SELECTING A PATH AGAINST HEPATITIS C VIRUS

A Dissertation

by

RUDO LYNDON SIMEON

Submitted to the Office of Graduate and Professional Studies of
Texas A&M University
in partial fulfillment of the requirements for the degree of

DOCTOR OF PHILOSOPHY

Chair of Committee,	Zhilei Chen
Committee Members,	Julian Leibowitz
	Arul Jayaraman
	Nazmul Karim
Head of Department,	Nazmul Karim

December 2013

Major Subject: Chemical Engineering

ABSTRACT

Hepatitis C virus (HCV) currently affects ~5% of the world's population and has relatively limited treatment options for infected patients. Genetic suppressor elements (GSE) derived from a gene or genome of interest can act as transdominant inhibitors of a particular biology function presumably by binding to and blocking an essential interaction surface for protein activity. Taking advantage of hepatoma cell line n4mBid, that supports all stages of the HCV life cycle and strongly report HCV infection by a cell-death phenotype, we developed an iterative selection/enrichment strategy for the identification of GSE against HCV. Using this strategy, a library expressing random fragments of the HCV genome was screened for sequences able to suppress HCV infection. A 244 amino acid gene fragment, B1, was strongly enriched after 5 rounds of selection. B1 has a very high net positive charge of 43 at neutral pH and a high charge-to-mass (kDa) ratio of 1.5. We show that B1 expression specifically inhibits HCV replication, apparently due to its high positive charge. We also show that recombinant positively charged proteins can inhibit HCV infection, when supplied *in vitro*.

In addition, eGFP-fused B1 potently penetrates both adherent and suspension cells with >80% of cells taking up the protein. Importantly, we show that B1 not only facilitates cellular uptake, but allows protein cargo to reach sites of biological relevance. B1 also delivers non-covalently conjugated RNA and DNA across the cell membrane to cytosolic and nuclear sites, with efficiency comparable to commercially available

cationic lipid reagents. Our data suggest that B1 utilizes cell-surface glycans and multiple competing endocytic pathways to enter and traffic through cells.

During a separate screening carried out in our lab, we identified a TACR3 inhibitor SB 222200 that had significant HCV activity. We go on to show that both TACR1 and TACR3 receptors are expressed in the HCV-permissive Huh 7.5 cell line. We also show that both TACR1 and TACR3 inhibitors significantly inhibit HCV infection. These results point to the potential for TACR1 antagonists in treating patients infected with both HCV and HIV.

DEDICATION

For my Mama and Papa.

ACKNOWLEDGEMENTS

I sincerely thank my advisor, Dr. Zhilei Chen, for her guidance over the past five years of my Ph.D. It has been an honor to work in her lab and to learn virology under her tutelage.

I thank the Chen lab members who were present during my stay: Dr. Karuppiah Chockalingam, Dr. Li Yi, Dr. Dongli Guan, Miguel Ramirez, Cory Klemashevich, Ana Maria Chamoun, Gunhye Lee, Nagarjun Kasareni, Thomas McMillin and John Rogers. Special thanks go to Dr Karuppiah Chockalingam for teaching me almost all the techniques I know, and to my former office mate, Cory Klemashevich, for making bacon, bread and pancakes.

I also thank: Jane Miller for teaching me flow cytometry techniques; Dr. Katy Kao for allowing my use of her flow cytometer; Dr. Roula Mouneimne for teaching me immunofluorescent microscopy techniques and for being extremely generous with her reagents; Dr. Julian Leibowitz for being an excellent professor and for taking the time to read the work of a lowly graduate student; Dr. Arul Jayaraman for generously allowing my use of his equipment; Dr. M. Nazmul Karim for agreeing to serve on my committee at the ‘eleventh hour’.

Finally, I thank my family for the ongoing love and support.

TABLE OF CONTENTS

Page

Page

LIST OF FIGURES

Page

Page

LIST OF TABLES

Page

1. INTRODUCTION

Hepatitis C virus (HCV) is a single-stranded, enveloped, positive-sense RNA virus of the *Flaviviridae* family (1). HCV infection affects over 180 million people worldwide (2) and is the leading cause of liver transplantation developed countries (3). Until recently the only currently approved HCV therapy involved a 24-48 week regimen of combination therapy involving pegylated interferon alpha and ribavirin (4). Interferon alpha-ribavirin treatment is costly, time-consuming and riddled with serious and debilitating side effects such as depression, fatigue and flu-like symptoms (5, 6), resulting in many patients being unable to complete the therapy. In addition, only 50% of treated patients infected with the most common genotype achieved sustained virological response (SVR) after receiving interferon-alpha-ribavirin therapy(7). The current standard of care for HCV infection involves a combination of two HCV protease inhibitors, boceprevir and telaprevir, along with interferon alpha-ribavirin (8). Though this treatment can achieve SVR rates approaching 80%, it is accompanied with more serious side effects and poses significant risks to patients with advanced liver disease (9). In addition, both boceprevir and telaprevir are prone to resistance development and they share resistant mutations (10). Thus, there remains an urgent need to develop new treatments to HCV outside the current paradigm of protease inhibition.

This research aimed to identify new genetic elements that inhibit HCV infection, and to characterize a new class of drugs that inhibit HCV infection. We first developed a

genetic screening approach that links HCV inhibition to cell survival. Using this approach, we identified a highly positively charged protein able to inhibit HCV replication. In addition, this protein was also found to have excellent cell penetration ability. These studies expands the repertoire of current anti-HCV molecules and hopefully will lead to safer, less demanding and more cost-effective treatment options for HCV-infected patients in the future.

1.1 Hepatitis C virus

1.1.1 HCV virology

HCV is a single-stranded, enveloped, positive-sense RNA virus of the *Flaviviridae* family (1). HCV exhibits an estimated mutation rate of 2.5×10^{-5} mutations per nucleotide per genome replication and exists as a quasispecies in each patient (11, 12). Six major genotypes and numerous subtypes of HCV have been identified around the world (13). HCV-induced liver cirrhosis and cancer is the leading cause for liver transplantation in developed countries (3).

The HCV RNA genome consists of approximately 9600 nucleotides, and is translated intracellularly into several structural and non-structural proteins. The structural proteins: capsid protein core and envelope proteins E1 and E2, form the virion that encloses the viral RNA. The non-structural proteins: p7, NS2, protease and helicase NS3 (14, 15), NS4A, NS4B, NS5A, and RNA dependent RNA polymerase NS5B (16), form the viral

replication complex and aid in the assembly of new virions. The HCV life cycle can be described in terms of three major steps: entry, replication, and virus assembly/release:

Entry. HCV requires a number of cell surface receptors to enter cells including SR-BI (17), CD81 (18), and the tight junction proteins claudin-1 (19), occludin (20) and the Neimann-Pick C1-like 1 (NPC1L1) cholesterol absorption receptor(21). After attachment, the HCV virion is internalized by the host cell via clathrin-mediated endocytosis. The acidic environment in the late endosome triggers fusion mediated by HCV E1 and E2 envelope proteins(22) between the viral and cellular membranes (23), causing the release of viral RNA into the cytoplasm.

Replication. With the viral RNA inside the cell, translation takes place at the rough endoplasmic reticulum (ER) (24). Unlike typical mRNAs, translation of HCV RNA is initiated at its internal ribosomal entry site (IRES) contained within the 5' untranslated region (UTR) of the viral RNA(25). All viral proteins are expressed in a single open reading frame, and are initially translated as a long polyprotein 3011 amino acids in length(26). The viral polyprotein is then processed into mature viral structural and non-structural proteins by cellular and viral proteases (27). HCV genome replication is believed to take place in a membranous web structure in the ER induced by HCV NS4B (28). In the membranous web, the HCV genome replication is carried out within the replication complex by the viral RNA-dependent RNA polymerase NS5B(16, 29). However, NS5B lacks a proof-reading mechanism, making viral RNA synthesis highly

error-prone(30). This leads to significant variations of the viral genome within a single patient, called a quasispecies (30). As is the case with human immunodeficiency virus (HIV) (31), the viral quasispecies facilitates the emergence of drug-resistant viral variants, making it difficult to eradicate HCV infection *in vivo* with any single drug therapy.

Virus assembly/release. Due to the presence of HCV core on the cytosolic side of the ER membrane, HCV assembly is thought to initiate in the cytosol. Nascent particles are transferred into the ER lumen to access cellular secretory pathways for release into the extracellular environment (32).

1.1.2 Systems available for the study of HCV

Even though HCV was first identified more than two decades ago (33), HCV antiviral development was hampered for many years by the lack of a suitable cell culture system(34). *In vitro*-transcribed HCV RNA of most genotypes proved infectious in animal models, but could not establish infection in cell culture(35). In 1999, a breakthrough was made with the discovery of the HCV replicon system, which is able to replicate efficiently in hepatocellular carcinoma cells (36). HCV replicon is a truncated form of the HCV genome encoding the HCV non-structural proteins NS3-NS5B. The replicon system facilitated the study of the replication aspects of the HCV life cycle, but did not support the production of infectious HCV particles. Another milestone in the

study of HCV was the development of infectious HCV pseudoparticles (HCVpp) in 2003.

HCVpp are lentiviral particles bearing HCV envelope glycoproteins E1 and E2. HCVpp recapitulate most of the steps of HCV entry, including cell surface receptor attachment, endocytosis and virus-host membrane fusion (37). However, HCVpp contain 94% more cholesterol than the authentic HCV and have reduced sensitivity toward cholesterol-modifying HCV inhibitors (21). Despite the availability of the HCV replicon and HCVpp systems to study HCV replication and entry, respectively, a convenient model system to study the entire life cycle of HCV was not available until a cell culture-produced strain of HCV (HCVcc) was discovered in 2005 (38) .

HCVcc was derived from JFH1, a genotype 2a isolate of HCV that was first found to be able to replicate efficiently *in vitro*, and then found to produce infectious virus particles in cell culture (39, 40). The HCVcc model enabled for the first time the study of all the steps of the HCV life cycle in a convenient cell culture format. Since then, a number of JFH-1 based intergenotypic recombinant viruses containing the core-NS2 sequence of prototype strains of HCV genotypes 1a, 2a, 3a, and 4a have been created, expanding the repertoire of infectious HCVcc genotypes (41, 42). Of these Jc1, the chimeric J6/JFH HCV genotype 2a isolate, and the JFH HCV genotype 2a isolate, are used in our lab. Jc1 was developed in a bid to obtain more infectious HCVcc recombinants. This isolate combines the Core, E1, E2 and p7 proteins of the patient-derived J6 isolate(43), with the

NS3-5B proteins of the patient-derived JFH-1 isolate(40, 41). When these two isolates were fused at the junction between the first and second transmembrane domains of the NS2 protein the resulting chimeric virus, termed Jc1, showed improved infectivity compared with the JFH isolate(41).

The final system developed involves a combination of the HCV replicon system, and HCV structural proteins. In this system, HCV virions are generated using J6 Core, E1 and E2 structural proteins, and then transcomplemented with JFH HCV replicon RNA resulting in transcomplemented HCV (HCVtcp)(44). HCVtcp can enter cells as HCVcc would, and then RNA replication can proceed via the JFH HCV replicon. However, due to the absence of HCV structural proteins in the JFH HCV replicon, no HCV virions can be produced in HCVtcp infected cells. Thus, the HCVtcp system allows for investigation of HCV entry and replication, in the absence of assembly/release. Since the virion used is a complete HCV virion, it is a potentially more accurate model of HCV entry than the HCVpp system. However, unlike HCVpp, HCVtcp virions are currently limited to using J6 HCV structural proteins(44).

1.1.3 Pharmacological advances in HCV inhibitor development

Since the development of the HCV replicon and HCVcc systems, there has been a great increase in the number of potential pharmacological treatments for HCV being identified and being pushed into clinical trials. These inhibitors may be organized into a number of

classes, based on the mechanism by which HCV infection is inhibited. All treatments may be classified as either direct acting or indirect acting antivirals.

1.1.3.1 Indirect acting antivirals

Indirect acting antivirals are compounds that do not specifically target viral protein or genetic material, and instead mediate antiviral activity by interacting specifically with the host. Indirect acting antivirals have a weaker tendency to foster drug-resistant mutants, but bear an increased risk of side effects. Interferon alpha, used in the standard of care for treating HCV, is an example of a non-direct acting antiviral since it functionally stimulates the host antiviral response by activating the JAK-STAT pathway (45).

1.1.3.2 Indirect acting antivirals: Cyclophillin inhibitors

Small molecule inhibitors of cyclophillins have been demonstrated to show significant inhibition of HCV infection *in vitro*. This has lead to significant interest in developing cyclophillin inhibitors as potential pharmacological treatments for HCV. Cyclophillin B has been demonstrated to bind to the HCV polymerase NS5B and enhance its RNA binding activity (46). Cyclophillin inhibitors can bind to cyclophillin B, preventing its interaction with the HCV polymerase and thereby inhibiting viral replication. As such, a number of cyclophillin inhibitors have entered into clinical trials. A promising cyclophillin inhibitor currently in clinical trials is NIM811. Despite previously having demonstrated excellent anti-HCV activity when used *in vitro*, NIM811 had no effect on

viral loads when used as a monotherapy. In addition, when used in combination with interferon, the drug failed to show a significant increase in sustained virological response (SVR) compared with control groups (47).

1.1.3.3 Indirect acting antivirals: HCV vaccines

Despite the development of an efficient *in vitro* model for studying HCV infection, the lack of a suitable animal model has greatly slowed the development of potential HCV vaccines. However, one such vaccine TG4040 has recently shown efficacy in a phase I clinical trial(48). TG4040 is a replication-deficient poxvirus that expresses HCV NS3, NS4 and NS5B proteins in patients. The expression of these proteins potentially leads to the induction of the host's natural immune response which constitutes its antiviral activity. TG4040 has been previously demonstrated to induce long lasting immune responses after initial vaccinations in animal models (49). Consistently, the phase I trial showed a sustained anti-HCV immune response in vaccinated patients. In addition, patients showed significantly reduced viral loads (53% reduction in viral RNA levels) and vaccine administration was relatively free of adverse effects apart from mild to moderate injection site reactions(48). Overall, TG4040 shows promise as a future anti-HCV vaccine.

1.1.3.4 Direct acting antivirals

Direct acting antivirals are compounds that specifically interact with a viral protein or nucleic acid. Drugs in this class are typically designed to be very specific to their target,

and tend to present a lower risk of side effects due to unintentional interactions. These drugs may be further grouped based on their specific target: protease inhibitors; nucleoside and non-nucleoside polymerase inhibitors; NS5A inhibitors; and monoclonal antibodies. However, this target specificity means an increased incidence of viral resistance, especially when treating viruses with high mutation rates like HCV (11). We will next discuss the development of the leading protease inhibitors.

1.1.3.5 Direct acting antivirals: protease inhibitors

Protease inhibitors are direct acting antivirals that selectively inhibit the protease activity of their target virus. Protease inhibitors developed for treatment of human immunodeficiency virus (HIV), such as darunavir and ritonavir, were found to be quite effective (50). The success of these and earlier anti-HIV protease inhibitors fueled interest in developing protease inhibitors against HCV. However, early development efforts were slowed both by the relatively shallow substrate binding site of the HCV protease (51), and the delay in developing an HCV infection model (HCVcc). Despite these initial limitations, Boehringer-Ingleheim developed a protease inhibitor (BILN 2061) that appeared to be very efficacious (52). However, this compound also exhibited high cardio toxicity which eventually lead to its failure as a potential treatment option (52). The proof of concept demonstrated with BILN fueled the development of candidate protease inhibitors by many pharmaceutical companies. Recently two of these drugs, boceprevir and telaprevir, became the first FDA-approved small molecule inhibitors of HCV.

1.1.3.6 Direct acting antivirals: Telaprevir

Telaprevir (marketed as Incivek) is a protease inhibitor initially developed and characterized by Vertex Pharmaceuticals. Telaprevir was designed as a peptidomimetic of the HCV protease cleavage site, and was demonstrated to be a selective, reversible inhibitor of the HCV protease(51). It was also found to be quite efficacious both in vitro and in a mouse model (51). In this study, telaprevir was demonstrated to have an oral bioavailability of at least 25%, and in particular was found to be present in the liver at concentrations at least 35 times that of the plasma(51). Telaprevir was also found to have a longer half-life when administered orally (~3 hours) compared to intravenous administration (~1.5 hours)(51).

Due to the relatively high chance of resistance mutants emerging during telaprevir treatment, the efficacy of telaprevir was tested in combination with interferon alpha therapy (53). A randomized, double blind, placebo controlled trial carried out in Europe achieved SVR in a significantly increased number of patients when telaprevir was administered in combination with interferon alpha (65% SVR) than the interferon alone group (48%) (53). In addition the effect of the presence of ribavirin on this expected synergy was also tested. This trial demonstrated the efficacy of the drug, and was particularly significant in that the overall treatment time could potentially be reduced from 48 weeks to 2 weeks (53). Reducing the treatment time of interferon therapy is important due to both the reduction in the cost to the patient, and the reduced duration of interferon's side effects which affects patient compliance. A significant result of this trial

was the relatively mild nature of the drug's adverse effects, which include pruritus and rash. These symptoms occurred significantly more frequently in patients receiving telaprevir/interferon (69%) compared with patients receiving interferon only (35%). The rashes found in the telaprevir group were found to be similar to those observed with drug reactions. Grade 3 rash was found in 7% of patients receiving telaprevir, but no grade 4 rash was reported(53). Overall 12% of patients receiving telaprevir discontinued treatment, compared with 7% of patients receiving interferon only. In a simultaneously conducted trial in the United States, similar efficacy was reported(54). A significant result of this trial was the reported efficacy of telaprevir when treating black patients. Black patients are typically less responsive to interferon therapy compared with other groups of patients due to the increased prevalence of the TT allele of the IL28b single nucleotide polymorphism, which was found to determine patient interferon response (55). The SVR obtained with black patients receiving telaprevir was significantly greater (44%) than those receiving interferon only (11%) (54). The efficacy of the treatment, reduction in treatment time, and relatively manageable side effects reported with telaprevir use eventually lead the drug to be approved for treatment of HCV by the Food and Drug Administration (FDA) in May of 2012.

1.1.3.7 Direct acting antivirals: Boceprevir

Boceprevir (marketed as Victrelis) is a protease initially developed by Schlering-Plough. Boceprevir contains a ketoamide moiety as the backbone and was designed to bind the active site of the HCV protease (56). Boceprevir was designed to be selective for the

HCV protease with irreversible binding (56), but later studies confirmed that its inhibition was indeed reversible (57). Boceprevir was also demonstrated to be extremely efficient at inhibiting both HCV replicon replication and HCV protease activity *in vitro*, with no reported cytotoxicity(56). Initial clinical trials tested the efficacy of boceprevir monotherapy as well its ability to induce drug resistant HCV mutants. In one such trial involving patients unresponsive to interferon-ribavirin therapy, SVR was not achieved in a significant percentage of patients tested (58). In addition, a number of drug resistant strains of HCV emerged which showed resistance to both boceprevir and telaprevir(58). The result of this and other studies lead to the development of boceprevir as a combination therapy with interferon alpha instead of as a monotherapeutic. Bocaprevir was then tested in an open label, randomized trial in North America and Europe to determine its efficacy as combination therapy with interferon alpha/ribavirin. In this study, patient groups received either the standard interferon/ribavirin therapy, or various combinations of interferon/bocaprevir therapy for at least 28 weeks and up to 48 weeks(59). The results indicated significantly higher SVR rates in all groups where bocaprevir was included as part of the therapeutic regimen, but it was noted that lower doses of ribavirin was associated with a higher rate of viral breakthrough (59). Similar to the results obtained in the trials of telaprevir, rapid clearance of viral loads was associated with SVR, which lead to the conclusion that treatment times in subsequent trial could be potentially be reduced. In addition, black patients receiving bocaprevir also showed a significantly increased SVR rate (53%) compared with those receiving interferon only (13%). Reported adverse effects included fatigue, anemia, nausea and

headache which are the side effects interferon/ribavirin treatment. Incidence of the reported side effect did not vary significantly between bocaprevir treatment and the control group. Given the success of this initial trial, subsequent phase 3 trials were carried out. The first of these trials tested the effect of bocaprevir/interferon combination therapy, while varying the bocaprevir treatment duration after a lead-in with interferon/ribavirin(60). The second tested the ability of boceprevir to induce a SVR in patients who did not respond to previous interferon/ribavirin treatment (61). In both these trials the SVR in boceprevir treated groups was significantly higher than that the control groups, and adverse effects were no more significant than appearing in control groups. As with telaprevir, the clinical efficacy and tolerability of boceprevir lead to its approval for treatment of HCV by the FDA in April of 2012.

1.2 Tachykinins

Tachykinins (also known as neurokinins) are peptides characterized by a common C-terminal sequence that binds to and activates a cell surface-localized tachykinin receptor (62). The three main tachykinin peptides (Substance P (SP), Neurokinin A (NKA) and Neurokinin B (NKB)) are distributed throughout the body, but are usually predominantly found in the central nervous system (CNS) (63, 64). The tachykinin receptor is a G-protein coupled receptor containing seven trans-membrane helices(65). Three different tachykinin receptors (TACR) have been identified – tachykinin receptors 1, 2 and 3 (TACR1, TACR2 and TACR3) – and each receptor can be activated by any of the three

main tachykinin peptides (66). This apparent lack of specificity is likely due to a high homology at the ligand-binding site among these receptors(67).

Typically the binding of an agonist to the receptor initiates a cascade of intracellular signaling events. Guanosine diphosphate (GDP) is first phosphorylated to guanosine triphosphate (GTP), activating the intracellular enzyme phospholipase C (PLC)(68). PLC can then, in turn hydrolyze phosphatidyl inositol bisphosphate (PIP_2) forming inositol triphosphate (IP_3) and diaglycerol (DAG)(68). These two molecules then act to increase the calcium concentration in the cytoplasm from two different sources. IP_3 can bind to and activate the IP_3 receptor on the ER membrane(69). This results in the release of calcium from the ER to the cytoplasm. DAG can activate protein kinase C (PKC) which opens L-type calcium channels in the cell membrane, enabling calcium influx from the extracellular environment(70). Perhaps due to this non-specific signal cascade, tachykinins can be responsible for a wide range of effects. This, combined with the relatively large tissue distribution, leads to tachykinins being involved in a number of functions including: neuronal survival and regeneration; gastric mobility; regulation of respiratory mechanisms; and the expression of pro-inflammatory cytokines (71-73).

Due to the large number of physiological functions mediated by tachykinin receptors, TACR antagonists, have been tested for a wide range of indications in clinical trials. TACR1 antagonist aprepitant has been tested as an antiemetic, an antidepressant, a CYP34A inhibitor, and to treat urge urinary incontinence (74-77). TACR1 antagonist CP

99994 has been tested as a post-operative analgesic (78). TACR2 antagonists nepadutant and saredutant have been tested for the treatment of irritable bowel syndrome, and the inhibition of NKA induced bronchoconstriction (79, 80). Finally, TACR3 antagonist osanetant has been tested as an anti-psychotic (81).

In addition to their roles in native body functions, tachykinin ligands and receptors have been implicated in the infection of some viruses (82, 83). For HIV it was observed that HIV-infected individuals had significantly increased levels of SP (84). It was also shown that SP binding lead to increased HIV replication in infected cells, including the activation of latently infected immune cells (85, 86). It was then shown that TACR1 antagonists inhibit HIV infection *in vitro* (83, 87, 88). Aprepitant, a TACR1 antagonist, was used in a clinical study for HIV treatment, but the study failed due to the inability to reach effective physiological concentrations at safe doses (89). The first, and only thus far implied role of tachykinins and HCV occurred when a TACR3 tachykinin receptor antagonist, SB 222200, appeared as a hit in a screen for anti-HCV small molecules carried out in our lab (90).

1.3 Genetic suppressor elements

Genetic suppressor elements (GSEs) are fragments of a genome that act to inhibit a function of the original gene from which they were derived (91). A GSE can exert its inhibitory function through a variety of mechanisms. For example, a GSE can encode a peptide that competes for a binding site or a substrate with the protein from which it was

derived, thereby suppressing the activity of the protein. GSEs have been identified against a number of different viruses, including rabies virus (92), HIV (93) and bovine viral diarrhea virus (94).

In addition to their role as tools for studying viruses, GSEs are potential therapeutic agents. GSEs have been found that decrease viral loads of bovine viral diarrhea virus (BVDV) by 100- to 1000-fold [20], a potency on par with some of the best BVDV antiviral candidates in preclinical and clinical trials [27]. Even if the GSEs themselves are not ideal drugs, suppressor elements can serve as templates for the creation of small molecule or peptide mimetics, which can in turn be used as potent antivirals. Such a peptide, called enfuvirtide, based on the fusiogenic domain of the HIV envelope protein, has been developed as an anti-HIV therapy (95). This treatment, marketed under the name Fuzeon, is used to great effect in treating patients who have become resistant to more traditional drugs used in Highly Active Anti-Retroviral Therapy (HAART)(96). No anti-HCV GSEs have yet been reported, partly due to the lack of a convenient cell culture system supporting HCV infection *in vitro* for many years.

GSE identification typically involves selection for a desired phenotype from a fragmented library derived from a target genome and the recovery of potential GSEs from the selected cells. The fragmented library is usually obtained by limited digestion of the target genome with DNaseI and purification of DNA fragments of a given size range. The potential library size depends on the size of the target genome. The HCV

genome has 9600 nucleotides and potentially contains 9600 distinct equal sized fragments. Depending on the size range of the purified fragments, the potential library size can be 10-100-fold larger than the target genome size. Due to the large complexity/size of genetic libraries generated from fragmented genomes, an effective phenotypic selection system is essential to separate true GSEs from genomic fragments that do not mediate the desired effect. The most convenient and commonly used selection pressure for viral systems is viral cytotoxicity. In such systems, virus-suppressing GSEs confer an easily selectable growth advantage phenotype to host cells(91).

HCV does not usually kill its target cells as a part of its infection cycle and is thus considered to be a non-cytopathic virus. To create of a selection system that allows anti-HCV molecules to confer a growth advantage to host cells, our lab engineered a hepatoma cell line, n4mBid, that supports high level of HCV infection and undergoes massive cell-death in response to HCV infection (97). The n4mBid cell line is a derivative of Huh 7.5, a cell line selected for its ability to support high levels of HCV replication(98). N4mBid contains a modified pro-apoptotic protein BH3 interacting domain death agonist (mBid) that is cleaved and activated by the HCV protease NS3-4A(99).

To select for anti-HCV GSEs, we transduced n4mBid cells with genetic libraries comprising a fragmented HCV genome and infected the transduced cell population with

cell culture-produced HCV (HCVcc). We hypothesized that, among the transduced n4mBid cell population, cells harboring HCV-neutral and pro-HCV genetic fragments will succumb to the HCV cytopathic effect and be gradually eliminated from the population, while cells harboring anti-HCV GSEs will resist the HCV cytopathic effect and gradually dominate the surviving cell population after several rounds of selection. As we will describe below, this led to the selection of an anti-HCV protein we call B1.

1.4 Cell penetrating proteins

Intracellular delivery of large, therapeutic biomolecules poses a significant challenge. Effective delivery entails not only crossing the outer cell membrane but transport and release of therapeutic cargo to cellular loci conducive to the attainment of a therapeutic effect. Several lipid-, polymeric- and inorganic-based vehicles for intracellular delivery of proteins and nucleic acids have been reported, including cationic lipids (100-102), polyethylenimine (PEI) (103, 104), carbon nanotubes (105-107), gold nanoparticles (108-110), and nanocapsules (111, 112).

The discovery that HIV Tat was capable of freely moving across the cell membrane inadvertently began a revolution of sorts in the field of protein transduction (113). Tat, which functions as a trans-activator of transcription of HIV genes, was shown to enter non-HIV infected cells, and eventually translocate into their nuclei (113). This discovery made Tat the first cell penetrating protein (CPP). Subsequent studies showed that an arginine–rich motif in Tat (GRKKRRQRRR) is responsible for cell-penetration (114).

This motif has been subjected to exhaustive analysis which lead to incremental improvements in its cell transduction capability (115, 116). Importantly, it was shown that fusing this Tat peptide to target proteins mediated the intracellular delivery of these proteins (117-120). Since then, a number of natural proteins have been found to have the capacity to penetrate cells, including the Antennapedia protein (Antp) from Drosophila (121, 122), VP22 protein from herpes simplex virus (123) and CaP from *Brome mosaic virus*(124). Similarly, several artificial CPPs have been created for protein and nucleic delivery, including highly positively charged peptides and proteins (e.g. poly arginine (125), supercharged +36 GFP (126) and related proteins (127)) and amphipathic peptides (e.g. Pep–1 (128), CADY (129)). Recently, an important discovery was made by the Liu group, who showed that many positively charged human proteins are also capable of cellular transduction(127). This study highlighted the importance of the ratio of positive charge and the molecular weight of each protein to efficient cellular transduction. The cellular uptake mechanisms of these CPPs are not yet fully understood, but many are believed to be internalized through endocytic pathways (130, 131).

In spite of their relatively high synthesis cost, cellular penetrating proteins are therapeutically relevant as gene or drug delivery agents. This both due to their relatively lack of intrinsic toxicity when compared with more traditional lipid based transfection reagents, and their potential to transduce cells previously determined to be problematic for traditional transfection reagents.

Several candidate peptide-delivered therapeutics have been developed, some of which are currently in clinical trials for a wide range of ailments including keloid scarring, myocardial infarction, hearing loss, wrinkles, cancer and psoriasis (132-138). One such therapeutic made use of a fusion of the Tat protein transduction domain and a positively charged poly-lysine motif in order to deliver a Botulinum Toxin Type A (BOTOX) analog across the skin without the need for painful injections (133). Another used a modified TAT ptd (called PTD4) fused to a C terminal peptide from heat shock-related protein HSP20 (139). This fusion protein, called AZX100, showed some promise in clinical trials aimed at treating keloid scarring(133).

2. INTRACELLULAR B1 INHIBITS JC1 HCV REPLICATION

2.1 Overview

Hepatitis C virus (HCV) currently affects ~5% of the world's population and has relatively limited treatment options for infected patients. Genetic suppressor elements (GSE) derived from a gene or genome of interest can act as transdominant inhibitor of a particular biology function presumably by binding to and blocking an essential interaction surface for protein activity. Taking advantage of hepatoma cell line n4mBid, that supports all stages of the HCV life cycle and strongly report HCV infection by a cell-death phenotype, we developed an iterative selection/enrichment strategy for the identification of GSE against HCV. Using this strategy, a library expressing random fragments of the HCV genome was screened for sequences able to suppress HCV infection. A 244 amino acid gene fragment, B1, was strongly enriched after 5 rounds of selection. Surprisingly, B1 is derived from a single-base frameshift of the enhanced green fluorescent protein (eGFP) which was used as filler during library cloning. B1 has a very high net positive charge of 43 at neutral pH and a high charge-to-mass (kDa) ratio of 1.5. We show that B1 expression specifically inhibits HCV replication. In addition, five B1 fragments with progressive truncation at the C-terminus all retain significant ability to inhibit HCV, suggesting that the high positive charge, rather than a particular motif in B1, is likely responsible for the anti-HCV activity. This study reports a new methodology for HCV inhibitor screening and points to the anti-HCV potential of positively charged proteins/peptides.

2.2 Introduction

Hepatitis C virus (HCV) is a single-stranded, enveloped, positive-sense RNA virus of the *Flaviviridae* family (1). HCV exhibits a high mutation rate and exists as a quasispecies in a single patient (11). Six major genotypes and numerous subtypes of HCV have been identified around the world (13). HCV infection affects over 180 million people worldwide (2) and is the leading cause of cirrhosis and cancer of the liver(140, 141). HCV induced end-stage liver disease is the leading indication for liver transplantation in developed countries (3).

Until recently the only approved HCV therapy involved a 24 or 48 week regimen of combination therapy involving pegylated interferon alpha and ribavirin (4, 142). Interferon alpha-ribavirin mono-treatment is costly, time-consuming and associated with serious and debilitating side effects such as depression, fatigue and flu-like symptoms (5, 6), resulting in many patients being unable to complete the therapy. In addition, only 50% of treated patients infected with the most common genotype achieved sustained virological response (SVR) after receiving interferon-alpha-ribavirin therapy(7). Recent pharmacological advances have led to the development and approval of two new drugs, boceprevir and telaprevir, which greatly improve the treatment response to up to 79% of the patients (60, 61). However, molecules that target specific viral proteins, including boceprevir, telaprevir and most of those in advanced clinical development, tend to foster drug-resistant variants (143, 144).

Genetic suppressor elements (GSEs) are short, biologically active gene fragments derived from a gene or genome of interest that inhibit the function of the associated gene or protein (93, 145). GSEs can exert their inhibitory effect as antisense RNAs, structural RNAs, or peptide/protein fragments that act as transdominant-negative mutants by binding to and blocking an interaction surface essential for protein activity. A significant feature of GSE technology is that it does not require any previous knowledge of the target gene(s)/protein(s) or the type of inhibitor (antisense RNAs, RNA decoys or transdominant mutants) that will most potently suppress the function of a specific gene. For example, GSE technology has been used to identify previously unknown viral genes that are essential for the infectious cycle of bacteriophage lambda, highlighting the power of the GSE approach for uncovering new biological information even in a very thoroughly investigated system (146). Other successes of GSE selection include the elucidation of human immunodeficiency virus type 1 (HIV-1) latency(93), bovine viral diarrhea virus entry(94), tumor suppressor genes(147), genes that mediate cellular sensitivity to anticancer drugs(148, 149), regulators of transcription(150), and potential anticancer(151) and antiviral(152) targets.

In addition to their role as tools for studying viruses, GSEs are potential therapeutic agents. GSEs have been found that decrease viral loads of bovine viral diarrhea virus (BVDV) by 100- to 1000-fold(94), a potency on par with some of the best BVDV antiviral candidates in preclinical and clinical trials (153). Even if the GSEs themselves

are not ideal drugs, suppressor elements can serve as templates for the creation of small molecule mimetics, which can in turn be used as potent antivirals.

In this section we aimed to identify GSEs with anti-HCV activity. Using a previously developed hepatoma cell line, n4mBid, that reports HCV infection by a cell-death phenotype, we developed an iteratively selection strategy which gradually enriches anti-HCV genetic fragments that confer resistance to HCV-induced cell death. Surprisingly, the most strongly enriched element, B1, is a 244 amino acid protein derived from a frame shifted enhanced green fluorescent protein (eGFP)(154) that was used as a filler during library cloning. B1 has a high net positive charge of 43 at pH 7, leading to a charge to molecular weight ratio of 1.5. B1 also possesses strong ability to delivery protein/nucleic acid cargo into the mammalian cell cytosol (section 3). We show here that B1 is able to inhibit HCV replication when expressed intracellularly and the inhibitory effect is largely mediated by its overall charge.

2.3 Results

2.3.1 GSE screens to identify genes involved in HCV infection

A schematic for GSE selection in mammalian cells is shown in Figure 2.1. Random DNA fragments of 100-200bp were obtained by DNaseI digestion of a plasmid encoding full-length Jc1 HCV(38). These fragments were first polished to form blunt ends and then cloned into retroviral vector pV1 previously digested with restriction enzyme *Pme*I.

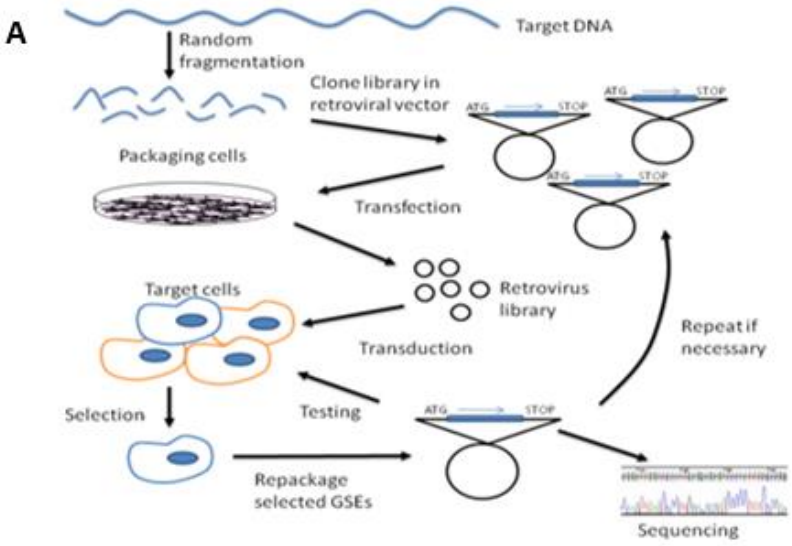

B

Round	Cell survival (%)	HCV infection (days)
1	6	5
2	6	7
3	11	8
4	21	9
5	60	9

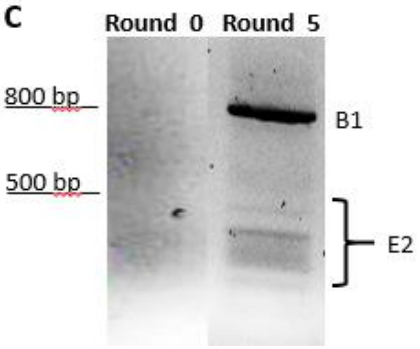

Figure 2.1. Overview of GSE selection. (A) Selection scheme. Randomly fragmented libraries were prepared by limited digestion of the HCV genome and fragments of 100-200 bp were cloned into pV1 lentiviral vector and packaged into VSV-G pseudotyped lentiviral particles. Library pseudoparticles were delivered into n4mBid cells such that each library fragment was expressed in at least 1000 cells. These cells were then infected with HCV to induce cytotoxicity until <10% of the initial cell population remained viable. The specific HCV inhibitor 2'C-MA was then added to rescue the remaining surviving cells. Library fragments were repackaged by transfecting the surviving cells with plasmids encoding VSV-G and HIV gag-pol. **(B)** The percentage of surviving cells after each round of selection. **(C)** Gel image of cDNA insert harvested from repackaged pseudoparticles.

pV1 is a minimal HIV-1 provirus lacking most HIV genes except for all necessary *cis* acting sequences such as Tat, Rev and Vpu ORF(155). The Nef gene was also deleted in pV1, and replaced by a cloning site for the insertion and expression of the cDNA interest. The fragment library is transcribed from the viral LTR. We chose the pV1 for library expression because viral particles can be repackaged from pV1-transduced cells when these cells are supplemented with envelope glycoprotein and HIV gag-pol, facilitating the iterative library screening through cyclic packaging(19).

We chose to express the fragmented library as C-terminal fusions to the transmembrane anchor of HCV NS4A (NS4Am) (156). Since HCV has been shown to replicate in replication complexes in association with the lipid raft membrane(157, 158), and HCV nonstructural (NS) proteins have been detected around lipid droplets in most HCV-permissive cells(159), attachment of the membrane-anchoring domains from HCV NS proteins to library fragments is designed to facilitate the interaction of the library fragments with viral/host factors located in the vicinity of the replication complexes, thus increasing the likelihood of identifying genetic suppressor elements from the library.

The random fragment library was prepared in lentiviral packaging cells and transferred to HCV reporter cell line n4mBid at a low multiplicity of infection (MOI) so that most transduced cells receive only one library fragment. The n4mBid cells contain a modified version of the pro-apoptotic protein Bid (mBid) and is able to induce apoptosis upon intracellular expression of HCV serine protease NS3-4A (97). Two days later, after the

expression of fragment library is established, these cells were infected with Jc1 HCVcc (MOI ~1) (38)and cultured until >90% of the cells succumbed to the induced cytopathic effect or up to 9 days. The surviving cells were 'cured' of any ongoing HCV infection by treatment with nucleoside analog 2'C-MA (1 μM) (160). Library fragments present in the surviving cells were repackaged by transfecting these cells with plasmid encoding VSV-G envelope protein. Repackaged lentiviruses were used in the next round of selection following the same procedure (Figure 2.1A). In some cases, the repackaged viruses were amplified in 293T cells to increase the viral titer prior to the next round of selection.

In total, we screened a random library containing an estimated 12, 000 individual fragments. For a library based on a fragmented retroviral HIV genome, the frequency of active perturbations (i.e. desirable GSE molecules) was estimated to be ~1/6000(93). As shown in Figure 2.1B, the time it takes for the cytopathic phenotype to be displayed, as well as the percentage of surviving cells at the end of selection period, increased with each successive round of selection, indicating that some library fragments able to inhibit HCV-induced apoptosis were being enriched. At the end of the fifth round, library fragments were recovered from the repackaged lentivirus and the insert cDNA were synthesized via RT-PCR. We observed a significant enrichment of a fragment of ~800 bp, and several fragments with sizes below 500 bp (Figure 2.1C). The 800 bp fragment was recovered and named B1 for convenience. Sequencing analysis showed that B1 is the product of a frameshift caused by an unintended single-base insertion preceding the

eGFP gene. Frameshifts in coding sequences typically yield very short polypeptides due to the concomitant introduction of new stop codons, but B1 contains 244 amino acids

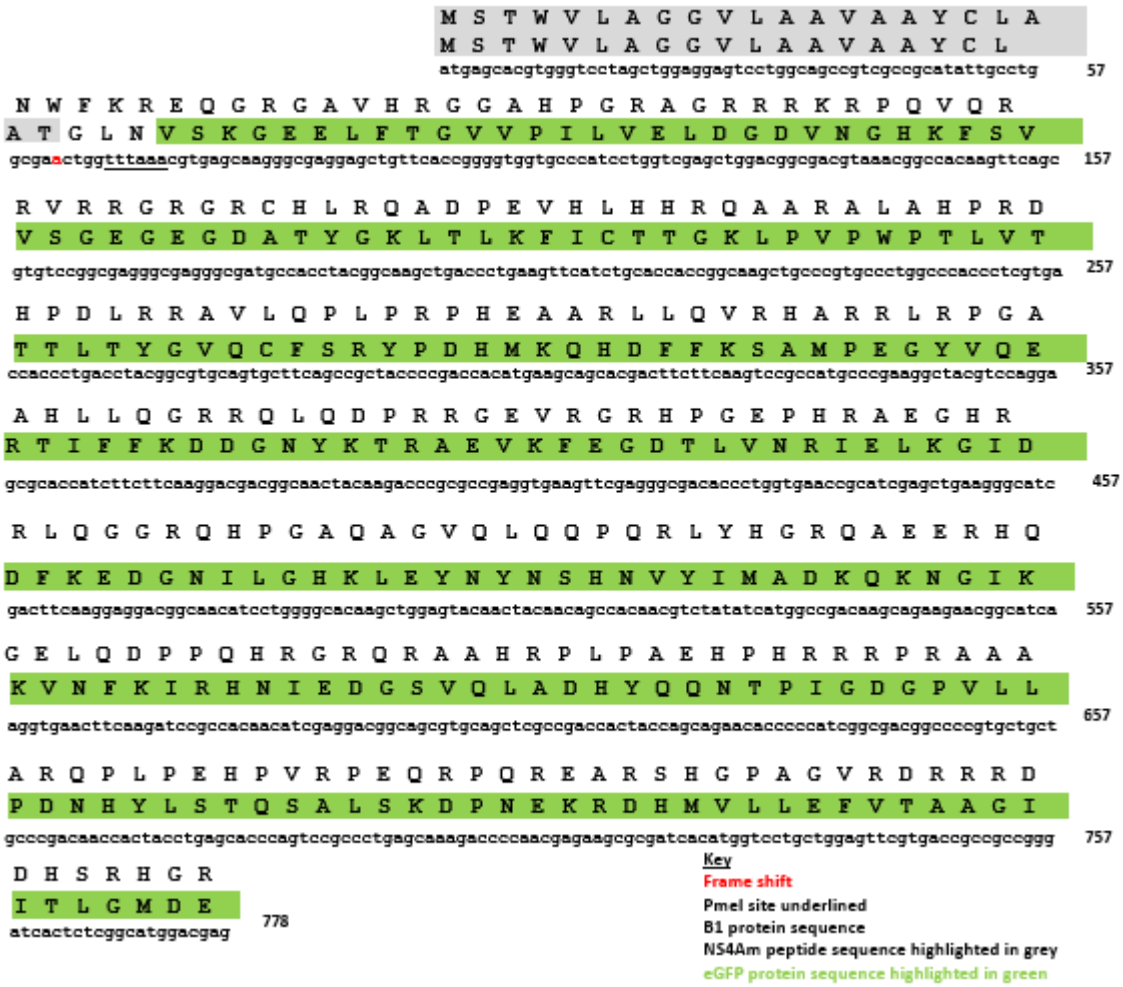

Figure 2.2. B1 nucleotide and amino acid sequence. Image showing comparative nucleotide and amino acid sequence of B1 and eGFP. Insertion which lead to the frame shift which generated B1 is shown in red.

and has a large positive charge of +43, making it similar in size to the original eGFP (238 amino acids). A protein database search of B1 using NCBI BLAST returned no matches, indicating no known homologs of B1. The eGFP gene is codon-optimized for expression in mammalian cells (154), and shares 71% nucleotide homology with the wild-type green fluorescent protein (GFP) from the jellyfish *Aequorea Victoria* (154, 161, 162) (Figure 2.2). Introduction of the same frameshift mutation into the original GFP sequence yields a translated sequence of only one amino acid. Most of the smaller enriched fragments shown in Figure 2.1C correspond to a region near the C-terminal of HCV E2 (Figure 2.3).

To confirm the expression of full-length B1 in Huh-7.5 cells, we constructed Flag-tagged B1 (Construct 3 & 4, Table 2.1). As shown in Figure 2.4A, the full length B1 is expressed both with and without the NS4Am anchor. The expression levels of the Flag-NS4Am-B1 appeared to be slightly lower than that of Flag-B1. We next determined the intracellular localization of both constructs using confocal microscopy. It was expected that Flag-NS4Am-B1 to be localized to the endoplasmic reticulum (ER) due to the presence of NS4Am membrane anchor. However, both Flag-NS4Am-B1 and Flag-B1 appeared to be predominantly localized to the cell nucleus and concentrated in nucleolar regions (Figure 2.4B). Since no known nuclear localization signal is present in B1, we speculate that the nuclear localization may due to its interaction with negatively charged genomic DNA during cell division.

A

```
MA-6*       TTTACCTTGCTCTTACTCGGACCTGCCCGCCTTGTCGACTGGTCTTCTCCACCTCCACCAAAACATCGTGGACGTACAATT
MA-7        TTT----------------ACCGGCCCGCCTTGTCGACTGGTCTTCTCCACCTCCGCCAAAACATCGTGGACGTACAAAC
MA-8        TTT----------------ACCTGCCCGCCTTGTCGACTGGTCTTCTCCACCTCCACCAAAACATCGTGGACGTACAAAC
MA-11       TTT----------------ACCTGCCCGCCTTGTCGACTGGTCTTCTCCACCTCCACCAAAACATCGTGGACGTACAAA-
MA-12       TTT----------------ACCTGCCCGCCTTGTCGACTGGTCTTCTCCACCTCCACCAAAACATCGTGGACGTACAATT
MA-13       TTT----------------ACCGGCCCGCCTTGTCGACTGGTCTTCTCCACCTCCACCAAAACATCGTGGACGTACAAAC
MA-14       TTT----------------ACCTGCCCGCCTTGTCGACTGGTCTTCTCCACCTCCACCAAAACATCGTGGACGTACAATT
MA-16       TTT----------------ACCTGCCCGCCTTGTCGACTGGTCTTCTCCACCTCCACCAAAACATCGTGGACGTACAAAC
MA-18       TTT----------------ACCTGCCCGCCTTGTCGACTGGTCTTCTCCACCTCCACCAAAACATCGTGGACGTACAATT
MA-19       TTT----------------ACCTGCCCGCCTTGTCGACTGGTCTTCTCCACCTCCACCAAAACATCGTGGACGTACAAAC
MA-20*      TTTACCTTGCTCTTACTCGGACCTGCCCGCCTTGTCGACTGGTCTTCTCCACCTCCACCAAAACATCGTGGACGTACAATT
HCV_J6_E2      ACCTTGCTCTTACTCGGACCTGCCCGCCTTGTCGACTGGTCTTCTCCACCTCCACCAAAACATCGTGGACGTACAATT
                          2430                                                        2490
```

B

Protein	Net charge	MW (kDa)	Charge/MW ratio
MA6*	-2.3	5	-0.5
MA7	+3	2.7	1.1
MA8	+5	3.9	1.3
MA11	+3.9	3.8	1.0
MA12	+4	4.5	0.9
MA13	+3	2.8	1.1
MA14	+6	5.1	1.2
MA16	+3.9	2.8	1.4
MA18	+4	4.5	0.9
MA19	+3.9	2.8	1.4
MA20*	-1.8	6.2	-0.3

Figure 2.3. E2-derived isolated fragment analysis. A.E2-derived fragment sequence alignment. Additional fragments isolated after the library selection were aligned with HCV J6 E2. Fragments matched 60 bases near the C-terminal of E2 (nucleotides 2430-2490). Bases showing complete homology among all sequences are highlighted in blue. The first base in each fragment is highlighted in red (start codons not shown). Bases remaining from original PmeI site are underlined. All fragments are -1 frame-shifted with the exception of MA-6 and MA-20.**B.** Table showing net charge and charge:MW(kDa) ratios of each peptide. *Indicates non-frame-shifted peptides.

Number	Name	Molecular weight (kDa)	Expression vectors
1	NS4Am-B1	30.6	pV1, pLenti6
2	B1	28.4	pV1, pLenti6
3	Flag-NS4Am-B1	33.3	pZsGreen (pTRIP)
4	Flag-B1	31.1	pZsGreen (pTRIP)
5	NS4Am-B2	17.8	pV1
6	NS4Am-B3	14.7	pV1
7	NS4Am-B4	13.2	pV1
8	NS4Am-B5	10.7	pV1
9	NS4Am-B6	6	pV1
10	+36GFP	28.4	pV1

Table 2.1. Protein constructs and vectors used in this section.

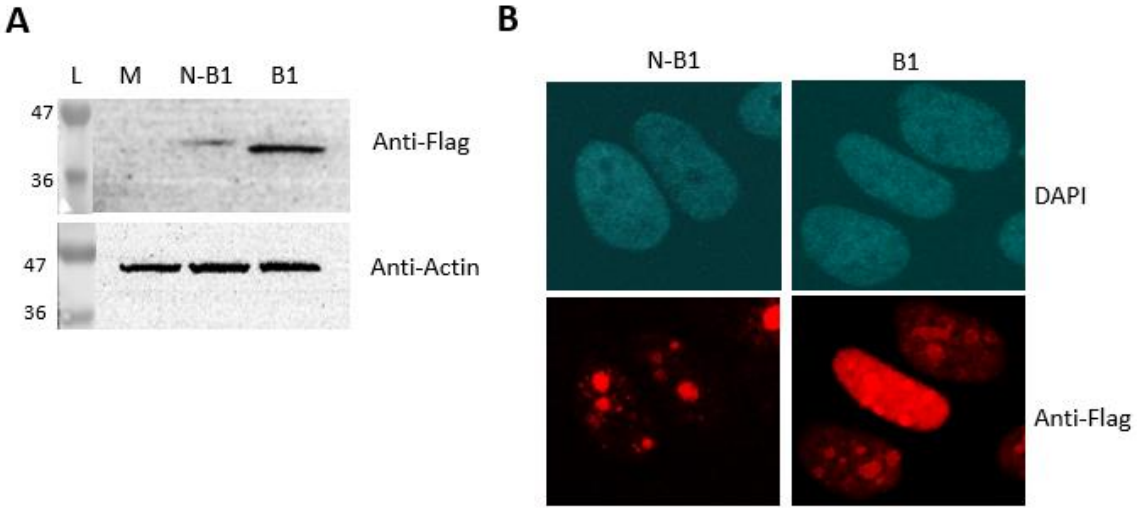

Figure 2.4. Expression of B1 in Huh 7.5 cells. A. Western blot of Flag-NS4Am-B1 (N-B1) and Flag-B1. **B** Confocal microscope image of Huh-7.5 cells transduced with Flag-NS4Am-B1 or Flag-B1 after immunohistochemical staining with anti-flag antibody.

2.3.2 Intracellular B1 inhibits HCV infection

To confirm the ability of B1 to confer HCV inhibition, the sequences of B1, NS4Am-B1 or eGFP were cloned into pLenti6 provirus and packaged into pseudoparticles used to transduce naïve Huh-7.5 cells at MOI ~1. After selection with blasticidin, the resulting cell population were infected with Jc1 Gluc HCVcc (163) or HIV-1 lentivirus pseudotyped with envelope protein from H77 HCV (23) or vesicular stomatitis virus (VSV) (164). As shown in Figure 2.5A, cells expressing either NS4Am-B1 or B1 showed significantly reduced infection level of Jc1 Gluc HCVcc when compared to that expressing eGFP, confirming the ability of B1 to inhibit HCV infection. No inhibition was observed in cells transduced with pseudotyped lentiviruses

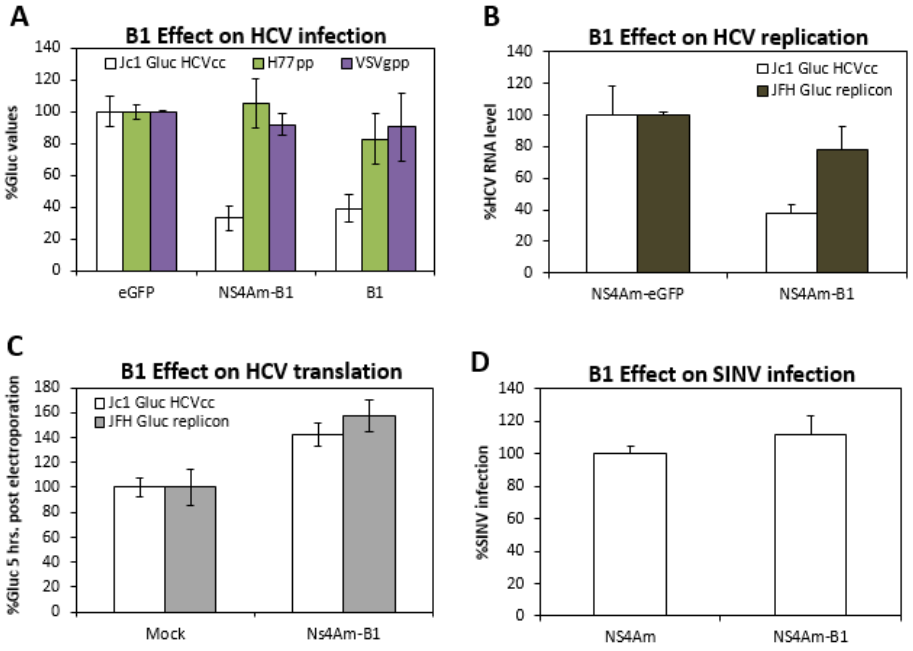

Figure 2.5. B1 inhibits HCV infection. A. Cells expressing B1 or NS4Am B1 have reduced HCV infection level. Huh 7.5 cells were transduced with lentiviral pseudoparticles encoding eGFP, NS4Am-B1 or B1 prior to infection with Jc1 Gluc HCVcc (MOI <0.1), H77 HCVpp (10-fold dilution) or VSV-Gpp (500-fold dilution) for 12 hours. The supernatant Gluc activity was quantified 24 hours later and used as indication of HCV infection level. Error bars represent the standard deviation of duplicate wells in two independent experiments. **B.** Cells expressing NS4Am-B1 have reduced HCV replication level. Huh 7.5 cells were transduced with lentiviral pseudoparticles expressing NS4Am-GFP or NS4Am-B1 at MOI 4. 48 hours later, these cells were electroporated with full length Jc1 Gluc HCVcc, or JFH Gluc replicon replicon HCV RNA. Intracellular HCV RNA levels were quantified 48 hours later using qRT-PCR. Error bars represent standard deviations of duplicate wells from two independent experiments. **C.** B1 does not inhibit HCV translation. Naïve Huh-7.5 cells or cells populations expressing NS4Am-B1 (as in B) were electroporated with Jc1 Gluc HCVcc or JFH Gluc HCV replicon RNA. HCV translation was quantified by measuring the activity of secreted Gluc 5 hours later. **D.** B1 does not inhibit SINV infection. BHK-J cells were transduced with lentiviral pseudoparticles expressing NS4Am-B1 or NS4Am alone at MOI ~4. Two days later, cells were infected with SINV for 12 hours and thoroughly washed. Infectious SINV in the supernatant collected 48 hours later were quantified by plaque assay. Error bars represent standard deviations of duplicate wells from two independent experiments.

regardless of the envelope protein, suggesting that B1 does not affect the entry step of HCV infection or lentiviral transduction.

Since B1 appears to be predominantly located in the nucleus, and some nuclear factors are required for HCV replication (165-167), we next considered whether B1 inhibits HCV replication. Cell populations expressing NS4Am-eGFP or NS4Am-B1 were electroporated with RNA encoding either full length Jc1 Gluc HCVcc(38) or JFH Gluc HCV subgenomic replicon(168). The amount of intracellular HCV RNA was quantified 48 hours post electroporation by qRT-PCR. Similar levels of inhibition were observed in cells electroporated with Jc1 Gluc HCVcc(38) (Figure 2.5B) and in cells infected with the same virus (Figure 2.5A). However, a much weaker but significant level of inhibition was observed with the JFH Gluc HCV replicon(168). The stronger inhibition seen in Jc1 Gluc HCVcc(38) may, in part, be due to the amplification of effects from multiple rounds of infection.

Next, we considered whether B1 might inhibit the translation/processing of HCV because 1) B1 was found to strongly associate with mRNA due to its high positive charge (section 3) and 2) B1 primarily localizes in the nucleus and HCV translation is potentially modulated by nuclear factors(165, 166). Cell populations expressing NS4Am-GFP or NS4Am-B1 were transfected with RNA expressing the full length Jc1 Gluc HCVcc (38) or the JFH Gluc subgenomic replicon(168). In the Jc1 HCVcc construct, the reporter Gluc gene was inserted between p7 and NS2 while in the replicon

construct, the Gluc is translated directly from the JFH HCV IRES. HCV IRES-mediated translation was quantified based on reporter activity measured at 5 hours post transfection (prior to the onset of replication (169)). No inhibition of Jc1 or JFH translation was observed in cells expressing (Figure 2.5C), indicating that B1 does not affect IRES-mediated translation.

Since B1 does not affect lentiviral transduction (Figure 2.5A), suggesting that B1 may not upregulate non-specific antiviral response mechanisms such as the interferon pathway or the unfolded protein response (170, 171). To confirm that B1 does not activate the innate antiviral machinery, we determined the ability of B1 to inhibit the infection of Sindbis Virus (SINV), a closely related positive sense RNA virus belonging to the *Alphavirus* genus(172). As anticipated, no inhibition of SINV was observed in cells expressing B1 (Figure 2.5D).

2.3.3 B1 fragments retain anti-HCV activity

Next, we decided to determine whether a specific domain/region in B1 is responsible for the anti-HCV activity. B1 is progressively truncated at the C-terminus to form shorter B2-6 (Figure 2.6A). The choice of truncation site is guided by the secondary structure predicted by the GOR4 algorithm(173). These truncated B1 fragments were cloned into pV1 lentiviral vector and packaged into lentiviruses. Huh-7.5 cell populations expressing the truncated B1 fragments were challenged with Jc1 Gluc HCVcc at MOI <0.1 and the

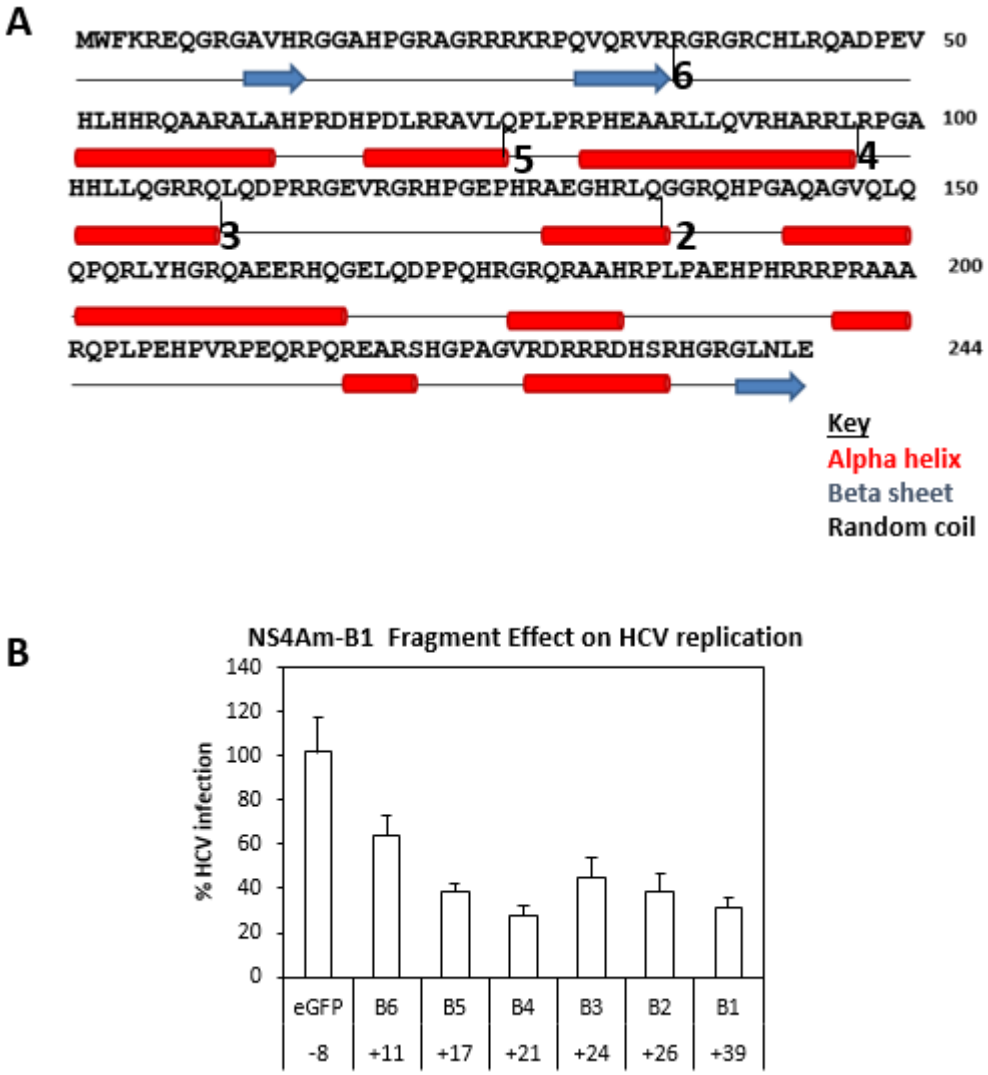

Figure 2.6. Truncated B1 retains significant anti-HCV activity. A. B1 was progressively truncated from the C-terminus to form B2-B6 based on secondary structure predicted by GOR4 algorithm(173). **B.** Anti-HCV activity of B1-B6. Huh-7.5 cells were transduced with lentiviral pseudoparticles encoding the indicated constructs at MOI ~4. 48 hours later, these cells were infected overnight with Jc1 Gluc HCVcc (MOI <0.1). Supernatant Gluc activities were quantified 48 hours later and used as indication of HCV infection level. Error bars represent the standard deviation of duplicate wells from two independent experiments.

HCV infection levels were quantified 3 days post infection. All shortened B1 constructs appear to significantly inhibit HCV infection to a level similar to the full-length B1 (Figure 2.6B), indicating that no specific region/domain in B1 is singly responsible for HCV inhibition. Fragments with a positive charge above 16 all appear to have similar anti-HCV activity, while B6, the shortest fragment with a lower predicted charge of +11, showed slightly reduced anti-HCV activity. The negative control protein eGFP, with a predicted net charge of -8, showed no anti-HCV activity.

2.3.4 Intracellular +36GFP is poorly expressed and does not inhibit HCV infection

Since the HCV inhibition of B1 appears to be due to its charge, we tested the potential anti-HCV activity of one of another proteins, +36 GFP that has a similar positive charge as NS4Am-B1 (+39). Fluorescent imaging of intracellular +36GFP indicated that it was predominantly localized in the cell nucleus, similar to B1 (Figure 2.7A). However, even after high MOI transduction (up to MOI 10), only a small percentage of the transduced cells showed detectable +36GFP expression (~20%) (Figure 2.7B). Consequently, no HCV inhibition was observed in cells expressing +36GFP (Figure 2.7C).

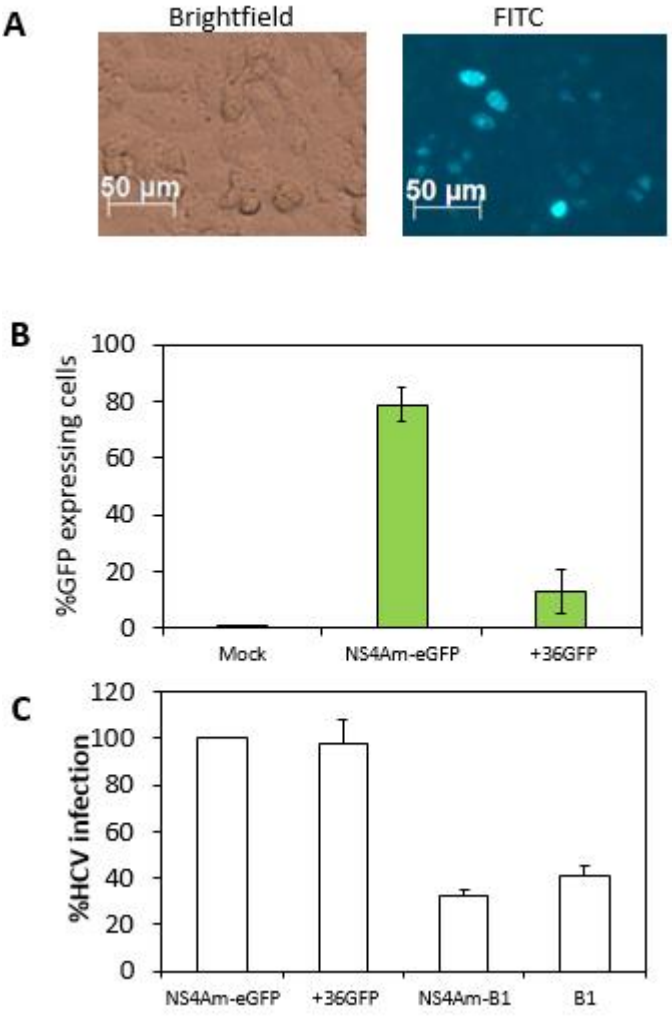

Figure 2.7. Intracellular +36GFP does not inhibit HCV infection. Huh 7 cells were transduced with lentiviral pseudoparticles expressing indicated constructs at MOI ~10. It was noted that using Huh 7 cells resulted in better expression of the +36GFP construct. Two days later, cells were infected with Jc1 Gluc HCVcc at <0.1 MOI for 12 hours. Cell supernatants were collected 48 hours post infection. At this time +36GFP expression was visualized with a fluorescent microscope (A). After imaging, cells were resuspended and the percentage +36GFP-expressing cells quantified with flow cytometry (B). HCV infection levels were quantified based on secreted Gluc levels in the collected supernatants (C).Error bars represent standard deviations of duplicate wells in two independent experiments.

2.3.5 Purified +36GFP but not GFP-L-B1 inhibits HCV infection

Although +36GFP is poorly expressed by Huh 7.5 cells, it has been shown to have significant cell transduction activity in mammalian cells (126). In addition, we also showed that purified B1 protein also has significant cell transduction activity (174). These observations made it possible to circumvent the lack of expression of +36GFP in Huh 7.5 cells, by treating cells with purified +36GFP. As shown in Figure 2.8A, cells treated with at least 0.5 μM +36GFP significantly inhibited Jc1 HCV infection. In addition, +36GFP did not inhibit H77 HCVpp entry (Figure 2.8B). In contrast, treating cells with purified GFP-L-B1 protein prior to and during HCV infection did not result in HCV inhibition (Figure 2.8).

2.4 Discussion

In this section we report the development of a method for identifying genetic suppressor elements of HCV. Despite recent advances in direct acting antivirals (DAAs) against HCV, there remain critical needs for new HCV inhibitors with novel antiviral mechanism of action. The screening method we developed takes advantage of a hepatoma cell line previously developed in our laboratory, n4mBid, which supports the entire HCV life-cycle and effectively reports HCV infection via a cell death phenotype(97). A randomly fragmented HCV genomic library was delivered to n4mBid cells via lentiviral transduction. Transduced cells were subsequently challenged with Jc1 HCVcc (38). The surviving cells were pooled and GSEs from these cells were harvested and repackaged, and used in subsequent rounds of selection and enrichment.

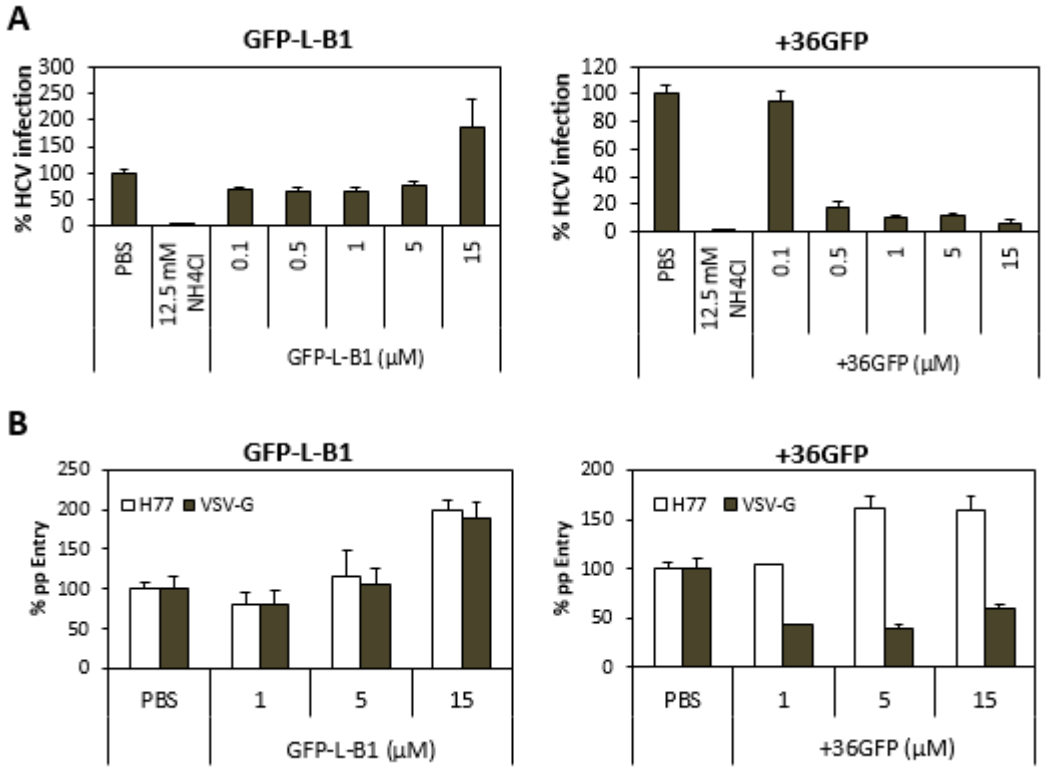

Figure 2.8. Purified +36GFP inhibits HCV infection. A. Anti-HCV activity of recombinant positively charged proteins. Huh 7.5 cells infected with Jc1 Gluc HCVcc in the presence of indicated concentrations of GFP-L-B1 or +36GFP for 12 hours. After infections cells were washed and protein dilutions replaced. HCV infection in each cell population was characterized based on secreted Gluc levels measured 48 hours later. HCV infection was inhibited by +36GFP but not GFP-L-B1. There was no significant inhibition of VSV-Gpp infection in these cells. Error bars represent the standard deviation of duplicate wells in two independent experiments. **B.** Anti-HCVpp activity of recombinant positively charged proteins. Huh 7.5 cells infected with H77pp or VSV-G in the presence of indicated concentrations of GFP-L-B1 or +36GFP for 12 hours. H77pp or VSV-Gpp infection in each cell population was characterized based on secreted Gluc levels measured 48 hours later. GFP-l-B1 enhanced H77 and VSV-Gpp infection at higher concentrations. +36GFP inhibited VSV-Gpp infection but enhanced H77pp infection at higher concentrations. Error bars represent the standard deviation of duplicate wells in two independent experiments.

After 5 rounds of screening, we identified B1, a 244 amino acid protein derived from a frame-shift in region immediately upstream of eGFP, a filler protein used during library cloning. B1 is a highly positively charged protein with significant cell-transduction capabilities and is capable of delivering cargo proteins and nucleic acids into the cytosol (section 3). In this section, we characterized the anti-HCV property of B1. The B1 sequence was not intended to be a part of the original library, as eGFP was only a filler in the vector during the cloning. It is even rarer that B1 derived from a single nucleotide insertion in the primer region upstream of eGFP (Figure 2.3). We showed that B1 was expressed as a full length protein in Huh-7.5 cells (Figure 2.2A). Surprisingly, B1 appeared to be almost exclusively localized in the nucleus even when fused to the NS4A membrane anchor (NS4Am) (Figure 2.2B). Despite its nuclear localization, both B1 and NS4Am-B1 exhibit similar anti-HCV potency (Figure 2.5A). Further characterization revealed that B1 does not affect HCV entry (Figure 2.5A) or virus production (data not shown) but specifically inhibits the replication step of the HCV life cycle (Figure 2.5B). Nuclear factors such as heterologous nuclear ribonucleoprotein L (hnRNP L)(165) and the nuclear La protein(166) have been demonstrated to affect HCV replication by upregulating HCV translation. This made it possible that B1 interacts with one of these such proteins, or their targets, leading to inhibition of viral translation. However, B1 does not appear to inhibit IRES-mediated HCV translation (Figure 2.5C).

To shed light on B1's anti-HCV mechanism of action, a series of truncated B1 with progressive deletions at the C-terminus were generated. We have shown that the cell

transduction activity of B1 is not due to its charge and not a specific motif within the protein(174). We reasoned that, if the anti-HCV activity is derived from the overall charge of B1, a point would be reached where the charge on the construct is no longer sufficient to effect the same level of inhibition. Conversely, if the charge was irrelevant and the inhibition is due to a structural motif or specific region in B1, then once the motif was removed from the construct, its HCV inhibition should be completely abrogated. We generated truncated B1 with predicted net charges ranging from +11 to +39 and showed that all these fragments, including the shortest fragment (35 amino acids with a predicted charge of +11), retain significant anti-HCV activity, albeit the shortest fragment showed reduced anti-HCV potency (Figure 2.6B). This result suggests that the overall positive charge, rather than a specific motif, is likely responsible for the anti-HCV activity of B1.

While positively charged proteins are relatively uncommon, many are expressed in mammalian cells (127). Previously, Liu and coworkers synthesized a series of highly charged GFP and showed that they can effectively transduce mammalian cells (126). We tested the potential anti-HCV activity of one of these charged proteins, +36 GFP that has a similar positive charge as NS4Am-B1 (+39). However, +36GFP was poorly expressed in Huh 7.5 cells, and did not inhibit HCV infection (Figure 2.7). This poor expression seems to indicate that the host (mammalian) cells negatively regulate or control the expression of highly positively charged protein. Indeed due to their high tendency to interact with negatively charged nucleic acids, the presence of large amount of positively

charged proteins in the cytosol may negatively affect the cell cycle and growth. With this in mind, it is perhaps fortuitous that B1 expresses at a level sufficient to inhibit HCV without causing any unintended cytopathic effects.

In addition to the B1, several shorter peptides were selected during the screen (Figure 2.1C). Among the 20 clones we sequenced, 11 correspond to a region near the C-terminal of HCV E2 (Figure 2.4A). These peptides had a modal charge of +3.9, and a charge to mass ratio of ~1 (Figure 2.4B). However, we were unable to observe consistent anti-HCV activity in cells expressing these fragments (data not shown). It would be expected that, based on results obtained with B1 and their enrichment during selection, these fragments should also have anti-HCV activity. However, due to their small sizes and low charges, their anti-HCV potencies are expected to be significantly weaker than that of B1. This, in addition to the fact that positively charged proteins are weakly expressed in these cells, will have undoubtedly contributed to our inability to observe any significant inhibition effect.

Taken at face value, the anti-HCV activity of B1 is comparable to the antiviral effects of defensins. Defensins are short (less than 100 amino acids), positively charged peptides that contain six cysteine residues(175). Defensins are broad-spectrum antimicrobials and have been shown to be active against bacteria, fungi and some enveloped viruses (176-180). The antiviral activity of defensing is largely attributed to its positive charge (177). However, defensins act directly on extracellular viruses while B1 inhibits intracellular

HCV replication. Treating cells with purified B1 protein prior to or during HCV infection did not result in HCV inhibition (Figure 2.8). Extracellularly delivered B1 exhibited punctate structure in the para-nucleus region (section 3), somewhat similar to that of extracellularly delivered +36 GFP (126). However, intracellularly expressed B1 appeared to exclusively localize in the nucleus (Figure 2.2B). The difference in subcellular localization of B1 may be critical to its ability to inhibit HCV replication. Human alpha defensins 1-3 was found to act intracellularly to inhibit PKC signaling, which results in inhibition of HIV infection (181). However, no inhibition of pseudotyped lentivirus was observed in cells expressing B1 (Figure 2.5A), implying that B1 does not significantly inhibit PKC signaling and B1 does not function like a defensin in these cells. In contrast, extracellularly delivered +36GFP did significantly inhibit HCV and pseudotyped lentivirus infection (Figure 2.8). This implies that unlike B1, recombinant +36GFP may possess some defensin-like antiviral activity.

In conclusion we have developed a new *in vitro* method for selecting GSEs against HCV. We identified a highly positively charged protein, B1, capable of inhibiting HCV replication. We showed that B1's positive charge is likely responsible for its anti-HCV activity, as a truncated B1 construct with less positive charge showed weaker HCV inhibition. This is a novel mechanism for inhibiting HCV replication and may open doors to new HCV antiviral design and synthesis. In addition, this GSE selection method can be applied to other protein or peptide libraries in the continued search for new anti-HCV factors.

2.5 Materials and methods

2.5.1 Reagents, bacterial strains and cell lines

TZM- bl cells were obtained from Dr. John C. Kappes, Dr. Xiaoyun Wu and Tranzyme Inc. through the NIH AIDS Reagent Program, Division of AIDS, NIAID. Huh 7 and Huh-7.5 cells were obtained from Prof. Charles Rice (Rockefeller University). 293T cells were purchased from Invitrogen.

All cell lines were cultured in complete growth medium (Dulbecco's Modified Eagle Medium (DMEM) containing 4500 mg/L glucose, 4.0 mM L- Glutamine, and 110 mg/L sodium pyruvate (Thermo Scientific HyClone, Logan, UT) supplemented with 10 % fetal bovine serum (Atlanta Biologicals, Lawrenceville, GA) and 1X non- essential amino acids (Thermo Scientific HyClone, Logan, UT)). *Escherichia coli* strains DH5α and Stbl3 (Invitrogen) were used for recombinant DNA cloning.

Biolux Gaussia Luciferase Assay Kit was purchased from New England Biolabs. Dulbecco's Phosphate- Buffered Saline (DPBS) was purchased from Thermo Scientific HyClone. OptiMEM and Lipofectamine 2000 were purchased from Invitrogen. Luria-Bertani (LB) broth, Mirus TransIT LT1 transfection reagent and ampicillin were obtained from Thermo Fisher Scientific. 0.25% trypsin- EDTA was from VWR International. All restriction enzymes, nucleases and polymerase were purchased from New England Biolabs.

2.5.2 Fragment library preparation

Plasmid DNA encoding full-length Jc1-NFlag2 HCVcc (38) was digested with DNaseI at 16 °C for ~2 minutes to obtain an average fragments size between 100-200 bp. The digested DNA were extracted by phenol-chloroform following standard protocol, sequentially treated with Mung Bean Nuclease, T4 DNA polymerase and Klenow Fragments to form blunt ends, and phosphorylated using T4 Polynucletide Kinase. Blunted fragments were inserted into the pV1 lentiviral vector downstream of NS4A membrane anchoring domain (NS4Am). pV1 is a minimal HIV-1 provirus lacking most of the HIV genes except for essential *cis*-acting elements and the tat, rev and vpu genes (155). The vector backbone was prepared by digesting pV1-NS4Am-eGFP with PmeI to remove the eGFP insert and dephosphorylated using Antarctic Phosphotase. The ligation mixture was electroporated into *E. coli* DH5α. Colonies were pooled and cultured, and the plasmid DNA library (Lib4) was isolated.

2.5.3 Pseudoparticle production and titering

Lib4 expressing pseudoparticles (Lib4pp) were generated based on a procedure described previously (90). Briefly, 293T cells were transfected with a 2:2:1 mass ratio of plasmids encoding HIV gag-pol, vesicular stomatitis virus glycoprotein (VSV-G), and Lib4 using TransIT-LT1 transfection reagent(19). Cell supernatants containing VSV-G coated, Lib4pp were collected 48 hours later, filtered and stored at -80 C until use. Collected Lib4pp were titered in TZM-bl indicator cells. TZM-bl cells were inoculated with serial dilutions of Lib4pp (10^{-1} - 10^{-6}). 48 hours later cells were washed with DPBS,

fixed in PBS/2% paraformaldehyde (PFA) and stained with X-Gal (VWR International). The $TCID_{50}$ of the Lib4pp in TZM-bl were calculated using the method of Reed and Meunch(182). The titer determined in TZM-bl cells was correlated to that in Huh 7.5 cells by comparing the infectivity of GFP expressing pseudoparticles (GFPpp) in both cell types. GFPpp was generated using the same protocol replacing Lib4 expressing plasmid with pTRIP-GFP(183). Huh 7.5 and TZM-bl cells were inoculated with serial dilutions of GFPpp (10^{-1} - 10^{-6}). 48 hours later, Huh-7.5 cells were collected and analyzed with flow cytometry (FACScan flow cytometer, BD Biosciences) while infection of TZM-bl cells were analyzed as described above. The infectivity of the pseudoparticles was estimated based on infection at low multiplicity of infection (MOI) and correlated between these two cell lines.

Lentivirus pseudotyped with envelope proteins from HCV H77 (H77pp) (23)and VSV-G (VSV-Gpp)(164) were generated from 293T cells as previously described (90). Both H77pp and VSV-Gpp harbor pTRIP-Gluc provirus. Briefly, 293T cells were transfected with a 1:4:1 mass ratio of HIV gag-pol, Gluc, and H77/VSV envelope expressing plasmid using TransIT-LT1 transfection reagent(19). Cell supernatants containing H77pp or VSVG-pp were collected 48 hours later, filtered and stored at -80 C until use.

2.5.4 Library selection

For each round of selection, a total 2.1 x 10^7 n4mBID cells were transduced with Lib4pp at MOI ~0.5. This allowed for the expression of each potential library fragment in at

least 1000 cells. Cells were cultured for 48 hours post transduction to allow for fragment expression. Next, these cells were challenged with Jc1 HCVcc at MOI~1, and cultured until less than 10% of cells remained viable or for up to 9 days. Surviving cells were 'rescued' from HCV infection by treatment with HCV polymerase inhibitor 2'C-MA (1 μM) for 72 hours. Library fragments in the surviving cells were recovered by transfecting these cells with plasmids encoding HIV gag-pol and VSV-G using Fugene-6 transfection reagent (Promega). The Fugene-6 reagent was used here due to its low cytotoxicity in these cells. Cell supernatants containing VSV-G coated Lib4pp were collected 48 hours later, filtered and stored at -80 °C. Since Huh-7.5 cells do not have high transfection efficiency, Lip4pp repackaged from Huh-7.5 cells need to be amplified prior to the next round of selection. Briefly, 293T cells were first transduced with ten-fold diluted Lib4pp. 48 hours later, these cells were transfected with plasmids encoding HIV gag-pol and VSV-G using Trans-IT LT1 transfection reagent (Mirus). Cell supernatants containing high titers of repackaged Lib4pp were collected 48 hours later, filtered and stored at -80 °C. This amplification step typically increases the lentiviral titer by ~100-fold. Recovered supernatants were titered in TZM-bl cells as described above and used for subsequent rounds of infection. After the final round of selection, viral RNA were isolated using RNeasy Mini Kit (Qiagen) and cDNA corresponding to the library fragment were amplified by RT-PCR (ImProm-II, Promega) using primers Lib4-F(5'-ACG GCC TCT AGA ATG AGC-3') and Lib4-R (5'- AGT GGC TAA GTC TAC AGC TG-3') . Amplified fragments were analyzed on a 1.5% agarose gel.

2.5.5 Immunofluorescent imaging and Western blotting

Huh 7.5 cells were seeded into wells of a glass chamber slide before being transduced with lentiviral pseudoparticles expressing Flag-tagged NS4Am-B1 and B1 (Constructs #3-4, Table 2.1). Two days post transduction, cells were fixed by incubating in PBS/2% PFA for 30 minutes at 4 °C, stained with mouse anti-Flag primary antibody (Genscript) and Alexa-Fluor 568-conjugated goat anti-mouse secondary antibody (Invitrogen), treated with anti-fade reagent (Promega) overnight and imaged using a Zeiss 510 Meta NLO Multiphoton microscope (Carl Zeiss Microscopy).

For Western blotting, these cells were lysed with Renilla luciferase assay lysis buffer (Promega) two days post transduction cells. Cell lysates were subsequently combined with an equal volume of 2X SDS loading buffer and heated at 95 °C for five minutes. Samples were separated on a SDS-PAGE (12% acrylamide) and transferred to a PVDF membrane. After transfer, the membranes were stained mouse anti-Flag primary antibody (Genscript) and HRP-conjugated donkey anti-mouse secondary antibody (Jackson ImmunoResearch), developed using West Pico Chemiluminescent HRP substrate (Pierce) and visualized in a ChemiDoc-It (UVP) chemiluminescence imager.

2.5.6 HCV infection assay

To confirm the anti-HCV activity of B1, Huh-7.5 cells were transduced with pLenti6-GFP/B1/NS4Am-B1pseudoparticles at low (<0.5) MOI, selected with blasticidin (10 µg/mL) for 8 days and infected with Jc1 Gluc HCVcc (MOI <0.1), H77pp (diluted 10-

fold) or VSV-Gpp (diluted 500-fold) for 12 hours. The cells were thoroughly washed with complete growth media to remove residual Gluc protein in the supernatant and the infection in each cell population was quantified by the amount of secreted Gluc in the supernatant 24 hours later.

2.5.7 HCV replication and translation assay

GFP or B1 construct expressing cells were electroporated with full length JC1 Gluc, or YSGR- JFH Gluc replicon(168) HCV RNA. At 5 hours post electroporation, HCV translation was quantified based on reporter Gluc activity in the cell supernatants (Figure 2.5C). 48 hours post electroporation, cells were harvested and intracellular HCV RNA levels as quantified by qRT-PCR as described previously(90) (Figure 2.5B).

2.5.8 SINV production and infection assay

Infectious SINV was generated and titered in BHK-J cells as described previously (184). Briefly, 1 x 10^7 BHK-J cells were suspended in 400 µl DPBS and electroporated with 3 µg SINV Toto1101 RNA(172) using an ECM 830 electroporator (Harvard Apparatus) at the following settings: 750 V, 99-µs pulse length, 5 pulses, 1.1-s interval. Cell supernatants were collected 24 hours post electroporation, filtered and stored at -80 °C. SINV titers were determined by infecting BHK-J cells with ten-fold serial dilutions of virus before carrying out a plaque assay 24 hours later.

To evaluate the ability of B1 to inhibit SINV, BHK-J cells were transduced with pV1-NS4Am-eGFP/B1 (Table 2.1, construct 1)-expressing pseudoparticles at MOI ~4. 48 hours later, these cells were infected overnight with SINV MOI ~10. Cell supernatants were collected 36 hours later upon cell lysis and the amount of infectious SINV in each supernatant were determined using plaque assays.

2.5.9 Protein sequences

Amino acids corresponding with the NS4Am sequence are highlighted in gray. Amino acids corresponding with the Flag tag used are highlighted in red.

(1) NS4Am-B1

MSTWVLAGGVLAAVAAYCLANWFKREQGRGAVHRGGAHPGRAGRRRKRPQ
VQRVRRGRGRCHLRQADPEVHLHHRQAARALAHPRDHPDLRRAVLQPLPRPHE
AARLLQVRHARRLRPGAHHLLQGRRQLQDPRRGEVRGRHPGEPHRAEGHRLQ
GGRQHPGAQAGVQLQQPQRLYHGRQAEERHQGELQDPPQHRGRQRAAHRPLP
AEHPHRRRPRAAARQPLPEHPVRPEQRPQREARSHGPAGVRDRRRDHSRHGRG
LN

(2) B1

MWFKREQGRGAVHRGGAHPGRAGRRRKRPQVQRVRRGRGRCHLRQADPEVH
LHHRQAARALAHPRDHPDLRRAVLQPLPRPHEAARLLQVRHARRLRPGAHHLL
QGRRQLQDPRRGEVRGRHPGEPHRAEGHRLQGGRQHPGAQAGVQLQQPQRLY

HGRQAEERHQGELQDPPQHRGRQRAAHRPLPAEHPHRRRPRAAARQPLPEHPV
RPEQRPQREARSHGPAGVRDRRRDHSRHGRGLN

(3) Flag-NS4Am-B1

MDYKDHDGDYKDHDIDYKDDDDKSTWVLAGGVLAAVAAYCLANWFKREQG
RGAVHRGGAHPGRAGRRRKRPQVQRVRRGRGRCHLRQADPEVHLHHRQAAR
ALAHPRDHPDLRRAVLQPLPRPHEAARLLQVRHARRLRPGAHHLLQGRRQLQD
PRRGEVRGRHPGEPHRAEGHRLQGGRQHPGAQAGVQLQQPQRLYHGRQAEER
HQGELQDPPQHRGRQRAAHRPLPAEHPHRRRPRAAARQPLPEHPVRPEQRPQRE
ARSHGPAGVRDRRRDHSRHGRGLN

(4) Flag-B1

MDYKDHDGDYKDHDIDYKDDDDKWFKREQGRGAVHRGGAHPGRAGRRRKR
PQVQRVRRGRGRCHLRQADPEVHLHHRQAARALAHPRDHPDLRRAVLQPLPRP
HEAARLLQVRHARRLRPGAHHLLQGRRQLQDPRRGEVRGRHPGEPHRAEGHRL
QGGRQHPGAQAGVQLQQPQRLYHGRQAEERHQGELQDPPQHRGRQRAAHRPL
PAEHPHRRRPRAAARQPLPEHPVRPEQRPQREARSHGPAGVRDRRRDHSRHGR
GLN

(5) NS4Am-B2

MSTWVLAGGVLAAVAAYCLANWFKREQGRGAVHRGGAHPGRAGRRRKRPQ
VQRVRRGRGRCHLRQADPEVHLHHRQAARALAHPRDHPDLRRAVLQPLPRPHE
AARLLQVRHARRLRPGAHHLLQGRRQLQDPRRGEVRGRHPGEPHRAEGHRLQ

(6) NS4Am-B3

MSTWVLAGGVLAAVAAYCLANWFKREQGRGAVHRGGAHPGRAGRRRKRPQ

VQRVRRGRGRCHLRQADPEVHLHHRQAARALAHPRDHPDLRRAVLQPLPRPHE

AARLLQVRHARRLRPGAHHLLQGRRQ

(7) NS4Am-B4

MSTWVLAGGVLAAVAAYCLANWFKREQGRGAVHRGGAHPGRAGRRRKRPQ

VQRVRRGRGRCHLRQADPEVHLHHRQAARALAHPRDHPDLRRAVLQPLPRPHE

AARLLQVRHARRL

(8) NS4Am-B5

MSTWVLAGGVLAAVAAYCLANWFKREQGRGAVHRGGAHPGRAGRRRKRPQ

VQRVRRGRGRCHLRQADPEVHLHHRQAARALAHPRDHPDLRRAVL

(9) NS4Am-B6

MSTWVLAGGVLAAVAAYCLANWFKREQGRGAVHRGGAHPGRAGRRRKRPQ

VQRVR

(10) +36GFP

MGHHHHHHGGASKGERLFRGKVPILVELKGDVNGHKFSVRGKGKGDATRGKL

TLKFICTTGKLPVPWPTLVTTLTYGVQCFSRYPKHMKRHDFFKSAMPKGYVQE

RTISFKKDGKYKTRAEVKFEGRTLVNRIKLKGRDFKEKGNILGHKLRYNFNSHK

VYITADKRKNGIKAKFKIRHNVKDGSVQLADHYQQNTPIGRGPVLLPRNHYLST
RSKLSKDPKEKRDHMVLLEFVTAAGIKHGRDERYK

2.5.10 Cloning

All constructs used in this study are listed in Table 2.1. The 800 bp fragment shown in Figure 2.2C was gel purified and named NS4Am-B1 DNA for convenience. To generate pV1-B1 (construct 2), the B1 sequence was PCR amplified from the NS4Am-B1 DNA template using primers XbaI-B1-F (5'-CAT ACT TCT AGA ATG TGG TTT AAA CGT GAG CAA GG-3') and Lib4-R. The PCR product was digested with XbaI and XhoI before ligation into the pV1 vector.

To generate pLenti6-NS4Am-B1 the NS4Am-B1 sequence was amplified from the pv1-NS4Am-B1 construct using primers BamHI-Lib4-F (5'- CAT ACT GGA TCC ATG TGG TTT AAA CGT GAG CAA GG-3') and Lib4-R. Similarly to generate pLenti6-B1, the B1 sequence was PCR amplified from the NS4Am-B1 DNA template using primers BamHi-Lib4-F and Lib4-R. PCR products were digested with BamHI and XhoI before ligation into the pLenti6 vector.

To generate pV1-NS4Am-B2, pV1-NS4Am-B3, pV1-NS4Am-B4, pV1-NS4Am-B5 and pV1-NS4Am-B6 (constructs 5-9), the sequences were each PCR amplified from the NS4Am-B1 DNA using forward primer Lib4-F and reverse primers: B2-R (5'-GAT ATG CTC GAG CTA TTG AAG TCG ATG CCC TTC-3'); B3-R (5'-GAT ATG CTC GAG CTA TTG CCG TCG TCC TTG A-3'); B4-R (5'-GAT ATG CTC GAG CTA

TAG TCT TCG GGC ATG G-3'); B5-R (5'-GAT ATG CTC GAG CTA AAG CAC TGC ACG CCG TA-3'); B6-R (5'-GAT ATG CTC GAG CTA CCG GAC ACG CTG AAC TT-3') respectively. The PCR products were digested with XbaI and XhoI before ligation into the pV1 vector.

To generate pZsGreen-NS4Am-B1 (construct 3), the Flag-NS4Am-B1 sequence was PCR amplified from the NS4Am-B1 DNA using a forward primer Flag-NS4Am-B1-F (5'- CATGATTCTAGAATG GACTACAAAGACGACGACGACAAG AGCACGTGGGTCCTAGCT-3'), containing the Flag-tag sequence at the 5' end, and reverse primer B1-BamHI-R (5'- GTA TAG GGA TCC AGT GGC TAA GTC TAC AGC TG-3'). Similarly to generate pZsGreen-Flag-B1, the Flag-B1 sequence was amplified from the NS4Am-B1 DNA using a forward primer Flag-B1-F (5'-CATGATTCTAGAATG GACTACAAAGACGACGACGACAAG TGGTTTAAACGTGAGCAAGGG-3'), that added the Flag-Tag sequence to the 5' end of the gene and reverse primer B1-BamHI-R. PCR products were digested with XbaI and BamHI before ligation into the pZsGreen vector (185), resulting in pZsGreen-Flag-NS4Am-B1 and pZsGreen-Flag-B1. The pZsGreen lentiviral vector expresses the target gene and the GFP reporter as a single mRNA controlled by a CMV promoter. In ZsGreen the target gene translation is controlled by the 5'cap, while the GFP reporter translation is controlled by an EMCV IRES.

To generate pv1-+36 GFP (construct 10), the +36GFP was PCR amplified from the pET-+36GFP plasmid (a generous gift from David Liu (Harvard University)) using forward primer +36GFP-F (5'- GCG TAG AGG ATC GAG ATC TC-3') and reverse primer +36GFP-R (5'- CTC AAG ACC CGT TTA GAG GC-3'). The PCR product was digested with XbaI and XhoI before ligation into the pV1 vector.

2.5.11 Protein expression and purification

BL21 (DE3) cells were transformed with the expression plasmid and plated on a Luria–Bertani (LB) agar plate containing 100 µg/mL ampicillin. The next day, a single colony was picked and cultured at 37°C with shaking at 250 rpm. At OD_{600} ~0.6, the cells were cooled to 18°C and isopropyl β–D–1–thiogalactopyranoside (IPTG, 0.5 mM) was added to the culture to induce protein expression. After overnight expression (~18 hours) at 18°C, cells were harvested by centrifugation at 6000 x g and 4°C for 20 minutes and pellets were stored at –80 °C until use.

For recombinant protein purification, cell pellets were resuspended in lysis buffer (500 mM NaCl, 50 mM Tris, pH 8, 10 mL per 1 g wet cell pellet), and disrupted by sonication on ice (QSonica Misonix 200 (Qsonica), 1 second pulse 6 second pause for 3 minutes 10 amp). Whole cell lysate was clarified by centrifugation at 20,000 *x g* for 20 minutes at 4°C. Soluble cell lysates were loaded onto 5 mL Ni–NTA agarose beads (Qiagen). For constructs expressing B1 or +36GFP, the loaded resin was washed with lysis buffer supplemented with 150 mM imidazole and the product was eluted in lysis buffer

supplemented 500 mM imidazole. For all other constructs the loaded resin was washed with lysis buffer supplemented with 50 mM imidazole and the product was eluted in lysis buffer supplemented 150 mM imidazole. Purified protein samples were dialyzed overnight at 4°C into Buffer A (2 M NaCl, 2.7 mM KCl, 10 mM $Na_2HPO_4.2H_2O$, 2 mM KH_2PO_4, pH 7.4). +36GFP was further purified by cation exchange chromatography using a GE HiTrap SP HP column (GE Biosciences, PA). Dialyzed proteins were diluted 1:5 into PBS to reduce the salt concentration and then loaded onto the SP column. The column was washed with Buffer B (0.5 M NaCl, 2.7 mM KCl, 10 mM $Na_2HPO_4.2H_2O$, 2 mM KH_2PO_4, pH 7.4) and the target protein was eluted in Buffer A. Purified proteins were concentrated via ultracentrifugation through an Amicon 10 kDa MWCO centrifugal column (EMD Millipore). The final protein concentrations were determined using a Pierce Coomassie Plus Protein Assay Kit (Thermo Fisher Scientific).

3. RECOMBINANT B1 IS A CELL-TRANSDUCING PROTEIN

3.1 Overview

In this section we describe a new cell-penetrating protein, B1, capable of delivering conjugated proteins and nucleic acids into mammalian cells. B1 is a 244-amino-acid product of a single-base frameshift in the gene encoding enhanced green fluorescent protein (eGFP). The molecule has a net positive charge of 43 and a very high charge-to-mass ratio of 1.5. eGFP-fused B1 potently penetrates both adherent and suspension cells with >80% of cells taking up the protein when exposed to concentrations as low as 1 μM. The protein was found to cluster in the paranuclear region of TZM-bl cells. Most importantly, we show that B1 not only facilitates cellular uptake, but allows biomolecular cargo to reach sites of biological relevance. For example, baby hamster kidney cells underwent DNA recombination when exposed to B1-tagged Cre recombinase at protein concentrations as low as 2.5 μM, indicating potent nuclear delivery of functional protein cargos. Additionally, B1 delivers non-covalently conjugated RNA and DNA across the cell membrane to cytosolic and nuclear sites accessible to the cellular translation and transcription machinery, as gauged by detection of encoded reporter functions, with efficiency comparable to commercially available cationic lipid reagents. B1 appears to utilize cell-surface glycans and multiple competing endocytic pathways to enter and traffic through cells. These studies provide both a new tool for intracellular delivery of biomolecules and insights that could aid in the design of more effective cell penetrating proteins.

3.2 Introduction

Intracellular targeting of large therapeutic biomolecules poses a significant challenge. Effective delivery entails not only crossing the outer cell membrane but transport and release of therapeutic cargo to cellular loci conducive to attainment of the therapeutic effect. Several lipid-, polymeric- and inorganic-based vehicles for intracellular delivery of proteins and nucleic acids exist, including cationic lipids (100-102), polyethylenimine (PEI) (103, 104), carbon nanotubes (105-107), gold nanoparticles (108-110), highly charged green fluorescent protein (GFP) (126, 186) and nanocapsules (111, 112). However, the field of intracellular delivery of large molecules is still in its infancy and major strides need to be made both in effectiveness of delivery and our understanding of the underlying mechanisms before this approach can be used in the clinic.

The first cell penetrating polypeptide (CPP) identified was the HIV Tat protein, which is able to enter cells and translocate into the nucleus (113). The Tat protein transduction domain has been fused to many target proteins to mediate cellular delivery (117-120). Since then, a number of natural proteins have been found to have the capacity to penetrate cells, including the Antennapedia protein (Antp) from Drosophila (121, 122), VP22 protein from herpes simplex virus (123) and CaP from *Brome mosaic virus*(124). Similarly, several artificial CPPs have been created for protein and nucleic delivery, including highly positively charged peptides and proteins (e.g. poly arginine (125), supercharged +36 GFP (126) and related proteins (127)) and amphipathic peptides (e.g. Pep–1 (128), CADY (129)). The cellular uptake mechanism of these CPPs is not yet

fully understood, but many are believed to be internalized through endocytic pathways (130, 131).

In this section, we describe the cell penetrating ability of B1. This study evaluates the effectiveness of B1 as a vehicle for intracellular delivery of two types of biomolecular payloads – genetically fused proteins and non-covalently conjugated nucleic acids. We demonstrate that B1 not only potently mediates cellular uptake of large molecules, but delivers the cargo to biologically relevant cellular sites. To our knowledge, the efficiency of mRNA delivery mediated by B1 is the highest reported for CPPs to date and is comparable to that mediated by commercially available cationic lipids. The ability of B1 to effectively deliver functional cargo to the cytosol may at least facilitate its use in *in vitro* stem cell engineering for which it is desirable to transiently deliver transcription factor(s) to cells to achieve cell fate reprograming(187).

This study also provides insights into the mechanism of cell penetration by B1. We show that (1) cell-surface glycans and several cellular endocytic pathways play a role in cellular entry and cargo delivery by B1, and (2) the contribution of specific endocytic pathways to cellular entry versus functional cargo delivery by B1 can be significantly different. B1 penetrates cells through a mechanism distinct from that of another high-positive-charge protein +36GFP as gauged from intracellular distribution and time-/temperature-dependent cell penetration profiles. Thus, B1 represents a complementary addition to the current toolkit for intracellular delivery.

3.3 Results

3.3.1 B1 penetrates mammalian cells and mediates cellular uptake of conjugated proteins

Testing the cell transduction potential of B1 required the expression and purification of the recombinant protein. 6xHis-tagged B1 (6H-B1, Table 3.1) was expressed as a soluble protein in *E. coli* BL21(DE3) cells and purified via one-step immobilized-metal affinity chromatography (IMAC), although a very high concentration of imidazole (0.5–1 M) is needed to elute resin-bound B1 (Figure 3.1A). The yield of purified 6H-B1 was ~4 mg per liter of *E. coli* culture, with an estimated purity > 90%. To remove excess imidazole, 6H-B1 was dialyzed in a modified PBS containing an increased concentration of NaCl (2 M NaCl, 2.7 mM KCl, 10 mM KH_2PO_4, 10 mM Na_2HPO_4, pH 7.4). Dialysis of purified 6H-B1 in unmodified PBS (containing 137 mM NaCl) yielded significant amounts of white precipitate in the dialysis tubing. Dialyzed 6H-B1 can be stored at 4°C for up to 2 weeks without significant loss of protein activity, or at -80°C.

To enable detection of intracellular B1, we fused the globular protein eGFP to the N-terminus of B1 via a flexible linker to form GFP-L-B1 (Table 3.1). We purified GFP-L-B1 by one-step IMAC, akin to our purification of B1 (Figure 3.1B). However, we noted the co-purification of a band at ~38 kDa that is presumed to be a truncation of 6 His tagged-GFP and part of the N terminal region of B1. Purified GFP-L-B1 exhibited greatly improved stability compared to B1. The purified protein can be easily dialyzed

with minimal precipitation and the dialyzed protein can be stored at 4°C for a few months without loss of activity. GFP-L-B1 is non-toxic to mammalian cells (Figure

Number	Short Name	Short sequence	Molecular weight (kDa)
1	6H-B1	HHHHHH-B1	30.3
2	GFP-L-B1	HHHHHH-GFP-2X(GGGGS)-B1	60.2
3	GFP-L-B1-F	HHHHHH-GFP-2X(GGGGS)-B1(F)	41.5
4	GFP-L-B1-M	HHHHHH-GFP-2X(GGGGS)-B1(M)	41.2
5	GFP-L-B1-R	HHHHHH-GFP-2X(GGGGS)-B1(R)	38.7
6	mCherry-L-B1	HHHHHH-mCherry-8X(GGS)-B1	58.9
7	mCherry-L-R10	HHHHHH-mCherry-8X(GGS)-10X(R)	32.4
8	mCherry-L-TAT	HHHHHH-mCherry-8X(GGS)-TAT(ptd)	32.2
9	Cre-L-B1	HHHHHH-Cre-8X(GGS)-B1	72.2
10	Cre-L-R10	HHHHHH-Cre-8X(GGS)-10X(R)	43.4

Table 3.1. Protein constructs used in this section.

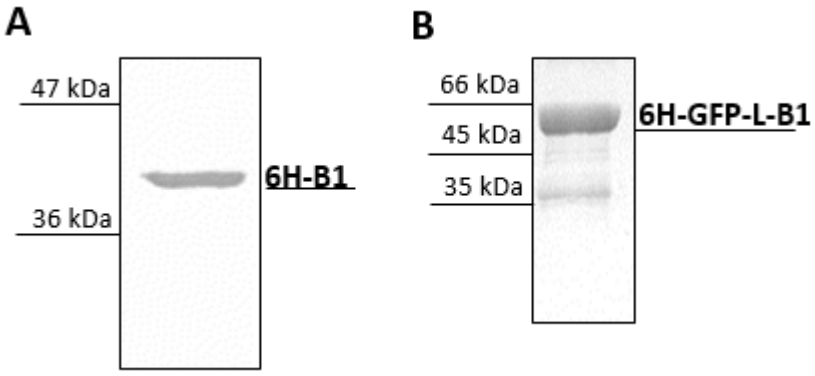

Figure 3.1. Purification of recombinant B1. A. E. coli expressing recombinant 6H-B1 were suspended in lysis buffer (500 mM NaCl, 50 mM Tris at pH 8) and lysed using French press (model number). The soluble lysate containing 6H-B1 was loaded onto a Ni-NTA agarose column. Impurities were removed by extensive washing with Lysis Buffer supplemented with 150 mM imidazole. 6H-B1 was eluted from the column with lysis buffer supplemented with 0.5 M imidazole. The purified protein was analyzed on SDS-PAGE gel (12 % acrylamide) **B.** E. coli expressing recombinant 6H-GFP-L-B1 were suspended in lysis buffer (500 mM NaCl, 50 mM Tris at pH 8) and lysed using French press (model number). The soluble lysate containing 6H-B1 was loaded onto a Ni-NTA agarose column. Impurities were removed by extensive washing with Lysis Buffer supplemented with 150 mM imidazole. 6H-B1 was eluted from the column with lysis buffer supplemented with 0.5 M imidazole. The purified protein was analyzed on SDS-PAGE gel (12 % acrylamide).

3.2). TZM-bl cells were incubated with 2 µM GFP-L-B1 at 37°C and 5% CO_2 for different amounts of time. After incubation, cells were treated with 0.04% Trypan Blue for two minutes to completely quench the signal from extracellular GFP (188), digested with 0.25% trypsin-EDTA for five minutes to completely remove the extracellular GFP and analyzed by flow cytometry (Figure 3.3A). GFP-L-B1 was found to rapidly and efficiently enter TZM-bl cells.

Two major differences were noticed between cells that had taken up GFP-L-B1 (+charge:MW ratio of 1.5) and those that had taken up the supercharged +36GFP

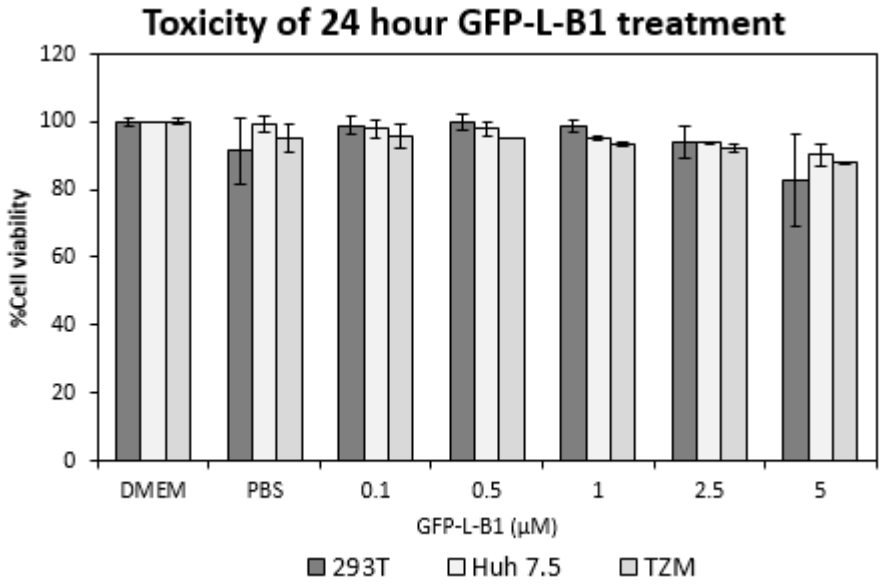

Figure 3.2. Cytotoxicity of GFP-L-B1 transduction. 293T, TZM and Huh 7.5 cells were seeded into 96 well plates at 2 x 10^4, 1.8 x 10^4 and 2 x 10^4 cells per well respectively. The next day, cells were washed with 100 µl OptiMEM before being treated with 0-5 µM GFP-L-B1, diluted in OptiMEM. 24 hours later, the relative cell viability was quantified using the CellTiter-Glo assay kit following the manufacturer's protocol.

(+charge:MW ratio of 1.3): (1) Fluorescence intensity. +36GFP-positive cells exhibited a much higher (up to 50-fold) fluorescence intensity on average than GFP-L-B1-positive cells (Figure 3.3A). (2) Intracellular distribution. Unlike +36GFP, which accumulated evenly in a large number of tiny, endosomal compartments, as gauged by the appearance of finely spotted cells, intracellular GFP-L-B1 was found to accumulate in much larger intracellular clusters in one subpopulation of cells while exhibiting an even diffuse distribution in another subpopulation (Figure 3.3B). Confocal microscopy confirmed that large GFP-L-B1 clusters formed in the paranuclear region of cells (Figure 3.3C).

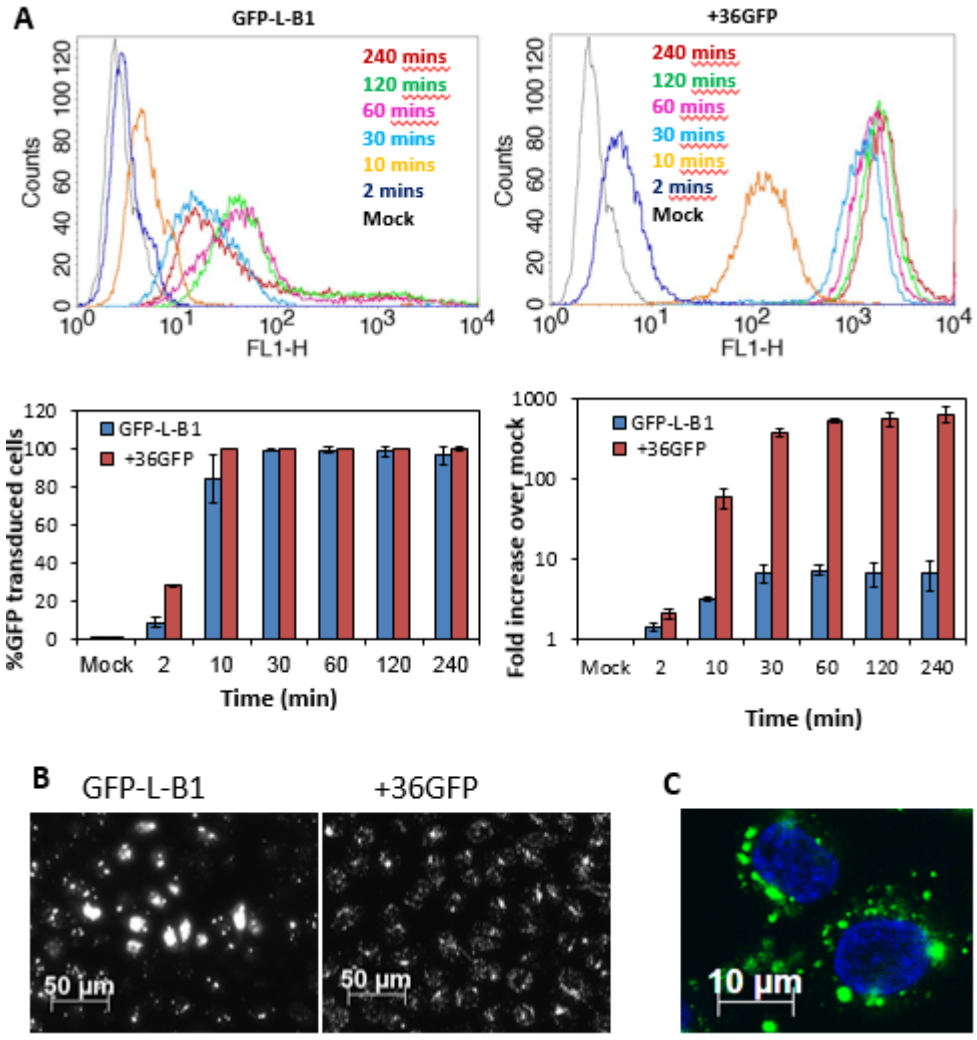

Figure 3.3. B1 mediates cell transduction. A. Flow cytometry analysis of TZM-bl cells incubated with GFP-L-B1 (2 µM)or +36GFP (2 µM) at 37 °C for indicated times. **B**. Fluorescent microscope images of TZM-bl cells treated with 2 µM of GFP-L-B1 or +36GFP at 37 °C for 1 hour. Cells were washed with PBS containing 0.04% trypan blue prior to imaging. **C**. Confocal microscopic image of TZM cells treated with 2 µM GFP-L-B1 at 37 °C for 1 hour. Cell nuclei were stained with DAPI (blue).

We also determined the ability of B1 to deliver covalently attached mCherry protein (32 kDa) (189) into different cell types and evaluated B1 against other known cell-penetrating

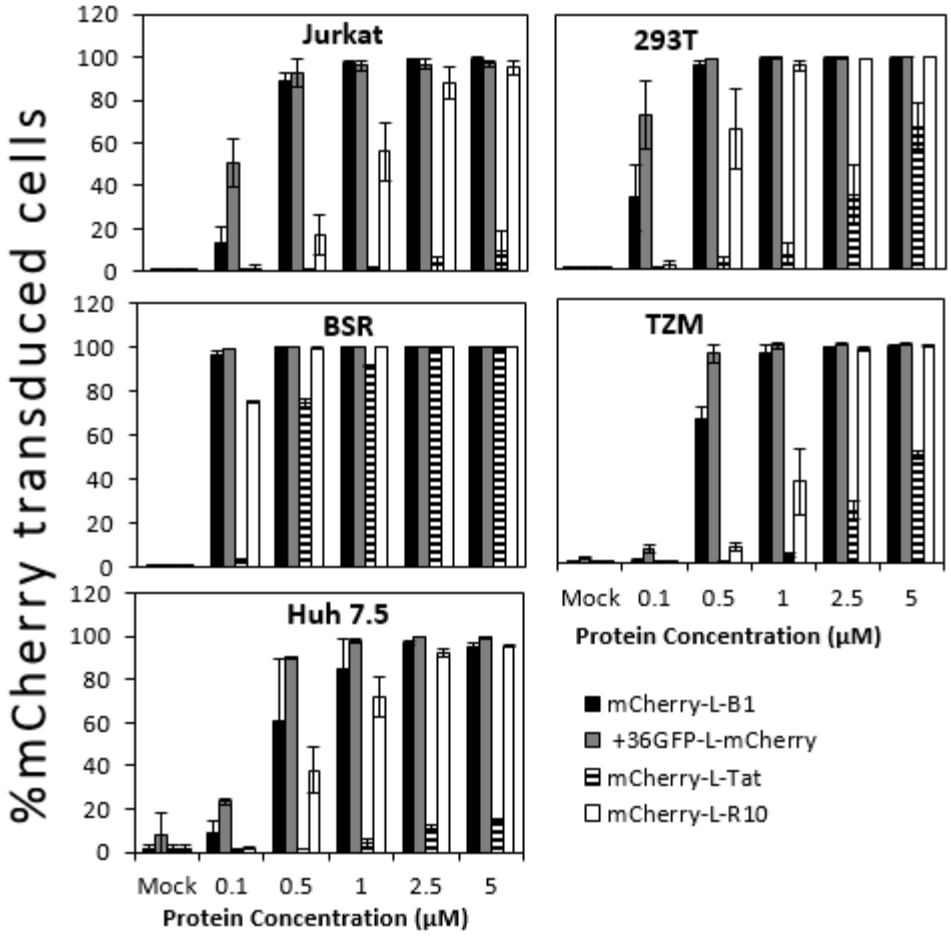

Figure 3.4. B1 mediated mCherry transduction in selected cell lines. Jurkat, 293T, BSR, TZM, or Huh 7.5 cells were treated with the indicated mCherry-protein fusions for 4 hours at 37 °C, prior to trypsin digestion and flow cytometry. Error bars represent the standard deviation of two independent experiments.

proteins/peptides. mCherry was attached to the N-terminus of B1, supercharged +36GFP, Tat and R10 (deca-arginine) via a flexible linker (Table 3.1). As shown in Figure 3.4, 80-100% of all the target cells take up mCherry-L-B1 when exposed to a protein concentration as low as 1 μM. The potency of B1-mediated delivery of mCherry into cells was comparable to R10 and +36GFP and significantly higher than Tat.

3.3.2 Abbreviated forms of B1 yield significantly weakened cell penetration

We sought to determine whether B1's cell penetration functionality could be traced to a specific region of the protein. B1 was segmented into three non-overlapping fragments that avoid the disruption of predicted structural motifs, named B1-F, B1-M, and B1-R (Figure 3.5A). As shown in the table at the bottom of Figure 3.5A, each segment comprises approximately one third of the mass of B1 and possesses a charge:MW ratio similar to the parental B1 (Figure 3.5B). Each segment was fused to the C-terminus of eGFP via a flexible linker (Table 3.1) and the ability of TZM-bl cells to take up these constructs was measured. All three segments of B1 mediated cell penetration, with >80% of cells taking up the proteins at 5 μM exposure (Figure 3.5B). However, the cell penetration potency of these abbreviated forms of B1 is significantly lower than that of full-length B1. It is noteworthy that, compared to B1-R, B1-M possesses a lower charge:kDa ratio but exhibits a higher cell penetration potency.

3.3.3 B1-delivered proteins are able to access the cytosol and nucleus

Many cellular functions require proteins to be able to access the cytosol or nucleus. The punctate subcellular distribution of GFP-L-B1 (Figure 3.3C) raised the concern that B1 may be trapped in subcellular compartments, without access to sites critical for cellular functions. To address this concern, we performed two major studies. The first study evaluated B1-mediated nuclear transport of protein cargo by measuring the ability of a B1-delivered recombinase to mediate DNA recombination. The second major study evaluated the ability of two types of nucleic acids – mRNA and DNA – to undergo processing by the cell's transcription/translation machinery in the cytosol (mRNA) and nucleus (DNA).

For the nuclear transport study, B1 was used to deliver covalently conjugated Cre recombinase into BSR.LNL.tdTomato cells (186). BSR.LNL.tdTomato cells contain two loxP recombination sites upstream of the reporter gene tdTomato, causing the gene to be silenced (189). Reporter gene expression is triggered by Cre-mediated DNA recombination (186). Cre fusions to B1 and R10 used in this study are depicted in Table 3.1. A comparable extent of transfection was observed with +36GFP-L-Cre, Cre-L-B1 and Cre-L-R10 based on fluorescence microscopic analysis (Figure 3.6A). We were unable to quantify the percentage of activated (tdTomato-expressing) cells in the +36GFP-L-Cre-exposed cell population via flow cytometry due to significant overlap in the fluorescence spectra of GFP and tdTomato (189, 190). Over 70% of cells were activated after exposure to 2.5 μM Cre-L-B1 or Cre-L-R10 (Figure 3.6B). As with

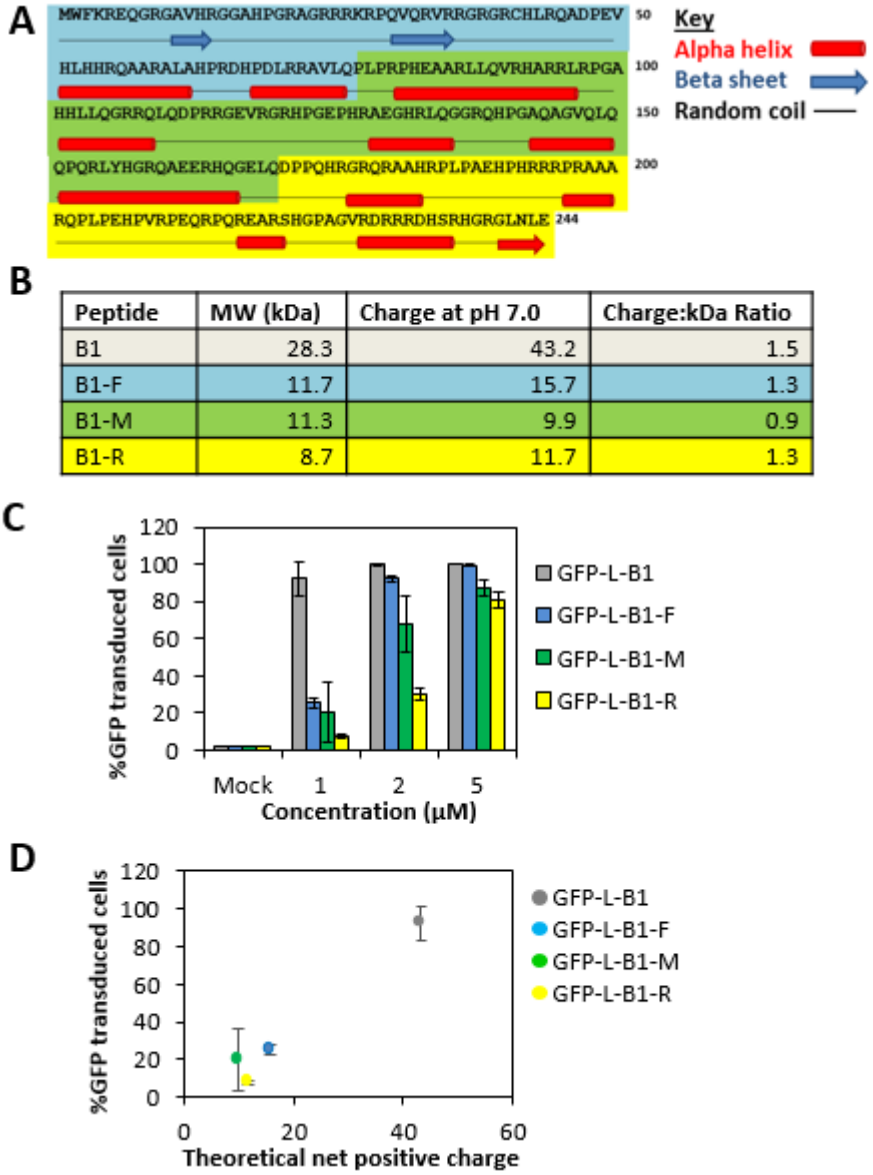

Peptide	MW (kDa)	Charge at pH 7.0	Charge:kDa Ratio
B1	28.3	43.2	1.5
B1-F	11.7	15.7	1.3
B1-M	11.3	9.9	0.9
B1-R	8.7	11.7	1.3

Figure 3.5. Transduction efficiency of truncated B1. A. B1 protein sequence including truncations resulting in B1-F (blue), B1-M (green), B1-R (yellow). Structural motifs were predicted using the GOR4 algorithm. **B.** Table showing the molecular weight and charge of B1 truncations. **C, D.** TZM cells were treated with the indicated GFP-protein fusions at 1, 2, 5 µM (C) or 1 µM (D) for 4 hours at 37 °C, prior to trypsin digestion and flow cytometry. The full length B1 mediates the most efficient GFP transduction. Error bars represent the standard deviation of two independent experiments.

+36GFP (186), chloroquine significantly enhanced Cre-induced recombination, particularly at low protein concentrations (Figure 3.6B). Chloroquine is a known inhibitor of lysosomal protein degradation (191) and likely extends the residence time of Cre fusion proteins in endosomes, allowing for increased escape.

We next determined the ability of B1 to transport conjugated nucleic acids to cytosolic and nuclear sites accessible to the cell's transcription/translation machinery, as assessed by the measurement of encoded reporter functions. To do this, we used two reporter constructs as payloads – the mRNA pIRF (3 kb) and the plasmid DNA pCMV5-Gluc (5.2 kbp). pIRF is a bicistronic mRNA containing a firefly luciferase (Fluc) gene expressed via cap-dependent translation and a Renilla luciferase (Rluc) gene expressed via the incorporated internal ribosome entry site (IRES) of hepatitis C virus (192). Only the Fluc reporter was quantified in this study. pCMV-Gluc encodes a *Gaussia* luciferase gene under the control of a CMV promoter (193). In this experiment and other studies described in this paper, GFP-L-B1 and not B1 was used as the CPP because of difficulties in obtaining large amounts of highly pure B1 protein. As seen in Figure 3.7A, GFP-L-B1 is able to bind pIRF mRNA, as gauged by the decreasing intensity of the mRNA band at increasing protein:mRNA molar ratios. At B1:pIRF molar ratios at and above 500, the mRNA was not able to migrate into the gel at all, indicating supershift of the mRNA. Similarly, B1 forms complexes with linearized plasmid DNA, although at a higher B1:nucleic acids ratio (Figure 3.7A). The higher molar ratio of B1 needed for DNA gel-shift likely derives from the larger molecular weight of the DNA.

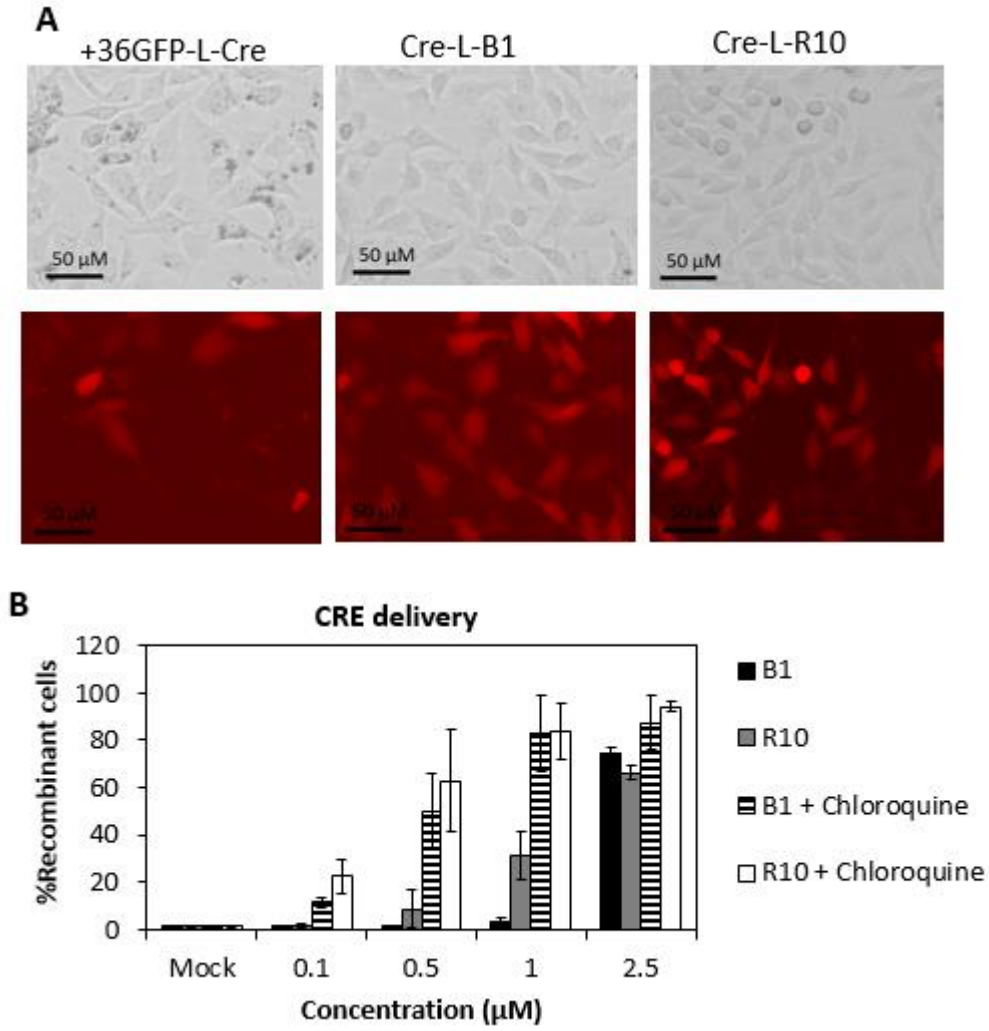

Figure 3.6. B1 mediated cytosolic delivery of Cre. A. Brightfield and fluorescent images of BSR.LNL.td.Tomato reporter cells 24 hours after transduction with 2.5 µM Cre-L-B1, Cre-L-R10 and +36GFP-L-Cre. **B.** Delivery of active CRE recombinase by B1 and R10 into BSR.LNL.td.Tomato reporter cells. Cells were treated with indicated concentrations of B1 or R10 in the presence or absence of 100 µM chloroquine for six hours at 37 °C. Chloroquine enhanced the delivery of active Cre into the cytosol at lower protein concentrations. Error bars represent the standard deviation of two independent experiments.

Each pCMV5-Gluc DNA molecule has approximately 3 times the number of nucleotides as pIRF mRNA. It is also possible that B1 interacts more strongly with single-stranded RNA than double-stranded DNA.

To determine the ability of B1 to transport nucleic acids to cytosolic sites accessible to the cell's transcription/translation machinery, 1000:1 mixtures of either GFP-L-B1:pIRF or GFP-L-B1:pCMV5-Gluc were incubated with 293T cells for 6 hours. Our rationale for using a higher ratio of protein to nucleic acids than the minimum amount required for gel-shift was that each RNA/DNA molecule needs to form a complex with multiple B1 proteins in order to be functionally delivered into cells (194). The activities of Fluc and Gluc deriving from intracellularly processed pIRF RNA (cytosol) and pCMV5-Gluc DNA (nucleus) were quantified several hours following exposure to cell penetration constructs. As a control, the same amounts of mRNA or DNA were transfected into 293T cells using commercially available cationic lipid reagents according to the manufacturers' protocols. As shown in Figure 3.7B, the efficiency of B1-mediated mRNA transfection is comparable to that obtained with the commercially available reagents TransMessenger and Lipofectamine 2000. Although +36GFP has been reported to support RNA interference by efficient delivery of siRNA (126), we found that exposure of 293T cells to +36GFP-conjugated pIRF reporter RNA did not yield a detectable Fluc reporter signal despite multiple attempts using different batches of purified proteins. The reason for this apparent discrepancy is unclear, but may derive from the much larger size of pIRF RNA (3 kb) relative to siRNA (22 bp).

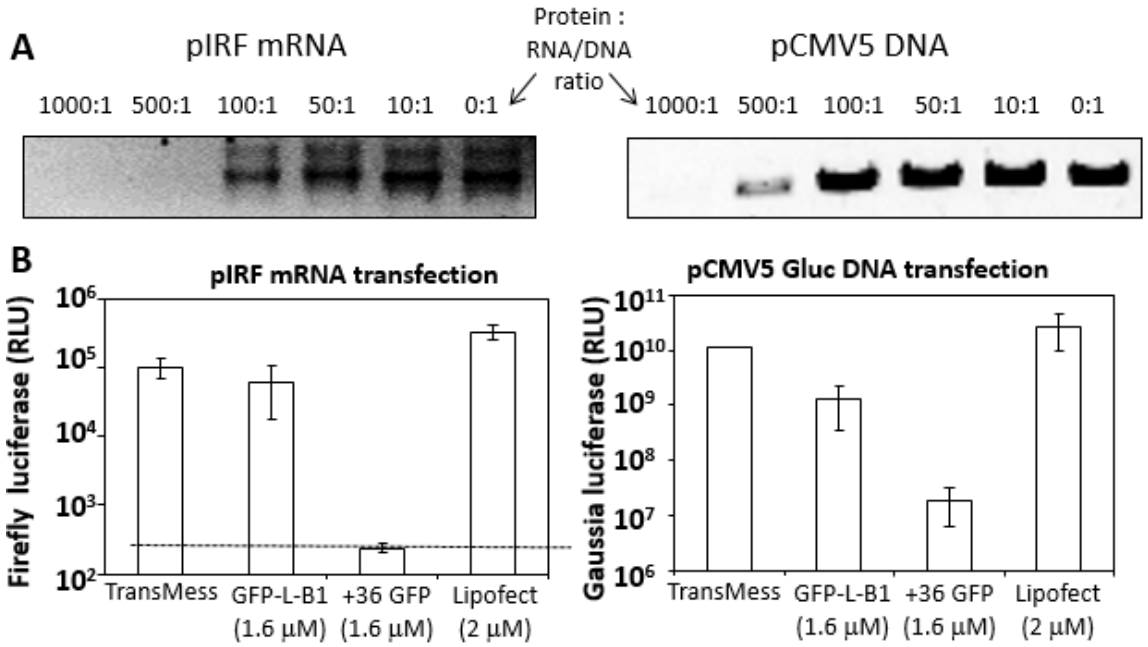

Figure 3.7. B1 mediated cytosolic delivery of RNA, DNA and proteins. (A) Gel-shift assays of GFP-L-B1 conjugated DNA/RNA. pIRF RNA (43 femto moles) or linearized pCMV5 DNA (14.5 femto moles) were incubated with B1 protein at the indicated molar ratios in EMSA buffer for 10 minutes at room temperature analyzed on an agarose gel (0.8 %). **(B)** 293T cells were transfected with 1.6 nM of pIRF mRNA/linearized pCMV5-Gluc DNA using GFP-L-B1, +36GFP or the indicated commercial reagents according to manufacture protocol. TransMess: TransMessenger. Lipofec: Lipofectamine. Error bars represent the standard deviation from 2 independent experiments.

Although +36GFP has been reported to support RNA interference by efficient delivery of siRNA (126), we found that exposure of 293T cells to +36GFP-conjugated pIRF reporter RNA did not yield a detectable Fluc reporter signal despite multiple attempts using different batches of purified proteins. The reason for this apparent discrepancy is unclear, but may derive from the much larger size of pIRF RNA (3 kb) relative to siRNA (22 bp). Another possible explanation is that pIRF RNA may interact with +36GFP in a way that inhibits its translation. DNA transfection mediated by GFP-L-B1 is 10-20-fold

weaker than that mediated by TransIT and Lipofectamine 2000, and ~100-fold stronger than that mediated by unmodified +36GFP (Figure 3.7C). It has previously been reported that the ability of free +36GFP to transport DNA into the nucleus is poor (126). However, +36GFP attached to a fusion peptide derived from hemagglutinin (126)can transfect DNA with similar efficiency as Lipofectamine (126). It is possible that an even higher DNA transfection efficiency can be achieved when B1 is fused to the same fusion peptide.

3.3.4 B1 penetrates and traffics through cells via multiple endocytic pathways

We attempted to elucidate the mechanism through which B1 penetrates cells. We first quantified cell penetration by GFP-L-B1 at different temperatures. As seen in Figure 3.8A, although cell penetration by GFP-L-B1 is significantly weaker at lower temperatures all cells are able to take up GFP-L-B1 even at 4°C. This result indicates that B1 can penetrate cells in a temperature-independent manner.

To determine the role of different cellular endocytic pathways in cell transduction by B1, we evaluated cellular uptake of GFP-L-B1 in the presence of selected inhibitors of macropinocytosis, clathrin-mediated endocytosis, mannan receptor-dependent phagocytosis, and caveolin-mediated endocytosis. No significant reduction in GFP-L-B1 uptake was observed in the presence of any of the inhibitors in either 293T or TZM-b1 cell line (Figure 3.8B), suggesting that any one of these pathways alone is not critical for GFP-L-B1 uptake by cells. In fact, GFP-L-B1 uptake by TZM-bl cells appeared to be

somewhat enhanced by the macropinocytosis inhibitor amiloride (195) and clathrin-mediated endocytosis inhibitor dynasore (196), and dramatically enhanced by chlorpromazine, another inhibitor of clathrin-mediated endocytosis (197) (Figure 3.8B, C). This result indicates that macropinocytosis and clathrin–mediated endocytosis may be "weak links" for cell transduction by B1 that obstruct B1–mediated protein entry through other, more energetically favorable pathways.

The monitoring of green fluorescent cells following exposure of cells to GFP-L-B1 provides a measure of cellular uptake of protein from the surroundings but does not provide information on its intracellular fate.

We therefore sought to investigate the ability of cellular endocytic pathways to support the B1-mediated transport of an mRNA payload to sites accessible to the cell's translation machinery. 293T cells were exposed to pIRF-mRNA-conjugated GFP-L-B1 in the presence of endocytic inhibitors. In contrast to the data shown in Figure 3.8B, RNA transfection efficiency was significantly reduced by inhibitors of clathrin-mediated endocytosis (chlorpromazine, dynasore) and mannan receptor-dependent phagocytosis (100 μg/ml mannan (198)) (Figure 3.8D).

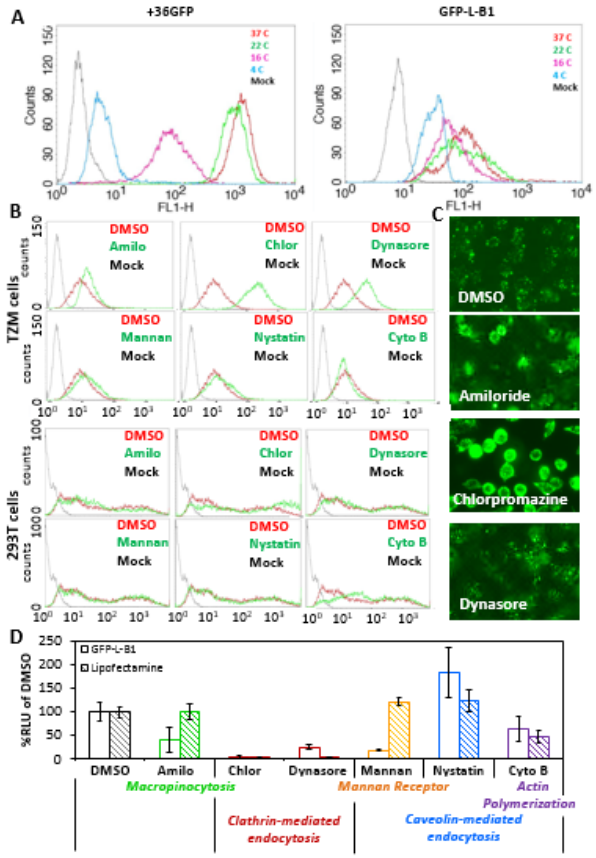

Figure 3.8. B1 enters/traffics through cells using multiple endocytic pathways. The ability of these pathways to mediate cellular uptake does not correlate with the ability to support payload delivery to sites where bioactivity can be realized. **A.** Effect of temperature on cellular internalization of B1. TZM-bl cells were incubated with 2 µM GFP-L-B1 or 2 µM +36GFP at 4, 16, 22 or 37°C for one hour, washed with DPBS containing 0.04% Trypan Blue to quench extracellular GFP and analyzed by flow cytometry. **B.** Role of different endocytic pathways in cellular uptake of B1. TZM-bl or 293T cells were pretreated with the endocytic inhibitors amiloride (5 mM) (195), chlorpromazine (55 µM) (197), dynasore (50 µM) (196), mannan (100 µg/ml) (198), nystatin (50 nM) (199) or cytochalasin B (4 µM) for one hour prior to the addition of GFP-L-B1 (2 µM). Part (D) indicates the endocytic pathways inhibited by these small molecules. One hour later, these cells were washed with DPBS containing 0.04% Trypan Blue and analyzed by flow cytometry. **C.** Fluorescence microscopic images of TZM-bl cells transfected with GFP-L-B1 in the presence of the indicated inhibitors. Data is representative of 4 independent experiments. **D.** Role of different endocytic pathways in supporting B1-mediated functional delivery of a RNA payload. 293T cells were pretreated with the indicated inhibitors for 1 hour prior to pIRF mRNA transfection using GFP-L-B1 or Lipofectamine 2000. The activity of Fluc deriving from translation of the delivered RNA was measured 6 hours post transfection. Error bars represent the standard deviation of two independent experiments.

Since cells are able to take up GFP-L-B1 even at 4°C and its transduction cannot be blocked by inhibiting known endocytic pathways, it is possible that B1 can penetrate cells in a temperature-independent mode. This observation raises the possibility that B1 could permeabilize the cell membrane to facilitate uptake. To evaluate the permeability of B1, we treated TZM-bl cells with the membrane-impermeable dye propidium iodide in the presence of GFP-L-B1 (Figure 3.9) (200). Intracellular propidium iodide was not detected in the presence of B1, indicating that B1 does not permeabilize cell membranes.

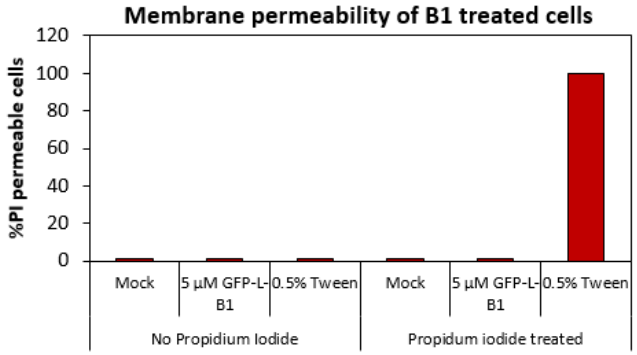

Figure 3.9. Cell membrane permeability of B1 treated cells. TZM cells were seeded into 24 well plates at 1.5 x 10^5 cells per well. The next day cells were washed once with OptiMEM before treatment with 5 µM GFP-L-B1 or 0.5% Tween for one hour at 37 °C in the presence of 3 ng/ml propidium iodide. After treatment cells were carefully washed once with cold DPBS followed by three washes with cold heparin solution (diluted to 50 µg/ml in OptiMEM). After treatment cells were trypsinized, suspended, and cell permeability quantified based on propidium iodide fluorescence measured with flow cytometry.

Finally, we investigated the role of negatively charged cell-surface glycans on cellular uptake/processing of B1. 293T cells and TZM-bl cells were treated for 24 hours with sodium chlorate (80 mM), an inhibitor of glycan synthesis (201), prior to exposure to GFP-L-B1. B1-mediated cell uptake was reduced by sodium chlorate treatment (Figure 3.10A). Similarly, GFP-L-B1-mediated RNA transfection was compromised in sodium chlorate-treated cells (Figure 3.10B). These results point to a role of cell-surface sulfated glycans in cell penetration by B1.

3.4 Discussion

This section describes a new cell penetrating polypeptide (CPP) – B1 – that derives from a frameshifted eGFP gene. B1 is able to rapidly and efficiently transport conjugated proteins (~30 kDa) and nucleic acids (~5 kbp DNA and 3 kb RNA) across cell membranes and to intracellular sites where bioactivity of the transported biomolecules can be realized. The kinetics of B1-mediated cell penetration is comparable to the published data for two other well-characterized CPPs – deca-arginine (R10) and Tat (125, 202).

B1 effectively transports covalently conjugated proteins across the cell membrane, as evidenced by the fluorescence of cells exposed to B1-fused GFP. It is important to note

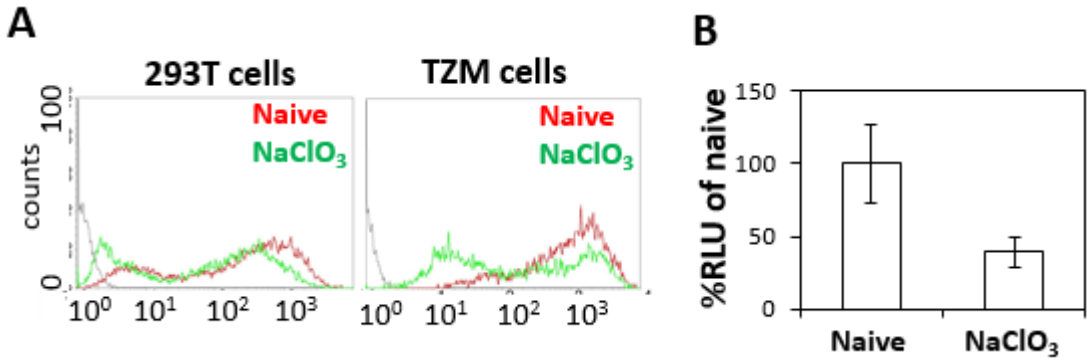

Figure 3.10. Probing the transduction mechanism of B1. A. Cell surface charge dependence of B1 mediated GFP transduction. TZM cells were treated with 80 mM sodium chlorate for 24 hours and then treated for one hour with 2 µM GFP-L-B1. Removing sulfated cell surface glycans did not consistently inhibit B1 mediated GFP transduction. **B.** Cell surface charge dependence on B1 mediated RNA transfection**.** 293T cells were treated with 50 mM sodium chlorate for 24 hours. After treatment cells were transfected with 5 ng pIRF mRNA using GFP-L-B1 for 6 hours. Transfection efficiency was quantified 6 hours later and compared with untreated cells. Error bars show the standard deviation from two independent experiments.

that this fluorescence analysis assesses cellular uptake of CPP-fused proteins but does not provide information on intracellular fate. It was found that, while mammalian cells readily take up B1-fused GFP, the mean fluorescence of the GFP-L-B1-exposed cells was significantly (~50-fold) lower than that of cells exposed to the supercharged +36GFP (186). Only a small proportion of GFP-L-B1-positive cells exhibit a fluorescence intensity on par with +36GFP-positive cells. The reduced intracellular fluorescence of GFP-L-B1 could be due to relatively quick transport from endosomes into lysosomes for degradation, preventing any increase in cellular fluorescence intensity after 30 minutes (Figure 3.3A). Another possibility is that GFP-L-B1 more readily escapes from endosomes relative to +36GFP, exposing it to degradation by cytosolic processes.

We demonstrated that B1 can efficiently penetrate many different mammalian cell lines, including both adherent and suspension cells. In all the tested cell lines, the percentage of mCherry-positive cells mediated by B1 delivery was comparable to +36GFP delivery, and was much higher than Tat delivery. Since cellular uptake was similar for both suspension cells (Jurkat) and adherent cells (HeLa, 293T, Huh-7.5), the amount of solution-exposed cell surface does not appear to be a limiting factor for cell penetration. Rather, given that the rate of uptake into cells is dependent primarily on association with the cell membrane, the overall turnover rate of the plasma membrane of a given cell line may more strongly influence protein uptake (203). As evidence of this hypothesis, it is noted that (1) BSR cells, which exhibit an unusually high metabolic rate (doubling time of ~12 h (186)), were observed to undergo the most potent cell penetration by B1, with essentially all cells being GFP-positive after exposure to 0.1 μM GFP-L-B1, and (2) the rate of uptake of B1 into TZM-bl cells is similar to published rates of membrane turnover (204).

Despite being derived from a frameshifted gene, B1 is predicted to possess significant secondary structure (Figure 3.11). Efforts to assess the presence of secondary structure via circular dichroism (CD) analysis proved challenging, mainly due to difficulties in obtaining large amounts of highly pure B1, but preliminary data obtained from CD analysis appeared to indicate the presence of significant secondary structural motifs (Figure 3.12).

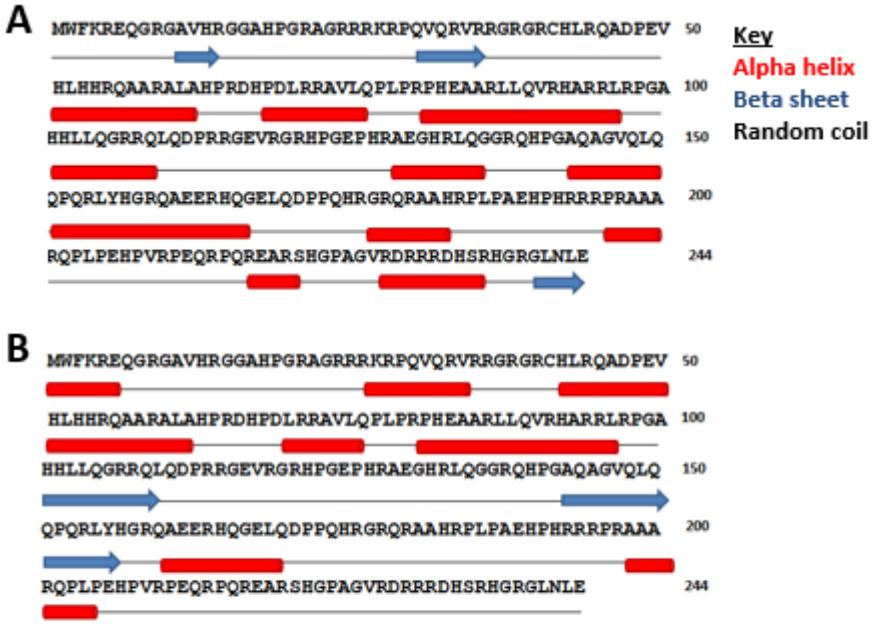

C

Prediction	Helix	Sheet	Turn	Coil
GOR4	42.62	7.38	0	50
Chou-Fasman	35.7	20.1	17.2	27

Figure 3.11. Secondary structure predictions of B1 amino acid sequence. Secondary structure predictions of the B1 protein were made using the GOR4 (A) (Garnier et al. 1996) and Chou-Fasman (B) (Privelege et al. 1989) algorithms. A significant number of helical motifs were predicted by both algorithms (C).

We segmented B1 into three non-overlapping fragments that avoid the disruption of predicted structural motifs (Figure 3.5A). Despite possessing similar charge:mass (kDa) ratios, these fragments were found to exhibit significantly weakened cell penetration relative to B1 (Figure 3.5B). This result implies that charge:mass ratio is not the only factor governing B1's ability to penetrate and transport cargo across cellular barriers.

It is tempting to speculate that secondary, or even the tertiary, structure may play a role in B1's cell penetration functionality.

We demonstrated that B1 can deliver functional Cre recombinase to the nucleus, as gauged by reconstitution of expression of a silenced recombinant reporter gene. This result also implies that B1 can escape endosomes and access the cytosol. In our study, Cre was fused to the N-terminus of B1 and R10 via a flexible linker. Cre-mediated recombination is greatly enhanced by the presence of chloroquine, an inhibitor of lysosomal protein degradation (191).

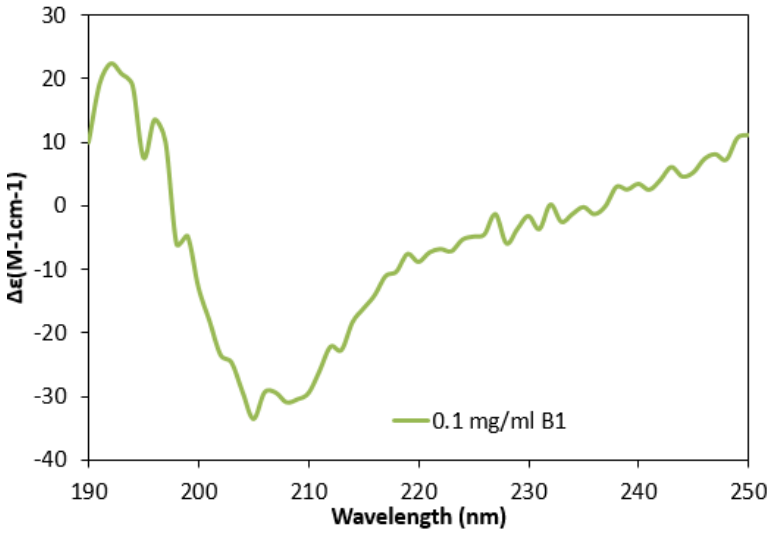

Figure 3.12. CD spectrum of 0.1 mg/ml B1 in ddH2O. Spectra were obtained from an AVIV 62DS spectropolarimeter by measuring every 1 nm between 190 and 250 nm with 30 s averages.

The potency of B1-mediated delivery of Cre recombinase as gauged by nuclear recombination activity is significantly lower than that of B1-mediated delivery of mCherry as reported by cell fluorescence (compare chart for BSR cells in Figure 3.4 with Figure 3.6B). This result indicates that the vast majority of covalently conjugated proteins delivered to cells by B1 are not accessible to the nucleus and perhaps also not accessible to the cytosol. These inaccessible proteins likely remain trapped in endosomes, consistent with the observation that GFP-L-B1 was found to accumulate in large intracellular patches (Figure 3.3B).

Presumably, any cargo protein can be covalently attached to B1 for cell delivery. Given that B1 is highly positively charged, a negatively charged cargo protein could potentially be non-covalently conjugated to B1 for cellular delivery. This strategy was successfully used by Waugh *et al.* to deliver negatively charged BOTOX into the skin of mice through conjugation with a Tat-polylysine fusion peptide (133). Alternatively, a disulfide bond could be inserted between the cargo protein and B1 through the introduction of a pair of cysteine substitutions in both proteins. Upon delivery to the reducing environment of the cytosol, the disulfide linkage is likely to break. Wiyagi *et al*. used this approach to deliver a δPKC inhibitor peptide into mice through using Tat as the CPP (134).

To determine the role of different cellular endocytic pathways in cell penetration by B1, we evaluated cellular uptake of GFP-L-B1 in the presence of selected inhibitors of

macropinocytosis, clathrin-mediated endocytosis, mannan receptor-dependent phagocytosis, and caveolin-mediated endocytosis. None of these inhibitors blocked uptake of GFP-L-B1, suggesting that any one of these cellular pathways alone is not critical for cellular entry of B1. In fact, B1 uptake by TZM-bl cells is enhanced by inhibitors of macropinocytosis and clathrin-mediated endocytosis (Figure 3.8B, C). This result indicates that macropinocytosis and clathrin-mediated endocytosis may be "weak links" for cell penetration by B1 that obstruct B1-mediated protein entry through other, more energetically favorable pathways. In contrast, nystatin, an inhibitor of caveolin–mediated endocytosis, was found to enhance the delivery of mRNA pointing to a possible inhibitory role of caveolin–mediated endocytosis in mRNA cargo delivery.

The discrepancy in the roles of endocytic pathways in cellular uptake versus successful processing of an mRNA cargo underscores the lack of correlation between B1's cell-transduction ability and its access to cellular sites conducive to cargo bioactivity. Clathrin-mediated endocytosis is an example of a pathway that is dispensable for cellular uptake of B1 (Figure 3.8B) but critical for providing cytosolic access to B1–conjugated cargo (Figure 3.8D). In this example, it is possible that blockage of clathrin–mediated endocytosis forces B1 to enter cells through other endocytic pathways whose endosomal compartments are less permissive to cytosolic access (131).

An endocytic pathway is presumed since fluorescence imaging indicates that the GFP–fused protein appears to be agglomerated in punctate regions presumed to be endosomes

(Figure 3.3B, C). Any form of direct membrane translocation is not expected, since B1 is composed of mainly hydrophilic residues, and since the cell membrane remains intact during transduction (Figure 3.9). Such pathways would presumably be responsible for the GFP transduction observed at 4 °C, and would as such possess a relatively limited energy dependence. Since the known mechanisms of cellular transport require considerable amounts of energy and cellular resources, such a pathway must therefore use a currently undescribed mechanism. It is likely that other cell transducing proteins also make use of this mechanism. Elucidating the details of this mechanism, however, will prove a challenge. This is because B1, and other cell transducing proteins, are capable of delivering their cargo via multiple mechanisms (205, 206).

Finally, we explored the role of negatively charged cell-surface glycans in cellular uptake/processing of B1 based on our hypothesis that cell-surface ionic interactions play a role in B1's ability to associate with and enter cells. We found that lowering the cell-surface content of sulfated glycans via sodium chlorate treatment does indeed retard the ability of GFP-L-B1 to penetrate and deliver functional cargo into cells. Previously, Cronican *et al.* observed that highly positively charged proteins can efficiently penetrate mammalian cells and predicted that proteins with a +charge:MW ratio greater than 0.75 represent candidate CPPs (126, 127). B1 possesses a +charge:MW ratio of 1.5, further supporting a role of ionic interactions in at least partially mediating its cell penetration functionality.

In conclusion we identified a new cell-penetrating protein, B1, which is able to potently deliver conjugated biomolecular cargo to several mammalian cell lines. Most importantly, we show that B1 not only mediates cellular uptake, but effectively transports cargo to intracellular sites of biological relevance. B1 appears to utilize cell-surface glycans for cellular entry and penetrates cells and transports its cargo via multiple competing cellular endocytic pathways. Interestingly, we found that the contribution of specific endocytic pathways to cellular entry versus functional cargo delivery by B1 can be significantly different. B1 provides a new tool for intracellular delivery of biomolecules. Additionally, insights garnered from these studies could aid in the design of more effective vehicles for the cellular delivery of therapeutic payloads.

3.5 Methods

3.5.1 Cellular uptake determination of fluorescent protein-fused CPPs

On the day prior to CPP exposure, the following cells were seeded in 24-well plates at the indicated densities: 293T cells (2 x 10^5 cells/well), Huh-7.5 and TZM cells (1.9 x 10^5 cells/well), BSR cells (1 x 10^5 cells/well). These seeding densities were chosen such that the cells reach ~70% confluency the following day. On the day of CPP exposure, Jurkat cells were transferred to V-bottom 96-well plates at 1 x 10^5 cells/well. All cells were washed once with OptiMEM to remove residual serum. Protein solutions were diluted in cold OptiMEM to the desired concentrations and equilibrated to room temperature before being added to cells. Cells were incubated at 37°C/5% CO_2 unless otherwise indicated. After incubation, these cells were washed once with cold DPBS.

For uptake determination of GFP-L-B1 or +36 GFP, cells were incubated with 0.04% Trypan Blue (in DPBS) for 2 minutes at room temperature to quench the fluorescence of extracellular GFP (188), washed again with cold DPBS and then imaged using a Zeiss Axiovert 200M fluorescent microscope (Carl Zeiss Microscopy, NY). For confocal microscopy, TZM cells (seeded on a glass chamber slide) that had been exposed to 2 µM GFP-L-B1 were incubated with 300 nM DAPI solution (Invitrogen, NY) for 5 minutes at room temperature and imaged using a Zeiss 510 Meta NLO Mulitphoton microscope (Carl Zeiss Microscopy). For flow cytometric analysis, cells that had been exposed to CPPs were incubated with 0.25% trypsin-EDTA at room temperature for 5 minutes and resuspended in complete growth medium (DMEM supplemented with 10% FBS and 1X NEAA) and analyzed on a BD FACScan flow cytometer (BD Biosciences) gated for GFP fluorescence (excitation/emission 488/530). At least 1 x 10^4 cells were analyzed for each sample.

For cellular uptake analysis of CPPs containing mCherry-fusion proteins, CPP-exposed cells were detached by incubation with 0.25% trypsin-EDTA at room temperature for five minutes, resuspended in complete growth medium and then analyzed by flow cytometry (excitation/emission 488/650). At least 1 x 10^4 cells were analyzed for each sample.

3.5.2 Cre recombinase delivery

BSR.LNL.tdTomato reporter cells were seeded in 24-well plates at 5 x 10^4 cells per well. The following day, the cells were washed once with OptiMEM to remove residual serum, exposed to Cre-fused CPPs in the presence or absence of 100 µM chloroquine and incubated at 37°C/5% CO_2 for 6 hours. Following CPP exposure, cells were washed once with OptiMEM to remove excess proteins, the supernatants were replaced with fresh, complete growth medium, and the cells were incubated at 37°C/5% CO_2 for another 24 hours followed by fluorescence microscopic analysis (Zeiss Axiovert 200M) to quantify Cre delivery. After imaging, cells were trypsinized, resuspended in complete growth medium and then analyzed by flow cytometry (excitation/emission 488/650). Cells were gated for at least 1 x 10^4 live cells in each sample.

3.5.3 Quantification of luciferase activity deriving from DNA/RNA delivery

293T cells were seeded in 96-well plates at 4 x 10^4 cells per well. The following day, 10X-concentrated protein samples were prepared in OptiMEM. Linearized pCMV5-Gluc DNA (46 ng/µL) and pIRF mRNA (10 ng/µL) were prepared in OptiMEM. 10 µL of 10X protein samples were mixed with 10 µl of the nucleic acids and the mixtures were incubated at room temperature for 10 minutes to allow protein/nucleic acids association. In the meantime, the cells were washed twice with OptiMEM to remove residual serum and incubated in 40 µL OptiMEM. 10 µL of the protein/nucleic acids mixtures were then added to cells followed by incubation at 37°C/5% CO_2 for 6 hours. The amount of RNA and DNA in individual wells was 50 ng (50.5 fmol) and 230 ng (67 fmol), respectively.

For control experiments utilizing commercial reagents for nucleic acids delivery, linearized pCMV5-Gluc (230 ng in 10 µL) was mixed with 0.8 µL Lipofectamine 2000 or TransIT reagent and pIRF mRNA (50 ng in 10 µL) was mixed with 0.4 µL Lipofectamine 2000 or TransMessenger reagent. The mixtures were incubated at room temperature for 20 minutes, diluted in 40 µL OptiMEM and added to 293T cells. 6 hours later, the cells were washed and the supernatants were replaced with the complete growth medium. DNA transfection was quantified by measuring the Gaussia luciferase (Gluc) activity in supernatants 24 hours post medium change using the Biolux Gaussia Luciferase Assay Kit (New England Biolabs). RNA transfection was quantified by measuring the intracellular firefly luciferase (Fluc) levels measured 6 hours post medium change using the Luciferase Assay System (Promega).

3.5.4 Chemicals, bacterial strains and cell lines

BSR.LNL.tdTomato reporter cells were a gift from Prof. David Liu (Harvard University). 293T cells were purchased from Invitrogen. TZM–bl cells were obtained from Dr. John C. Kappes, Dr. Xiaoyun Wu and Tranzyme Inc. through the NIH AIDS Reagent Program, Division of AIDS, NIAID. Jurkat cells were obtained from Prof. Paul Lindahl (Texas A&M University). Huh–7.5 cells were obtained from Prof. Charles Rice (Rockefeller University).

All adherent cell lines were cultured in complete growth medium (Dulbecco's Modified Eagle Medium (DMEM) containing 4500 mg/L glucose, 4.0 mM L–Glutamine, and 110 mg/L sodium pyruvate (Thermo Scientific HyClone) supplemented with 10 % fetal

bovine serum (Atlanta Biologicals) and 1X non–essential amino acids (Thermo Scientific HyClone)). Jurkat cells were cultured in Roswell Park Memorial Institute Medium (RPMI) 1640 (Lonza) supplemented with 10% fetal bovine serum. *Escherichia coli* strains DH5α (Invitrogen) and BL21 (DE3) (New England Biolabs) were used for recombinant DNA cloning and recombinant protein expression, respectively.

Amiloride and dynasore were purchased from Enzo Life Sciences. Chlorpromazine, mannan and cytochalasin B were obtained from Sigma–Aldrich. Nystatin was purchased from Amresco. CellTiter–Glo Luminescent Cell Viability Assay Kit and Luciferase Assay System were purchased from Promega. Biolux Gaussia Luciferase Assay Kit was purchased from New England Biolabs. Dulbecco's Phosphate–Buffered Saline (DPBS) was purchased from Thermo Scientific HyClone. OptiMEM and Lipofectamine 2000 were purchased from Invitrogen. 0.4% Trypan Blue solution was purchased from Lonza. Luria–Bertani (LB) broth, Mirus TransIT LT1 transfection reagent and ampicillin were obtained from Thermo Fisher Scientific. Isopropyl–β–D–thiogalactopyranoside (IPTG), 0.25% trypsin–EDTA and imidazole were from VWR International. TransMessenger transfection reagent was purchased from Qiagen.

3.5.5 Protein purification

BL21 (DE3) cells were transformed with the expression plasmid and plated on a Luria–Bertani (LB) agar plate containing 100 µg/mL ampicillin. The next day, a single colony

was picked and cultured at 37°C with shaking at 250 rpm. At OD_{600} ~0.6, the cells were cooled to 18°C and isopropyl β–D–1–thiogalactopyranoside (IPTG, 0.5 mM) was added to the culture to induce protein expression. After overnight expression (~18 hours) at 18°C, cells were harvested by centrifugation at 6000 x g and 4°C for 20 minutes and pellets were stored at –80 °C until use.

For recombinant protein purification, cell pellets were resuspended in lysis buffer (500 mM NaCl, 50 mM Tris, pH 8, 10 mL per 1 g wet cell pellet), and disrupted by sonication on ice (QSonica Misonix 200 (Qsonica), 1 second pulse 6 second pause for 3 minutes 10 amp). Whole cell lysate was clarified by centrifugation at 20,000 *x g* for 20 minutes at 4°C. Soluble cell lysates were loaded onto 5 mL Ni–NTA agarose beads (Qiagen). For constructs expressing B1 or +36GFP, the loaded resin was washed with lysis buffer supplemented with 150 mM imidazole and the product was eluted in lysis buffer supplemented 500 mM imidazole. For all other constructs the loaded resin was washed with lysis buffer supplemented with 50 mM imidazole and the product was eluted in lysis buffer supplemented 150 mM imidazole. Purified protein samples were dialyzed overnight at 4°C into Buffer A (2 M NaCl, 2.7 mM KCl, 10 mM $Na_2HPO_4.2H_2O$, 2 mM KH_2PO_4, pH 7.4). The proteins +36GFP and Cre-L-B1 were further purified by cation exchange chromatography using a GE HiTrap SP HP column (GE Biosciences, PA). Dialyzed proteins were diluted 1:5 into PBS to reduce the salt concentration and then loaded onto the SP column. The column was washed with Buffer B (0.5 M NaCl, 2.7 mM KCl, 10 mM $Na_2HPO_4.2H_2O$, 2 mM KH_2PO_4, pH 7.4) and the target protein was

eluted in Buffer A. Purified proteins were concentrated via ultracentrifugation through an Amicon 10 kDa MWCO centrifugal column (EMD Millipore). The final protein concentrations were determined using a Pierce Coomassie Plus Protein Assay Kit (Thermo Fisher Scientific).

Typically the purification yield of GFP-L-B1 using this approach is ~15 mg per liter of *E. coli* culture. It is worth noting that although a high concentration of NaCl (0.5M) is needed to maintain B1-fusion protein soluble at the stock concentration (i.e. when B1 is concentrated at ~100 µM), such high concentrations of NaCl were not needed during cell transduction. The highest final salt concentration used in these experiments was ~230 mM (Figure 3.4, 5 µM GFP-L-B1). Minimal cellular toxicity was observed under this condition (Figure 3.2).

3.5.6 Gel shift of GFP-L-B1-conjugated DNA/RNA

pCMV5–Gluc DNA was linearized by digestion with XbaI. pIRF mRNA was transcribed and capped from the XhoI digested plasmid DNA template using the Ampliscribe T7 High Yield Transcription Kit (Epicentre) with the addition of the monomethlyated RNA cap analog (Cell Script) following the manufacturer's protocol. Linearized pCMV5–Gluc plasmid DNA (14.5 femtomoles or 50 ng) or pIRF mRNA (86 femtomoles or 80 ng) were mixed with GFP–L–B1 at the following protein:DNA/RNA molar ratios: 0:1, 10:1, 50:1, 100:1, 500:1, 1000:1 in EMSA buffer (4% glycerol, 1 mM $MgCl_2$, 0.5 mM EDTA, 0.5 mM DTT, 50 mM NaCl, 10 mM Tris–HCl, pH 7.4). The

mixtures were incubated at room temperature for 10 minutes to allow protein–DNA/RNA association. Formation of protein/nucleic acids complexes was confirmed by analysis on a 0.8% agarose gels (100 V for 40 minutes for DNA and 120 V for 15 minutes for RNA). The ethidium bromide–stained gel was then visualized under UV exposure.

3.5.7 Interrogation of role of cellular endocytic pathways

293T and TZM–bl cells were seeded in 24–well plates at 1.5 x 10^5 cells per well. The following day, cells were washed with 500 µl OptiMEM to remove residual serum and incubated in 200 µL OptiMEM containing endocytic inhibitors for 1 hour at 37°C/5% CO_2. 20 µM GFP–L–B1 (in 20 µL) or mixtures of GFP–L–B1 (8 µM) and pIRF mRNA (5 ng (5 fmol))were added to the cells in the continued presence of the inhibitors and incubation at 37°C/5% CO_2 for one hour. For analysis of cellular uptake/functional cargo delivery, cells were washed once with cold DPBS, incubated with DPBS containing 0.04% Trypan Blue at room temperature for 2 minutes to quench the fluorescence of extracellular GFP (188), and analyzed via fluorescence microscopy (Zeiss Axiovert 200M) or flow cytometry (excitation/emission 488/530). At least 1 x 10^4 cells were analyzed for each sample. Firefly luciferase (Fluc) activity deriving from pIRF mRNA delivery was quantified 6 hours post exposure to GFP–L–B1/mRNA complex using the Luciferase Assay System (Promega).

3.5.8 Interrogation of role of cell–surface glycans

For GFP–L–B1 delivery, 293T and TZM–bl cells were seeded in 24–well plates at 7.5 x 10^4 and 1.5 x 10^5 cells/well, respectively. For the assessment of functional mRNA delivery, 293T cells were seeded in 96–well plates at 1.5 x 10^4 cells per well. The following day, cells were washed with OptiMEM to remove residual serum and incubated with either 2 μM GFP–L–B1 for one hour or mixtures of 1.6 μM GFP–L–B1 and 5 ng (5 fmol) pIRF mRNA for 6 hours. For assessment of GFP–L–B1 uptake, cells were washed once with cold DPBS, incubated in DPBS containing 0.04% Trypan Blue at room temperature for 2 minutes, and analyzed via fluorescence microscopy (Zeiss Axiovert 200M) or flow cytometry (excitation/emission 488/530). At least 1 x 10^4 cells were analyzed for each sample. Functional delivery of pIRF mRNA was determined by measuring intracellular Fluc activity 6 hours post transfection using the Luciferase Assay System.

3.5.9 Cloning

The codon–optimized B1 gene was synthesized by Genscript (Piscataway). All constructs were expressed using the pET15b vector, which contains an N–terminal 6xHistidine tag. mCherry was amplified from pET–+36GFP–L–mCherry (a gift from Prof. David Liu, Harvard University). Cre was amplified from pET–+36GFP–L–Cre (gift from Prof. David Liu). DNA fragments encoding linkers were synthesized by Integrated DNA Technologies and inserted into the appropriate vectors via overlap extension PCR.

3.5.10 Sequences of Proteins used in this section

(1) B1

MGSSHHHHHHSSGLVPRGSHMWFKREQGRGAVHRGGAHPGRAGRRRKRPQV
QRVRRGRGRCHLRQADPEVHLHHRQAARALAHPRDHPDLRRAVLQPLPRPHEA
ARLLQVRHARRLRPGAHHLLQGRRQLQDPRRGEVRGRHPGEPHRAEGHRLQG
GRQHPGAQAGVQLQQPQRLYHGRQAEERHQGELQDPPQHRGRQRAAHRPLPA
EHPHRRRPRAAARQPLPEHPVRPEQRPQREARSHGPAGVRDRRRDHSRHGRGL
N

(2) GFP-L-B1

MGSSHHHHHHSSGLVPRGSHMVSKGEELFTGVVPILVELDGDVNGHKFSVSGE
GEGDATYGKLTLKFICTTGKLPVPWPTLVTTLTYGVQCFSRYPDHMKQHDFFKS
AMPEGYVQERTIFFKDDGNYKTRAEVKFEGDTLVNRIELKGIDFKEDGNILGHK
LEYNYNSHNVYIMADKQKNGIKVNFKIRHNIEDGSVQLADHYQQNTPIGDGPVL
LPDNHYLSTQSALSKDPNEKRDHMVLLEFVTAAGITLGMDELEACGGGGSGGG
GSASWFKREQGRGAVHRGGAHPGRAGRRRKRPQVQRVRRGRGRCHLRQADPE
VHLHHRQAARALAHPRDHPDLRRAVLQPLPRPHEAARLLQVRHARRLRPGAHH
LLQGRRQLQDPRRGEVRGRHPGEPHRAEGHRLQGGRQHPGAQAGVQLQQPQR
LYHGRQAEERHQGELQDPPQHRGRQRAAHRPLPAEHPHRRRPRAAARQPLPEH
PVRPEQRPQREARSHGPAGVRDRRRDHSRHGRGLN

(3) GFP-L-B1-F

MGSSHHHHHHSSGLVPRGSHMVSKGEELFTGVVPILVELDGDVNGHKFSVSGE
GEGDATYGKLTLKFICTTGKLPVPWPTLVTTLTYGVQCFSRYPDHMKQHDFFKS
AMPEGYVQERTIFFKDDGNYKTRAEVKFEGDTLVNRIELKGIDFKEDGNILGHK
LEYNYNSHNVYIMADKQKNGIKVNFKIRHNIEDGSVQLADHYQQNTPIGDGPVL
LPDNHYLSTQSALSKDPNEKRDHMVLLEFVTAAGITLGMDELEACGGGGSGGG
GSASWFKREQGRGAVHRGGAHPGRAGRRRKRPQVQRVRRGRGRCHLRQADPE
VHLHHRQAARALAHPRDHPDLRRAVLQPLPRPLEDPAANKARKEAELAAATAE
Q

(4) GFP-L-B1-M

MGSSHHHHHHSSGLVPRGSHMVSKGEELFTGVVPILVELDGDVNGHKFSVSGE
GEGDATYGKLTLKFICTTGKLPVPWPTLVTTLTYGVQCFSRYPDHMKQHDFFKS
AMPEGYVQERTIFFKDDGNYKTRAEVKFEGDTLVNRIELKGIDFKEDGNILGHK
LEYNYNSHNVYIMADKQKNGIKVNFKIRHNIEDGSVQLADHYQQNTPIGDGPVL
LPDNHYLSTQSALSKDPNEKRDHMVLLEFVTAAGITLGMDELEACGGGGSGGG
GSASQPLPRPHEAARLLQVRHARRLRPGAHHLLQGRRQLQDPRRGEVRGRHPG
EPHRAEGHRLQGGRQHPGAQAGVQLQQPQRLYHGRQAEERHQGELQDPP

(5) GFP-L-B1-R

MGSSHHHHHHSSGLVPRGSHMVSKGEELFTGVVPILVELDGDVNGHKFSVSGE
GEGDATYGKLTLKFICTTGKLPVPWPTLVTTLTYGVQCFSRYPDHMKQHDFFKS

AMPEGYVQERTIFFKDDGNYKTRAEVKFEGDTLVNRIELKGIDFKEDGNILGHK
LEYNYNSHNVYIMADKQKNGIKVNFKIRHNIEDGSVQLADHYQQNTPIGDGPVL
LPDNHYLSTQSALSKDPNEKRDHMVLLEFVTAAGITLGMDELEACGGGGSGGG
GSASELQDPPQHRGRQRAAHRPLPAEHPHRRRPRAAARQPLPEHPVRPEQRPQR
EARSHGPAGVRDRRRDHSRHGRGLN

(6) mCherry-L-B1

MGSSHHHHHHSSGLVPRGSHMVSKGEEDNMAIIKEFMRFKVHMEGSVNGHEFE
IEGEGEGRPYEGTQTAKLKVTKGGPLPFAWDILSPQFMYGSKAYVKHPADIPDY
LKLSFPEGFKWERVMNFEDGGVVTVTQDSSLQDGEFIYKVKLRGTNFPSDGPV
MQKKTMGWEASSERMYPEDGALKGEIKQRLKLKDGGHYDAEVKTTYKAKK
PVQLPGAYNVNIKLDITSHNEDYTIVEQYERAEGRHSTGGMDELYKTGGSGGSG
GSGGSGGSGGSGGSGGSSASWFKREQGRGAVHRGGAHPGRAGRRRKRPQVQR
VRRGRGRCHLRQADPEVHLHHRQAARALAHPRDHPDLRRAVLQPLPRPHEAAR
LLQVRHARRLRPGAHHLLQGRRQLQDPRRGEVRGRHPGEPHRAEGHRLQGGR
QHPGAQAGVQLQQPQRLYHGRQAEERHQGELQDPPQHRGRQRAAHRPLPAEH
PHRRRPRAAARQPLPEHPVRPEQRPQREA
RSHGPAGVRDRRRDHSRHGRGLN

(7) mCherry-L-Arg10

MGSSHHHHHHSSGLVPRGSHMVSKGEEDNMAIIKEFMRFKVHMEGSVNGHEFE
IEGEGEGRPYEGTQTAKLKVTKGGPLPFAWDILSPQFMYGSKAYVKHPADIPDY

LKLSFPEGFKWERVMNFEDGGVVTVTQDSSLQDGEFIYKVKLRGTNFPSDGPV
MQKKTMGWEASSERMYPEDGALKGEIKQRLKLKDGGHYDAEVKTTYKAKK
PVQLPGAYNVNIKLDITSHNEDYTIVEQYERAEGRHSTGGMDELYKTGGSGGSG
GSGGSGGSGGSGGSGGSSASRRRRRRRRRR

(8) mCherry-L-Tat

MGSSHHHHHHSSGLVPRGSHMVSKGEEDNMAIIKEFMRFKVHMEGSVNGHEFE
IEGEGEGRPYEGTQTAKLKVTKGGPLPFAWDILSPQFMYGSKAYVKHPADIPDY
LKLSFPEGFKWERVMNFEDGGVVTVTQDSSLQDGEFIYKVKLRGTNFPSDGPV
MQKKTMGWEASSERMYPEDGALKGEIKQRLKLKDGGHYDAEVKTTYKAKK
PVQLPGAYNVNIKLDITSHNEDYTIVEQYERAEGRHSTGGMDELYKTGGSGGSG
GSGGSGGSGGSGGSGGSSASGRKKRRQRRR

(9) Cre-L-B1

MGSSHHHHHHSSGLVPRGSHMASNLLTVHQNLPALPVDATSDEVRKNLMDMF
RDRQAFSEHTWKMLLSVCRSWAAWCKLNNRKWFPAEPEDVRDYLLYLQARG
LAVKTIQQHLGQLNMLHRRSGLPRPSDSNAVSLVMRRIRKENVDAGERAKQAL
AFERTDFDQVRSLMENSDRCQDIRNLAFLGIAYNTLLRIAEIARIRVKDISRTD
GGRMLIHIGRTKTLVSTAGVEKALSLGVTKLVERWISVSGVADDPNNYLFCRVR
KNGVAAPSATSQLSTRALEGIFEATHRLIYGAKDDSGQRYLAWSGHSARVGAA
RDMARAGVSIPEIMQAGGWTNVNIVMNYIRNLDSETGAMVRLLEDGDGAPSGG
GGSGGGGSASWFKREQGRGAVHRGGAHPGRAGRRRKRPQVQRVRRGRGRC

HLRQADPEVHLHHRQAARALAHPRDHPDLRRAVLQPLPRPHEAARLLQVRHAR
RLRPGAHHLLQGRRQLQDPRRGEVRGRHPGEPHRAEGHRLQGGRQHPGAQAG
VQLQQPQRLYHGRQAEERHQGELQDPPQHRGRQRAAHRPLPAEHPHRRRPRAA
ARQPLPEHPVRPEQRPQREARSHGPAGVRDRRRDHSRHGRGLN

(10) Cre-L-Arg10

MGSSHHHHHHSSGLVPRGSHMASNLLTVHQNLPALPVDATSDEVRKNLMDMF
RDRQAFSEHTWKMLLSVCRSWAAWCKLNNRKWFPAEPEDVRDYLLYLQARG
LAVKTIQQHLGQLNMLHRRSGLPRPSDSNAVSLVMRRIRKENVDAGERAKQAL
AFERTDFDQVRSLMENSDRCQDIRNLAFLGIAYNTLLRIAEIARIRVKDISRTD
GGRMLIHIGRTKTLVSTAGVEKALSLGVTKLVERWISVSGVADDPNNYLFCRVR
KNGVAAPSATSQLSTRALEGIFEATHRLIYGAKDDSGQRYLAWSGHSARVGAA
RDMARAGVSIPEIMQAGGWTNVNIVMNYIRNLDSETGAMVRLLEDGDGAPSGG
GGSGGGGSASRRRRRRRRRR

(11) +36GFP

MGHHHHHHGGASKGERLFRGKVPILVELKGDVNGHKFSVRGKGKGDATRGKL
TLKFICTTGKLPVPWPTLVTTLTYGVQCFSRYPKHMKRHDFFKSAMPKGYVQE
RTISFKKDGKYKTRAEVKFEGRTLVNRIKLKGRDFKEKGNILGHKLRYNFNSHK
VYITADKRKNGIKAKFKIRHNVKDGSVQLADHYQQNTPIGRGPVLLPRNHYLST
RSKLSKDPKEKRDHMVLLEFVTAAGIKHGRDERYK

(12) +36GFP-L-mCherry

MASKGERLFRGKVPILVELKGDVNGHKFSVRGKGKGDATRGKLTLKFICTTGK
LPVPWPTLVTTLTYGVQCFSRYPKHMKRHDFFKSAMPKGYVQERTISFKKDGK
YKTRAEVKFEGRTLVNRIKLKGRDFKEKGNILGHKLRYNFNSHKVYITADKRK
NGIKAKFKIRHNVKDGSVQLADHYQQNTPIGRGPVLLPRNHYLSTRSKLSKDPK
EKRDHMVLLEFVTAAGIKHGRDERYKGGSGGSGGSGGSGGSGGSGGSGGSGGS
VSKGEEDNMAIIKEFMRFKVHMEGSVNGHEFEIEGEGEGRPYEGTQTAKLKVTK
GGPLPFAWDILSPQFMYGSKAYVKHPADIPDYLKLSFPEGFKWERVMNFEDGG
VVTVTQDSSLQDGEFIYKVKLRGTNFPSDGPVMQKKTMGWEASSERMYPEDG
ALKGEIKQRLKLKDGGHYDAEVKTTYKAKKPVQLPGAYNVNIKLDITSHNEDY
TIVEQYERAEGRHSTGGMDELYKLEHHHHHH

(13) +36GFP-L-Cre

MASKGERLFRGKVPILVELKGDVNGHKFSVRGKGKGDATRGKLTLKFICTTGK
LPVPWPTLVTTLTYGVQCFSRYPKHMKRHDFFKSAMPKGYVQERTISFKKDGK
YKTRAEVKFEGRTLVNRIKLKGRDFKEKGNILGHKLRYNFNSHKVYITADKRK
NGIKAKFKIRHNVKDGSVQLADHYQQNTPIGRGPVLLPRNHYLSTRSKLSKDPK
EKRDHMVLLEFVTAAGIKHGRDERYKGGSGGSGGSGGSGGSGGSGGSGGSGGS
ASNLLTVHQNLPALPVDATSDEVRKNLMDMFRDRQAFSEHTWKMLLSVCRSW
AAWCKLNNRKWFPAEPEDVRDYLLYLQARGLAVKTIQQHLGQLNMLHRRSGL
PRPSDSNAVSLVMRRIRKENVDAGERAKQALAFERTDFDQVRSLMENSDRCQDI
RNLAFLGIAYNTLLRIAEIARIRVKDISRTDGGRMLIHIGRTKTLVSTAGVEKALS

LGVTKLVERWISVSGVADDPNNYLFCRVRKNGVAAPSATSQLSTRALEGIFEAT

HRLIYGAKDDSGQRYLAWSGHSARVGAARDMARAGVSIPEIMQAGGWTNVNI

VMNYIRNLDSETGAMVRLLEDGDGGSHHHHHH

4. TACHYKININ RECEPTOR 1 & 3 ANTAGONISTS INHIBIT HCV INFECTION

4.1 Overview

Tachykinin receptors (TACR) are G-protein coupled receptors that are ubiquitously found in humans. Tachykinin receptors are usually stimulated by small signaling peptides, called tachykinins.

Due to their expression in a wide range of tissues, tachykinin receptors mediate a wide range of functions *in vivo*. TACR antagonists have long been developed for a wide range of clinical indications, including HIV infection. During a screening carried out in our lab, we identified a TACR3 inhibitor SB 222200 that had significant anti-HCV activity. In this section, we show that both TACR1 and TACR3 receptors are expressed in the HCV-permissive Huh 7.5 cell line. We also show that both TACR1 and TACR3 inhibitors significantly inhibit HCV infection. These results point to the potential for TACR1 antagonists in treating patients infected with both HCV and HIV.

4.2 Introduction

Tachykinins (also known as neurokinins) are peptides characterized by a common C-terminal sequence that binds to and activates a cell surface-localized tachykinin receptor (62). The three main tachykinin peptides (Substance P (SP), Neurokinin A (NKA) and Neurokinin B (NKB)) are distributed throughout the body, but are usually predominantly found in the CNS(63, 64). The tachykinin receptor is a G-protein coupled receptor

containing seven trans-membrane helices(65). Three different tachykinin receptors (TACR) have been identified – tachykinin receptors 1, 2 and 3 (TACR1, TACR2 and TACR3) – and although each receptor can be activated by any of the three main tachykinin peptides, SP, NKA, and NKB have higher affinities for TACR1, TACR2 and TACR3 respectively (66). This apparent lack of specificity is likely due to a high homology at the ligand-binding site among these receptors(67).

The binding of an agonist to the receptor initiates a cascade of intracellular signaling events leading to the activation of phospholipase C (PLC), inositol triphosphate (IP_3) and diaglycerol (DAG)(68). These two molecules can then act to increase the calcium concentration in the cytoplasm from two different sources. IP_3 can bind to and activate the IP_3 receptor on the ER membrane (69). This results in the release of calcium from the ER to the cytoplasm. DAG can activate protein kinase C (PKC) which opens L-type calcium channels in the cell membrane, enabling calcium influx from the extracellular environment(70). Perhaps due to this non-specific signal cascade, tachykinins can be responsible for a wide range of effects. This, combined with the relatively large tissue distribution, leads to tachykinins being involved in a number of functions including: neuronal survival and regeneration; gastric mobility; regulation of respiratory mechanisms; and the expression of pro-inflammatory cytokines (71-73). As such TACR antagonists, have been tested for a wide range of indications in clinical trials. TACR1 antagonist aprepitant has been tested as an antiemetic, an antidepressant, a CYP34A inhibitor, and to treat urge urinary incontinence (74-77). TACR1 antagonist CP 99994

has been tested as a post-operative analgesic (78). TACR2 antagonists nepadutant and saredutant have been tested for the treatment of irritable bowel syndrome, and the inhibition of NKA induced bronchoconstriction (79, 80). Finally, TACR3 antagonist osanetant has been tested as an anti-psychotic (81).

In addition to their roles in native body functions, tachykinin ligands and receptors have been implicated in the infection of some viruses (82, 83). For HIV it was observed that HIV-infected individuals had significantly increased levels of SP (84). It was also shown that SP binding lead to increased HIV replication in infected cells, including the activation of latently infected immune cells (85, 86). And finally that TACR1 antagonists inhibit HIV infection *in vitro* (83, 87, 88). Aprepitant, a TACR1 antagonist, was used in a clinical study for HIV treatment, but the study failed due to the inability to reach effective physiological concentrations at safe doses (89). The first implied role of tachykinins and HCV occurred when a TACR3 tachykinin receptor antagonist, SB 222200, appeared as a hit in a screen for anti-HCV small molecules carried out in our lab (90). Tachykinin receptors are also known to be expressed in the liver, albeit at low levels (207). Put together, those two initial observations point to a likely involvement of one or more tachykinin receptors in the HCV life cycle. However, due to the relative lack of specificity of the antagonists used, and the number of enzymes and processes potentially activated by the receptor, the role of the tachykinin receptor in the HCV life cycle is not immediately apparent. Characterization of the anti-HCV activity of SB 222200, a tachykinin receptor antagonist, could therefore shed light on previously

unknown or poorly understood virus-host interactions and open the door to a new class of anti-HCV drugs. Here we show that both the TACR1 and TACR3 receptors are expressed in the HCV-permissive Huh 7.5 cell line (98). In addition, we demonstrate that antagonists of both receptors inhibit HCV infection.

4.3 Results

4.3.1 TACR1 and TACR3 antagonists inhibit HCV infection

TACR1 and TACR3 receptors are expected to be expressed in the liver, and we previously demonstrated the ability of TACR3 antagonist SB 222200 to inhibit HCV infection. We first tested the anti-HCV capability of an additional TACR3 antagonist, and two selected TACR1 antagonist (Figure 4.1). As shown in Figure 4.2, all tested antagonists showed significant anti-HCV activity at low micromolar concentrations. However, it was noted that these drugs also have significant cytotoxicity at high concentrations. In fact, with the exception of SB 222200, the median toxic dose (TD_{50}) of tested drugs was less than or equal to the 90% inhibitory dose (EC_{90}) (Table 4.1). For this reason we used SB 222200 and TACR3 as models for further experiments.

4.3.2 TACR1 and TACR3 are expressed in Huh 7.5 cells

Given the activity of TACR1 and TACR3 antagonists in their inhibition of HCV infection, we next confirmed the presence of both receptors in Huh 7.5 cells. As shown in Figure 4.2C, both TACR1 (~53 kDa) and TACR3 (~55 kDa) appeared to be expressed in Huh 7.5 cells. However, the expression of both receptors appeared to be relatively

low. In addition, there appeared to be significant expression of both highly glycosylated, and truncated TACR1 and TACR3.

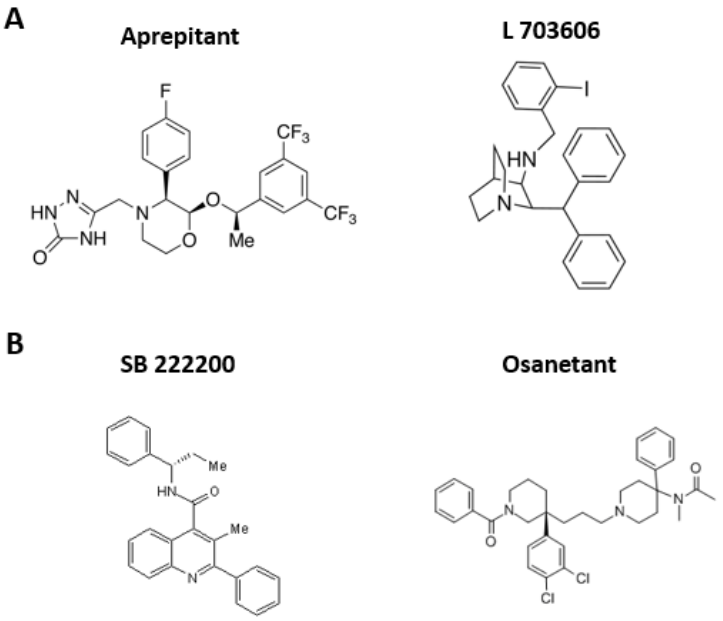

Figure 4.1. Chemical structures of inhibitors used. A. TACR1 antagonists aprepitant and L 703606. **B.** TACR3 antagonists SB 222200 and osanetant.

4.3.3 Blocking TACR3 reduces interferon stimulated gene expression in Huh 7.5 cells

PKC has been shown to be required for STAT phosphorylation and interferon-stimulated gene activation during IFN signaling(208). Since activating TACR potentially results in PKC activation, it is possible that TACR expression in Huh 7.5 cells is involved in

interferon signaling in this cell line. To confirm the receptor functionality in this cell line, we transfected Huh 7.5 cells with a plasmid expressing a reporter controlled by a promoter responsive to interferon stimulation. As shown in Figure 4.3, reporter activity was increased when cells were stimulated with IFN-β. As expected, IFN-stimulated reporter activity was reduced significantly upon treatment with 30 μM SB 222200 (Figure 4.3). This indicates the potential functionality of TACR in Huh 7.5 cells.

Compound	EC50 (μM)	EC90 (μM)	TD50 (μM)	TD90 (μM)
Aprepitant	4.1	14.6	15.9	30.9
L 703606	2.6	23.2	6.2	7
SB 222200	7.3	24.6	>30	>30
Osanetant	1.3	3.4	4.3	8.8

Table 4.1. Dose response of TACR antagonists to HCV infection in Huh 7.5 cells. EC50, EC90, TD50 and TD90 values were calculated using OriginLab software.

4.4 Discussion

In this work we describe that the HCV inhibition of by TACR3 antagonists is not limited to SB 222200. We also show for the first time that TACR1 antagonists aprepitant and L 703606 also significantly inhibit HCV infection. The TACR2 antagonist we tested, Men 10376, did not show significant anti-HCV activity (data not shown).

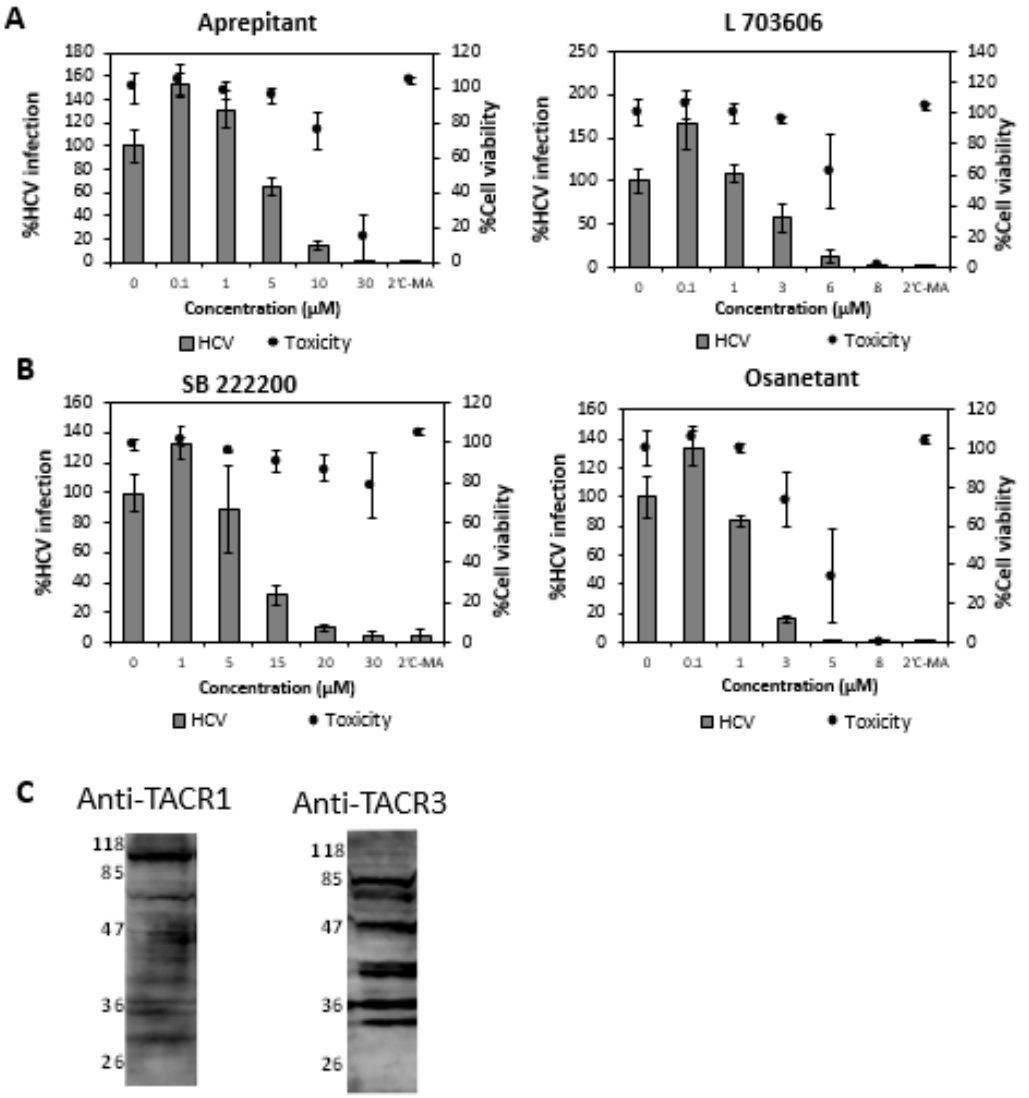

Figure 4.2. TACR antagonists inhibit HCV infection. Huh 7.5 cells were treated with indicated inhibitors of TACR1 (A), or TACR3 (B) for 30 minutes prior to infection with Jc1 Gluc HCVcc for 12 hours. After incubation cells were washed and supernatants replaced with drug dilutions. HCV infection levels (shaded bars) were quantified based on secreted reporter Gluc in supernatants collected 48 hours later. Cytotoxicity (shaded circles) was quantified on these cells by using the CellTiter-Glo assay kit (Promega). Error bars represent the standard deviation of duplicate wells of two independent experiments. **C.** Western blots of Huh 7.5 cells showing expression of TACR1 or TACR3 as indicated.

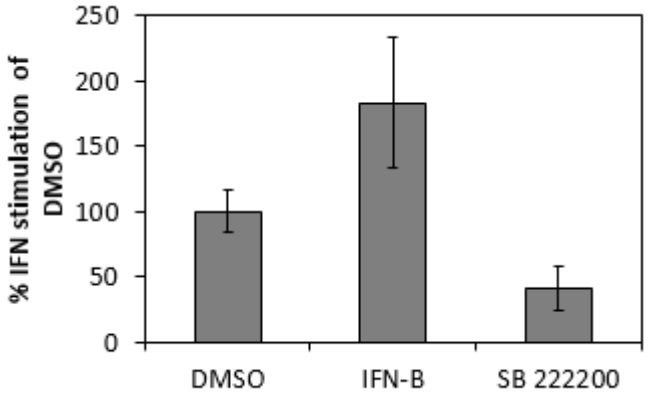

Figure 4.3. TACR3 antagonist SB 222200 reduces interferon signaling. Huh 7.5 cells were transfected with plasmids encoding an interferon stimulated reporter (Fluc) gene and a control plasmid encoding another reporter (Rluc) gene for 8 hours. After transfection cells were treated with 30 μM SB 222200 or 4 U/ml IFN-α for 24 hours. IFN stimulation was quantified based on relative reporter levels (Fluc/Rluc) measured from cell lysates. Error bars represent the standard deviation of duplicate wells of two independent experiments.

The high cytotoxicity exhibited by the tested drugs may be due to the fact that a hepatoma cell line was used, and TACR antagonists potentially have significant anti-tumor effects (209, 210).

The expression of both receptors in liver tissue has been implied based on an RT-PCR done by Pinto *et al.*, but their protein expression in these cells has never been published(207). Consistent with the published RNA levels, protein expression level of both receptors appeared to be relatively weak (Figure 4.2C). In addition, there appeared to be a number of bands on the Western blot potentially due to the presence of glycosylated and truncated forms of the receptors. It should be noted that expression of

both truncated and glycosylated forms of TACR1 has been described in lymphoblastic leukemia cells by Munoz *et al.* (211). We also attempted to reduce the expression TACR3 in these cells in order to study its effect on HCV infection. However our attempts to knockdown the expression using both commercial siRNA pools (Figure 4.4A) and shRNA expressed from a lentiviral expression vector (Figure 4.4B) were unsuccessful.

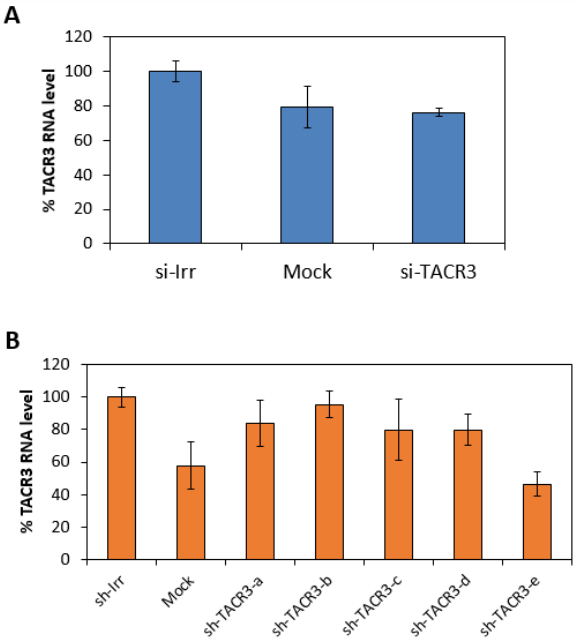

Figure 4.4. Attempted knockdown of TACR3 in Huh 7.5 cells. A. 2.8 x 10^6 Huh 7.5 cells were electroporated with 500 pmoles siRNA pools against TACR3, with irrelevant, scrambled siRNA (Irr), or PBS (mock). Relative TACR3 RNA levels were quantified 48 hours post electroporation by qRT-PCR. Error bars indicated the standard error obtained from duplicate wells. **B.** Huh 7.5 cells were transduced with pseudoparticles expressing shRNA against five different sequences of TACR3 mRNA (sh-TACR3-a-e). Three days post transduction, cellular RNA was isolated. Relative TACR3 mRNA levels were quantified by qRT-PCR. Error bars indicate the standard deviation obtained from duplicate wells.

The role of TACR in liver cells is currently unknown, but we were able to show to some extent that it may be functional in Huh 7.5 cells. This was done based on the known reliance of the interferon-pathway on PKC stimulation, and the fact that TACR has been involved in PKC activation in some cell lines (62, 208). By showing that TACR3 antagonist SB 222200 reduces the expression of an interferon-stimulated reporter gene, we indicate that receptor stimulation may lead to PKC activation in these cells. Interferon stimulation effectively inhibits HCV infection, therefore reducing interferon stimulation, *ceteris paribus,* should increase HCV infection. Therefore the role of the receptor in the HCV life cycle appears to not be limited to this pathway. In addition, the fact that there is a competing response to HCV replication (inhibition and potential enhancement) potentially explains why concentrations needed for HCV inhibition in these cells appear to be significantly greater than needed for receptor antagonism in other cell lines (212).

Here we demonstrated that both TACR1 and TACR3 antagonists significantly inhibit HCV infection. This makes TACR1 antagonists more attractive as antiviral drug candidates, due to their ability to inhibit both HCV and HIV. However their path to becoming approved drugs remains limited by the lack of bioavailability and the high dosage requirement of the only currently approved TACR1 antagonist, aprepitant (89, 213).

4.5 Materials and methods

4.5.1 Chemicals, bacterial strains and cell lines

Huh- 7.5 cells were obtained from Prof. Charles Rice (Rockefeller University).
Cell lines were cultured in complete growth medium (Dulbecco's Modified Eagle Medium (DMEM) containing 4500 mg/L glucose, 4.0 mM L- Glutamine, and 110 mg/L sodium pyruvate (Thermo Scientific HyClone) supplemented with 10 % fetal bovine serum (Atlanta Biologicals) and 1X non- essential amino acids (Thermo Scientific HyClone)).

CellTiter- Glo Luminescent Cell Viability Assay Kit and Luciferase Assay System were purchased from Promega. Biolux Gaussia Luciferase Assay Kit was purchased from New England Biolabs. Dulbecco's Phosphate- Buffered Saline (DPBS) was purchased from Thermo Scientific HyClone. OptiMEM was purchased from Invitrogen. Luria-Bertani (LB) broth, Mirus TransIT LT1, Fugene-6 transfection reagent and ampicillin were obtained from Thermo Fisher Scientific. 0.25% trypsin- EDTA was obtained from VWR International. Aprepitant was obtained from Toronto Research Chemicals. L 703606 was obtained from Sigma-Aldrich. SB 222200 was obtained from Tocris Bioscience. Osanetant was obtained from Axon MedChem.

4.5.2 shRNA expressing pseudoparticle production

shRNA-expressing pseudoparticles were generated based on a procedure previously described(90). Briefly, 293T cells were transfected for 6 hours with a 2:2:1 mass ratio of

HIV gag-pol, VSV-G, and shRNA expressing plasmid pLVTHM (19). The pLVTHM vector allows for expression of shRNA, and for identification of transduced cells based on GFP expression induced by a separate promoter. Cell supernatants containing VSV-G coated, shRNA expressing pp were collected 48 hours later, filtered and stored at -80 °C.

4.5.3 Production and titering of infectious HCVcc

JC1 HCVcc was generated from Huh 7.5 cells and titered as previously described(90). Briefly, 1 x 10^7 Huh 7.5 cells were suspended in 400 µl DPBS and electroporated with 5 µg JC1-nsGauss HCV RNA using using an ECM 830 electroporator (Harvard Apparatus) at the following settings: 650 V, 99-µs pulse length, 5 pulses, 1.1-s interval. Cell supernatants were collected at 72, 96, 120, 144, 168 hours post electroporation, filtered and stored at -80 °C.

4.5.4 HCV infection assay

Huh 7.5 cells were seeded into wells of a 96 well plate at ~20% confluency. 6 hours later, cells were treated with drugs at indicated concentrations before infection with Jc1 Gluc HCVcc at >0.1 MOI. 12-16 hours cells were washed and drug dilutions replaced. Cell supernatants were collected 48 hours post washing. HCV infection was quantified based on assayed Gluc levels in collected supernatants. Cell viability was quantified at this time using the CellTiter-Glo assay kit and by following the manufacturer's instructions.

4.5.5 Interferon stimulation assay

Huh 7.5 cells were seeded in a 24-well plate at 4 x 10^4 cells/well. The next, day cells were transfected with 0.5 µg/well of IFN-β reporter plasmid p125-Luc (214) and control plasmid pRL-TK at 10:1 mass ratios respectively, using Fugene-6 DNA transfection reagent. 24 hours later, cells were washed and treated with 30 µM SB 222200 or 4 U/ml IFN-α. Interferon signaling was determined based on intracellular Fluc levels measured 24 hours later. Fluc generation was normalized to transfection efficiency in each well based on assayed Rluc values in that well.

4.5.6 Western blotting

Huh 7.5 cells were seeded into wells of a 6 well plate at 6 x 10^5 cells per well. Two days post seeding cells were lysed using Renilla lysis buffer (Promega). Cell lysates were denatured by combining with an equal volume of 2X SDS loading buffer and heating at 95 °C for five minutes. Samples were separated using SDS-PAGE by running in a 12% acrylamide gel at 150 V for 60 minutes. After running samples were transferred to a PVDF membrane by running at 100 V for 80 minutes. Membranes were blocked in PBS containing 1% skim milk/0.1% Tween-20 (blocking buffer) for 30 minutes at room temperature. Next, membranes were incubated in blocking buffer containing 1000-fold diluted rabbit anti-TACR3 or 200-fold diluted goat anti-TACR1 primary antibodies (Santa Cruz Biotechnology), for 1 hour at room temperature. After incubation membranes were thoroughly washed with PBS before incubation with blocking buffer containing 1000-fold diluted HRP-conjugated goat anti-rabbit or donkey anti-goat

secondary antibodies as appropriate (Jackson ImmunoResearch) for 30 minutes at room temperature. Membranes were washed with PBS to remove blocking buffer, before development with West Femto Chemiluminescent HRP substrate (Pierce) and imaging.

5. CONCLUSIONS AND RECOMMENDATIONS

In this work, we have developed an *in vitro* screening method that identified HCV inhibiting proteins. This screen identified a positively charged protein, B1, which significantly inhibited Jc1 HCV replication. We also identified a number of positively charged peptides during the screen, but were unable to verify their HCV inhibition. Our work indicates that the expression of positively charged proteins may be tightly regulated by expressing cells. This regulation reduces the overall inhibition seen by such proteins. In addition, we showed that a recombinant positively charged protein, +36GFP, significantly inhibited HCV infection. While this inhibition was not observed with B1, it marks the first incidence of defensin-like inhibition of HCV infection. We went on to show that recombinant B1 had significant cell-transduction capability. We showed that B1 was capable of delivery covalently-attached protein cargo into a wide range of mammalian cell lines. We also showed that B1 was capable of complexing and then transfecting mRNA into target cells as efficiently as commercially available transfection reagents. While we were unable to determine the mechanism of B1 mediated protein transduction, we found that B1 mediated RNA transfection was strongly dependent on clathrin-mediated endocytosis, and mannan receptor-dependent phagocytosis. Finally, we described the HCV inhibition of TACR1 and TACR3 antagonists. However, this is not intended to be the end of the line for any of these findings and it is hoped that these

findings will stimulate further interest in these fields. In fact, we believe that these results may be built upon in several ways.

Firstly, the HCV inhibitor selection methodology outlined in section 2can potentially be enhanced and applied in different ways. Although the methodology was developed with the flexibility to identify inhibitors from any stage of the HCV life cycle, it can modified for more focused selection. This can be accomplished by using the fact that the developed cell line, n4mBID, uses a cell death based infection phenotype. Since only active HCV NS3-4A is required for initiation of the apoptotic cascade, n4mBID cells expressing only HCV NS3-4A are expected to be as apoptotic as HCV-infected n4mBID cells. As such, these cells can be used to screen for an HCV protease inhibitors. For example, in order to find small molecule inhibitors, seeded cells can be treated with inhibitor libraries, followed by transduction with pseudotyped lentivirals expressing HCV NS3-4A. In cells not treated with a protease inhibitor, significant cell death is expected at 3-4 days post transduction. Thus potential HCV protease inhibitors should be present in wells lacking significant cytotoxicity. Similarly, in order to find protein or peptide inhibitors of the HCV protease, a batch cells can first be transduced with a library of peptides/proteins using a lentiviral expression vector as done in section 2. After allowing time for gene expression, cells can then be transduced with lentivirals expressing HCV NS3-4A. After allowing 4-5 days for cell death, surviving cells can be rescued with the addition of a small molecule protease inhibitor such as VX950 (215). Selected lentivirals can be repackaged and used for subsequent rounds of selection, as

illustrated in Figure 2.1A. The advantages of this system, are that selected molecules will possess relatively little cytotoxicity, since they would be selected based on cell survival. Another advantage lies in the fact that the system allows for relatively easy validation of inhibition any of the genotypes of the HCV protease. This can be done simply by transducing cells treated with selected drugs, or expressing selected proteins with lentivirals expressing HCV NS3-4A of the desired genotype. However, disadvantages lie in the fact that drugs or proteins inhibiting lentiviral infection into these cells may be selected as false positives. In addition, drugs or proteins that inhibit caspase-mediated apoptosis may also be selected as false positives.

Secondly, the HCV inhibition of positively charged proteins can be explored further. Though our data indicates potential for HCV inhibition by both intracellularly expressed and externally supplied positively charged proteins, in both cases their overall expression levels result in less inhibition than could be possible. We can attempt to improve the intracellular expressional stability of these proteins by including short, negatively charged, covalently linked expressing partners. This approach can be attempted since it has been shown that some defensins are expressed with negatively charged propieces hypothesized to aid their expression and folding(216). As such, each expression partner should be designed such that the net charge on the construct approaches zero. In addition the cationic protein/peptide and its expression partner can be linked with a short repeat of a sequence such as: (glycine-glycine-serine) in order to promote proteolytic cleavage after expression, and release the ‘mature’ peptide/protein.

In addition, further work can be done to characterize the mechanism of inhibition of recombinant positively charged proteins.

Thirdly, the cellular transduction efficiency of B1 can be improved upon. Unfortunately, the crystal structure of B1 is currently unknown, and so modifications based on surface charge or surface residues cannot readily be made. In addition, since a single 'cell transduction' motif within B1 cannot be identified, no straight-forward truncations can be made that would result in a smaller, more active protein. As such, in order to generate a more active version of B1, we can generate a library of B1 mutants, and select for mutants with increased cellular transduction activity. These mutants can be selected based on their ability to gain access to the cytosol, and then nucleus in a high percentage of cells. To accomplish this, the transduction of Cre-B1 fusion proteins can be quantified within target cells expressing a LoxP-recombination-dependent Gluc reporter gene. The advantage of using Cre is that the gene expression in each cell is dependent on whether transduction happened, or not. As such the results will not be biased towards mutants which might be able to transduce large amounts of protein into some cells, and smaller amounts into the remaining cells. To accomplish the screening, individual mutants should be used to transduce single wells of Cre reporter cells seeded into individual wells. In addition, both any selected mutants, and the original B1 should be subjected to further biochemical analyses in order to solve their crystal structure. This will potentially allow for improved understanding of residues positively affecting cell transduction. In addition, the cytosolic delivery of B1 can also potentially be improved by the addition of

a fusiogenic peptide to the C or N terminal of B1. This should be attempted since addition of such peptides have been demonstrated to improve the endosomal escape of other cell transducing proteins(126).

We can also attempt to more conclusively determine the cellular transduction mechanism of B1. While we have shown that B1 mediated RNA transfection is dependent on endocytic and phagocytic processes (Figure 3.8), the mechanism of B1's protein transduction remains elusive. In the absence of direct membrane penetration, many cellular proteins must be involved in B1-mediated cellular transduction. We will attempt to identify some of these proteins by determining B1 transduction efficiency in their absence. Any cellular process involves a combination of many proteins working together, and so some must necessarily be more critical than others. For example while clathrin mediated endocytosis involves at least 30 intracellular proteins, blocking some of these (for example clathrin) has a much more detrimental effect than blocking others(217). However, we have shown that B1 mediated protein transduction may not be inhibited by blocking known endocytic pathways. This means that blocking or monitoring the activity of common markers of endocytic processes, such as the regulation of Rho and Rac GTAases, cannot be expected to yield very meaningful data. Since B1 appears to use an alternate or non-canonical pathway to enter cells, a broader approach to identifying these proteins must be taken (218, 219). In order to efficiently identify these genes, we will screen for activity from a library of candidates. Such an approach has been used to identify viral entry factors by using siRNA libraries to knock

down cellular proteins (220, 221). We can accomplish this by using an siRNA library designed to knock down genes associated with membrane trafficking, and then quantifying B1 protein transduction in their absence. Genes appearing as hits can be further characterized by using shRNA targeting identified genes to generate stable cell populations with these genes knocked out. At the same time, we can generate cell lines that over-express these genes, and determine the relative transduction efficiency in these cells, compared with naïve cells. If the targeted genes are solely responsible, or represent a limiting step in the process, then overexpressing them should increase transduction efficiency. We can also confirm the role of identified genes by attempting transduction in the presence of drugs that block their action, if such drugs are available. Finally we can compare the role of the identified genes in B1 transduction with the transduction of other CPPs. Using our knock-out cell lines and naïve cell lines, we will compare the transduction efficiency of Cre-Tat, Cre-R10, and Cre-+36GFP with Cre-B1. These experiments should provide some definitive comparisons of the mechanisms used by these CPPs.

Finally, we can find an improved TACR1 or TACR3 antagonist that may have a more favorable pharmacological profile *in vivo*. This can be done by testing the anti-HCV activity TACR1/3 antagonists with more limited ability to cross the blood-brain barrier, and with increased oral bioavailability. Though such drugs would be less attractive for the more traditional antiemetic and analgesic indications of TACR antagonists, they would undoubtedly present less unintended side effects when used *in vivo*.

REFERENCES

1. Lohmann V, Hoffmann S, Herian U, Penin F, & Bartenschlager R (2003) Viral and cellular determinants of hepatitis C virus RNA replication in cell culture. *Journal of Virology* 77(5):3007-3019.
2. Mohd Hanafiah K, Groeger J, Flaxman AD, & Wiersma ST (2013) Global epidemiology of hepatitis C virus infection: New estimates of age-specific antibody to HCV seroprevalence. *Hepatology* 57(4):1333-1342.
3. Brown RS (2005) Hepatitis C and liver transplantation. *Nature* 436(7053):973-978.
4. McHutchison JG*, et al.* (1998) Interferon alfa-2b alone or in combination with ribavirin as initial treatment for chronic hepatitis C. *New England Journal of Medicine* 339(21):1485-1492.
5. Manns MP*, et al.* (2001) Peginterferon alfa-2b plus ribavirin compared with interferon alfa-2b plus ribavirin for initial treatment of chronic hepatitis C: a randomised trial. *The Lancet* 358(9286):958-965.
6. Dusheiko G (1997) Side effects of alpha interferon in chronic hepatitis C. *Hepatology* 26(3):S112-S121.
7. Zeuzem S*, et al.* (2006) Efficacy of 24 weeks treatment with peginterferon alfa-2b plus ribavirin in patients with chronic hepatitis C infected with genotype 1 and low pretreatment viremia. *Journal of Hepatology* 44(1):97-103.

8. Maasoumy B*, et al.* (2013) Eligibility and safety of triple therapy for hepatitis C: lessons learned from the first experience in a real world setting. *PLoS ONE* 8(2):e55285.

9. Lok AS*, et al.* (2012) Preliminary study of two antiviral agents for hepatitis C genotype 1. *New England Journal of Medicine* 366(3):216-224.

10. Dusheiko G & Wedemeyer H (2012) New protease inhibitors and direct-acting antivirals for hepatitis C: interferon's long goodbye. *Gut* 61(12):1647-1652.

11. Martell M*, et al.* (1992) Hepatitis C virus (HCV) circulates as a population of different but closely related genomes: quasispecies nature of HCV genome distribution. *Journal of Virology* 66(5):3225-3229.

12. Ribeiro RM*, et al.* (2012) Quantifying the diversification of hepatitis C virus (HCV) during primary infection: estimates of the *in vivo* mutation rate. *PLoS Pathogens* 8(8):e1002881.

13. Simmonds P*, et al.* (2005) Consensus proposals for a unified system of nomenclature of hepatitis C virus genotypes. *Hepatology* 42(4):962-973.

14. Tomei L, Failla C, Santolini E, De Francesco R, & La Monica N (1993) NS3 is a serine protease required for processing of hepatitis C virus polyprotein. *Journal of Virology* 67(7):4017-4026.

15. Kim DW, Gwack Y, Han JH, & Choe J (1995) C-terminal domain of the hepatitis C virus NS3 protein contains an RNA helicase activity. *Biochemical and Biophysical Research Communications* 215(1):160-166.

16. Behrens SE, Tomei L, & De Francesco R (1996) Identification and properties of the RNA-dependent RNA polymerase of hepatitis C virus. *The EMBO Journal* 15(1):12-22.

17. Scarselli E*, et al.* (2002) The human scavenger receptor class B type I is a novel candidate receptor for the hepatitis C virus. *The EMBO Journal* 21(19):5017-5025.

18. Cormier EG*, et al.* (2004) CD81 is an entry coreceptor for hepatitis C virus. *Proceedings of the National Academy of Sciences of the United States of America* 101(19):7270-7274.

19. Evans MJ*, et al.* (2007) Claudin-1 is a hepatitis C virus co-receptor required for a late step in entry. *Nature* 446(7137):801-805.

20. Ploss A*, et al.* (2009) Human occludin is a hepatitis C virus entry factor required for infection of mouse cells. *Nature* 457(7231):882-886.

21. Sainz B*, et al.* (2012) Identification of the Niemann-Pick C1-like 1 cholesterol absorption receptor as a new hepatitis C virus entry factor. *Nature Medicine* 18(2):281-285.

22. Lavillette D*, et al.* (2007) Characterization of fusion determinants points to the involvement of three discrete regions of both E1 and E2 glycoproteins in the membrane fusion process of hepatitis C virus. *Journal of Virology* 81(16):8752-8765.

23. Hsu M*, et al.* (2003) Hepatitis C virus glycoproteins mediate pH-dependent cell entry of pseudotyped retroviral particles. *Proceedings of the National Academy of Sciences of the United States of America* 100(12):7271-7276.

24. Appel N, Schaller T, Penin F, & Bartenschlager R (2006) From structure to function: new insights into hepatitis C virus RNA replication. *Journal of Biological Chemistry* 281(15):9833-9836.

25. Fukushi S*, et al.* (1997) The sequence element of the internal ribosome entry site and a 25-kilodalton cellular protein contribute to efficient internal initiation of translation of hepatitis C virus RNA. *Journal of Virology* 71(2):1662-1666.

26. Grakoui A, Wychowski C, Lin C, Feinstone SM, & Rice CM (1993) Expression and identification of hepatitis C virus polyprotein cleavage products. *Journal of Virology* 67(3):1385-1395.

27. Bartenschlager R & Lohmann V (2000) Replication of hepatitis C virus. *Journal of General Virology* 81(7):1631-1648.

28. Egger D*, et al.* (2002) Expression of hepatitis C virus proteins induces distinct membrane alterations including a candidate viral replication complex. *Journal of Virology* 76(12):5974-5984.

29. Gosert R*, et al.* (2003) Identification of the hepatitis C virus RNA replication complex in Huh-7 cells harboring subgenomic replicons. *Journal of Virology* 77(9):5487-5492.

30. Moradpour D, Penin F, & Rice CM (2007) Replication of hepatitis C virus. *Nature Reviews in Microbiology* 5(6):453-463.

31. Clavel F & Hance AJ (2004) HIV drug resistance. *The New England Journal Of Medicine* 350(10):1023-1035.

32. Jones DM & McLauchlan J (2010) Hepatitis C virus: assembly and release of virus particles. *Journal of Biological Chemistry* 285(30):22733-22739.

33. Choo Q*, et al.* (1989) Isolation of a cDNA clone derived from a blood-borne non-A, non-B viral hepatitis genome. *Science* 244(4902):359-362.

34. Bartenschlager R (2002) Hepatitis C virus replicons: potential role for drug development. *Nature Reviews in Drug Discovery* 1(11):911-916.

35. Bartenschlager R (2006) Hepatitis C virus molecular clones: from cDNA to infectious virus particles in cell culture. *Current Opinion in Microbiology* 9(4):416-422.

36. Lohmann V*, et al.* (1999) Replication of subgenomic hepatitis C virus RNAs in a hepatoma cell line. *Science* 285(5424):110-113.

37. Bartosch B, Dubuisson J, & Cosset F-L (2003) Infectious hepatitis C virus pseudo-particles containing functional E1–E2 envelope protein complexes. *The Journal of Experimental Medicine* 197(5):633-642.

38. Lindenbach BD*, et al.* (2005) Complete replication of hepatitis C virus in cell culture. *Science* 309(5734):623-626.

39. Kato T*, et al.* (2003) Efficient replication of the genotype 2a hepatitis C virus subgenomic replicon. *Gastroenterology* 125(6):1808-1817.

40. Kato T*, et al.* (2001) Sequence analysis of hepatitis C virus isolated from a fulminant hepatitis patient. *Journal of Medical Virology* 64(3):334-339.

41. Pietschmann T*, et al.* (2006) Construction and characterization of infectious intragenotypic and intergenotypic hepatitis C virus chimeras. *Proceedings of the National Academy of Sciences* 103(19):7408-7413.

42. Scheel TKH*, et al.* (2008) Development of JFH1-based cell culture systems for hepatitis C virus genotype 4a and evidence for cross-genotype neutralization. *Proceedings of the National Academy of Sciences* 105(3):997-1002.

43. Yanagi M, Purcell RH, Emerson SU, & Bukh J (1999) Hepatitis C virus: an infectious molecular clone of a second major genotype (2a) and lack of viability of intertypic 1a and 2a chimeras. *Virology* 262(1):250-263.

44. Steinmann E, Brohm C, Kallis S, Bartenschlager R, & Pietschmann T (2008) Efficient trans-encapsidation of hepatitis C virus RNAs into infectious virus-like particles. *Journal of Virology* 82(14):7034-7046.

45. Horvath CM (2004) The Jak-STAT Pathway Stimulated by Interferon alpha or Interferon beta. *Science Signalling* 2004(260):tr10-.

46. Watashi K*, et al.* (2005) Cyclophilin B is a functional regulator of hepatitis C virus RNA polymerase. *Molecular Cell* 19(1):111-122.

47. Lawitz E*, et al.* (2011) Safety, pharmacokinetics, and antiviral activity of the cyclophilin inhibitor NIM811 alone or in combination with pegylated interferon in HCV-infected patients receiving 14 days of therapy. *Antiviral Research* 89(3):238-245.

48. Habersetzer F*, et al.* (2011) A poxvirus vaccine is safe, induces T-cell responses, and decreases viral load in patients with chronic hepatitis C. *Gastroenterology* 141(3):890-899.e894.

49. Fournillier A*, et al.* (2007) An accelerated vaccine schedule with a poly-antigenic hepatitis C virus MVA-based candidate vaccine induces potent, long lasting and *in vivo* cross-reactive T cell responses. *Vaccine* 25(42):7339-7353.

50. Ortiz R*, et al.* (2008) Efficacy and safety of once-daily darunavir/ritonavir versus lopinavir/ritonavir in treatment-naive HIV-1-infected patients at week 48. *AIDS* 22(12):1389-1397 1310.1097/QAD.1380b1013e32830285fb.

51. Perni RB*, et al.* (2006) Preclinical profile of VX-950, a potent, selective, and orally bioavailable inhibitor of hepatitis C virus NS3-4A serine protease. *Antimicrobial Agents and Chemotherapy* 50(3):899-909.

52. Hinrichsen H*, et al.* (2004) Short-term antiviral efficacy of BILN 2061, a hepatitis C virus serine protease inhibitor, in hepatitis C genotype 1 patients. *Gastroenterology* 127(5):1347-1355.

53. Hézode C*, et al.* (2009) Telaprevir and Peginterferon with or without Ribavirin for Chronic HCV Infection. *New England Journal of Medicine* 360(18):1839-1850.

54. McHutchison JG*, et al.* (2009) Telaprevir with peginterferon and ribavirin for chronic HCV genotype 1 infection. *New England Journal of Medicine* 360(18):1827-1838.

55. Abu Dayyeh BK*, et al.* (2011) Il28b alleles exert an additive dose effect when applied to HCV-HIV coinfected persons undergoing peginterferon and ribavirin therapy. *PLoS ONE* 6(10):e25753.

56. Malcolm BA*, et al.* (2006) SCH 503034, a mechanism-based inhibitor of hepatitis C virus NS3 protease, suppresses polyprotein maturation and enhances the antiviral activity of alpha interferon in replicon cells. *Antimicrobial Agents and Chemotherapy* 50(3):1013-1020.

57. Venkatraman S*, et al.* (2006) Discovery of (1R,5S)-N-[3-Amino-1-(cyclobutylmethyl)-2,3-dioxopropyl]- 3-[2(S)-[[[(1,1-dimethylethyl)amino]carbonyl]amino]-3,3-dimethyl-1-oxobutyl]- 6,6-dimethyl-3-azabicyclo[3.1.0]hexan-2(S)-carboxamide (SCH 503034), a selective, potent, orally bioavailable hepatitis C virus NS3 protease inhibitor: a potential therapeutic agent for the treatment of hepatitis C infection. *Journal of Medicinal Chemistry* 49(20):6074-6086.

58. Susser S*, et al.* (2009) Characterization of resistance to the protease inhibitor boceprevir in hepatitis C virus–infected patients. *Hepatology* 50(6):1709-1718.

59. Kwo PY*, et al.* (Efficacy of boceprevir, an NS3 protease inhibitor, in combination with peginterferon alfa-2b and ribavirin in treatment-naive patients with genotype 1 hepatitis C infection (SPRINT-1): an open-label, randomised, multicentre phase 2 trial. *The Lancet* 376(9742):705-716.

60. Poordad F*, et al.* (2011) Boceprevir for untreated chronic HCV genotype 1 infection. *New England Journal of Medicine* 364(13):1195-1206.

61. Bacon BR, *et al.* (2011) Boceprevir for previously treated chronic HCV genotype 1 infection. *New England Journal of Medicine* 364(13):1207-1217.

62. Khawaja AM & Rogers DF (1996) Tachykinins: receptor to effector. *The International Journal of Biochemistry & Cell Biology* 28(7):721-738.

63. Bucsics A, Holzer P, & Lembeck F (1983) The substance P content of peripheral tissues in several mammals. *Peptides* 4(4):451-455.

64. Metwali A, *et al.* (1994) Eosinophils within the healthy or inflamed human intestine produce substance P and vasoactive intestinal peptide. *Journal of Neuroimmunology* 52(1):69-78.

65. Luber-Narod J, Boyd ND, & Leeman SE (1990) Guanine nucleotides decrease the affinity of substance P binding to its receptor. *European Journal Pharmacology* 188(4-5):185-191.

66. Maggi CA, Patacchini R, Rovero P, & Giachetti A (1993) Tachykinin receptors and tachykinin receptor antagonists. *Journal of Autonomic Pharmacology* 13(1):23-93.

67. Gerard NP, Bao L, Xiao-Ping H, & Gerard C (1993) Molecular aspects of the tachykinin receptors. *Regulatory Peptides* 43(1-2):21-35.

68. Grandordy BM, Frossard N, Rhoden KJ, & Barnes PJ (1988) Tachykinin-induced phosphoinositide breakdown in airway smooth muscle and epithelium: relationship to contraction. *Molecular Pharmacology* 33(5):515-519.

69. Mikoshiba K (2007) IP3 receptor/Ca2+ channel: from discovery to new signaling concepts. *Journal of Neurochemistry* 102(5):1426-1446.

70. Gallacher DV*, et al.* (1990) Substance P and bombesin elevate cytosolic Ca2+ by different molecular mechanisms in a rat pancreatic acinar cell line. *Journal of Physiology* 426:193-207.

71. Munoz M & Covenas R (2010) Neurokinin-1 receptor: a new promising target in the treatment of cancer. *Discovery Medicine* 10(53):305-313.

72. Hokfelt T, Pernow B, & Wahren J (2001) Substance P: a pioneer amongst neuropeptides. *Journal of Internal Medicine* 249(1):27-40.

73. Ho W-Z & Douglas SD (2004) Substance P and neurokinin-1 receptor modulation of HIV. *Journal of Neuroimmunology* 157(1–2):48-55.

74. Keller M*, et al.* (2006) Lack of efficacy of the substance P (Neurokinin1 receptor) antagonist aprepitant in the treatment of major depressive disorder. *Biological Psychiatry* 59(3):216-223.

75. de Wit R*, et al.* (2004) The oral NK1 antagonist, aprepitant, given with standard antiemetics provides protection against nausea and vomiting over multiple cycles of cisplatin-based chemotherapy: a combined analysis of two randomised, placebo-controlled phase III clinical trials. *European Journal of Cancer* 40(3):403-410.

76. Nygren P*, et al.* (2005) Lack of effect of aprepitant on the pharmacokinetics of docetaxel in cancer patients. *Cancer Chemotherapy and Pharmacology* 55(6):609-616.

77. Green SA*, et al.* (2006) Efficacy and safety of a Neurokinin-1 receptor antagonist in postmenopausal women with overactive bladder with urge urinary incontinence. *The Journal of Urology* 176(6):2535-2540.

78. Dionne RA*, et al.* (1998) The substance P receptor antagonist CP-99,994 reduces acute postoperative pain[ast]. *Clinical Pharmacology & Therapeutics* 64(5):562-568.

79. Lecci A, Capriati A, & Maggi CA (2004) Tachykinin NK2 receptor antagonists for the treatment of irritable bowel syndrome. *British Journal of Pharmacology* 141(8):1249-1263.

80. Van Schoor J, Joos G, Chasson B, Brouard R, & Pauwels R (1998) The effect of the NK2 tachykinin receptor antagonist SR 48968 (saredutant) on neurokinin A-induced bronchoconstriction in asthmatics. *European Respiratory Journal* 12(1):17-23.

81. Meltzer HY, Arvanitis L, Bauer D, & Rein W (2004) Placebo-controlled evaluation of four novel compounds for the treatment of schizophrenia and schizoaffective disorder. *American Journal of Psychiatry* 161(6):975-984.

82. Zimmer G*, et al.* (2003) Virokinin, a bioactive peptide of the tachykinin family, is released from the fusion protein of bovine respiratory syncytial virus. *Journal of Biological Chemistry* 278(47):46854-46861.

83. Wang X*, et al.* (2007) Neurokinin-1 receptor antagonist (aprepitant) inhibits drug-resistant HIV-1 infection of macrophages *in vitro*. *Journal of Neuroimmune Pharmacology* 2(1):42-48.

84. Douglas SD*, et al.* (2001) Elevated substance P levels in HIV-infected men. *AIDS* 15(15):2043-2045.

85. Ho WZ*, et al.* (1996) Substance P modulates human immunodeficiency virus replication in human peripheral blood monocyte-derived macrophages. *AIDS Research and Human Retroviruses* 12(3):195-198.

86. Li Y, Douglas SD, Song L, Sun S, & Ho WZ (2001) Substance P enhances HIV-1 replication in latently infected human immune cells. *Journal of Neuroimmunology* 121(1-2):67-75.

87. Lai J-P*, et al.* (2001) Substance P antagonist (CP-96,345) inhibits HIV-1 replication in human mononuclear phagocytes. *Proceedings of the National Academy of Sciences of the United States of America* 98(7):3970-3975.

88. Wang X, Douglas S, Song L, Wang Y-J, & Ho W-Z (2008) Neurokinin-1 receptor antagonist (aprepitant) suppresses HIV-1 infection of microglia/macrophages. *Journal of Neuroimmune Pharmacology* 3(4):257-264.

89. Tebas P*, et al.* (2011) A randomized, placebo controlled, double masked phase IB study evaluating the safety and antiviral activity of aprepitant, a Neurokinin-1 receptor antagonist in HIV-1 infected adults. *PLoS ONE* 6(9):e24180.

90. Chockalingam K, Simeon RL, Rice CM, & Chen Z (2010) A cell protection screen reveals potent inhibitors of multiple stages of the hepatitis C virus life cycle. *Proceedings of the National Academy of Sciences* 107(8):3764-3769.

91. Gudkov AV & Roninson IB (1997) Isolation of genetic suppressor elements (GSEs) from random fragment cDNA libraries in retroviral vectors. *Methods in Molecular Biology*), pp 221-240.

92. Wunner WH, Pallatroni C, & Curtis PJ (2004) Selection of genetic inhibitors of rabies virus. *Archives of Virology* 149(8):1653-1662.

93. Dunn SJ*, et al.* (1999) Isolation of efficient antivirals: genetic suppressor elements against HIV-1. *Gene Therapy* 6(1):130-137.

94. Tscherne DM, Evans MJ, MacDonald MR, & Rice CM (2008) Transdominant inhibition of bovine viral diarrhea virus entry. *Journal of Virology* 82(5):2427-2436.

95. Lalezari JP*, et al.* (2003) A phase II clinical study of the long-term safety and antiviral activity of enfuvirtide-based antiretroviral therapy. *AIDS* 17(5):691-698.

96. Robertson D (2003) US FDA approves new class of HIV therapeutics. *Nature Biotechnology* 21(5):470-471.

97. Chen Z, Simeon RL, Chockalingam K, & Rice CM (2010) Creation and characterization of a cell-death reporter cell line for hepatitis C virus infection. *Antiviral Research* 86(2):220-223.

98. Blight KJ, McKeating JA, & Rice CM (2002) Highly permissive cell lines for subgenomic and genomic hepatitis C virus RNA replication. *Journal of Virology* 76(24):13001-13014.

99. Strasser A (2005) The role of BH3-only proteins in the immune system. *Nature Reviews in Immunology* 5(3):189-200.

100. Felgner PL*, et al.* (1987) Lipofection: a highly efficient, lipid-mediated DNA-transfection procedure. *Proceedings of the National Academy of Sciences* 84(21):7413-7417.

101. Rose JK, Buonocore L, & Whitt MA (1991) A new cationic liposome reagent mediating nearly quantitative transfection of animal cells. *BioTechniques* 10(4):520.

102. Vigneron J-P*, et al.* (1996) Guanidinium-cholesterol cationic lipids: efficient vectors for the transfection of eukaryotic cells. *Proceedings of the National Academy of Sciences* 93(18):9682-9686.

103. Pun SH*, et al.* (2004) Cyclodextrin-modified polyethylenimine polymers for gene delivery. *Bioconjugate Chemistry* 15(4):831-840.

104. Boussif O*, et al.* (1995) A versatile vector for gene and oligonucleotide transfer into cells in culture and *in vivo*: polyethylenimine. *Proceedings of the National Academy of Sciences* 92(16):7297-7301.

105. Kam NWS, Liu Z, & Dai H (2005) Functionalization of carbon nanotubes via cleavable disulfide bonds for efficient intracellular delivery of siRNA and potent gene silencing. *Journal of the American Chemical Society* 127(36):12492-12493.

106. Pantarotto D*, et al.* (2004) Functionalized carbon nanotubes for plasmid DNA gene delivery. *Angewandte Chemie* 116(39):5354-5358.

107. Bianco A, Kostarelos K, Partidos CD, & Prato M (2005) Biomedical applications of functionalised carbon nanotubes. *Chemical Communications* (5):571-577.

108. Rosi NL*, et al.* (2006) Oligonucleotide-modified gold nanoparticles for intracellular gene regulation. *Science* 312(5776):1027-1030.

109. Sandhu KK, McIntosh CM, Simard JM, Smith SW, & Rotello VM (2002) Gold nanoparticle-mediated transfection of mammalian cells. *Bioconjugate Chemistry* 13(1):3-6.

110. Han G, Ghosh P, De M, & Rotello VM (2007) Drug and gene delivery using gold nanoparticles. *Nanobiotechnology* 3(1):40-45.

111. Gu Z, Biswas A, Zhao M, & Tang Y (2011) Tailoring nanocarriers for intracellular protein delivery. *Chemical Society Reviews* 40(7):3638-3655.

112. Biswas A*, et al.* (2011) Endoprotease-mediated intracellular protein delivery using nanocapsules. *ACS Nanotechnology* 5(2):1385-1394.

113. Frankel AD & Pabo CO (1988) Cellular uptake of the tat protein from human immunodeficiency virus. *Cell* 55(6):1189-1193.

114. Vives E (2005) Present and future of cell-penetrating peptide mediated delivery systems: "Is the Trojan horse too wild to go only to Troy?". *Journal of Controlled Release* 109(1–3):77-85.

115. Ho A, Schwarze SR, Mermelstein SJ, Waksman G, & Dowdy SF (2001) Synthetic protein transduction domains: enhanced transduction potential *in vitro* and *in vivo*. *Cancer Research* 61(2):474-477.

116. Wadia JS, Stan RV, & Dowdy SF (2004) Transducible TAT-HA fusogenic peptide enhances escape of TAT-fusion proteins after lipid raft macropinocytosis. *Nature Medicine* 10(3):310-315.

117. Fawell S*, et al.* (1994) Tat-mediated delivery of heterologous proteins into cells. *Proceedings of the National Academy of Sciences* 91(2):664-668.

118. Becker-Hapak M, McAllister SS, & Dowdy SF (2001) TAT-mediated protein transduction into mammalian cells. *Methods* 24(3):247-256.

119. Xia H, Mao Q, & Davidson BL (2001) The HIV Tat protein transduction domain improves the biodistribution of beta-glucuronidase expressed from recombinant viral vectors. *Nature Biotechnology* 19(7):640-644.

120. Wadia JS & Dowdy SF (2003) Modulation of cellular function by TAT mediated transduction of full length proteins. *Current Protein & Peptide Science* 4(2):97-104.

121. Thorén PEG, Persson D, Karlsson M, & Nordén B (2000) The Antennapedia peptide penetratin translocates across lipid bilayers – the first direct observation. *FEBS Letters* 482(3):265-268.

122. Joliot A, Pernelle C, Deagostini-Bazin H, & Prochiantz A (1991) Antennapedia homeobox peptide regulates neural morphogenesis. *Proceedings of the National Academy of Sciences* 88(5):1864-1868.

123. Kueltzo LA, Normand N, O'Hare P, & Middaugh CR (2000) Conformational lability of herpesvirus protein VP22. *Journal of Biological Chemistry* 275(43):33213-33221.

124. Qi X, Droste T, & Kao CC (2010) Cell-penetrating peptides derived from viral capsid proteins. *Molecular Plant-Microbe Interactions* 24(1):25-36.

125. Mitchell DJ, Steinman L, Kim DT, Fathman CG, & Rothbard JB (2000) Polyarginine enters cells more efficiently than other polycationic homopolymers. *The Journal of Peptide Research* 56(5):318-325.

126. McNaughton BR, Cronican JJ, Thompson DB, & Liu DR (2009) Mammalian cell penetration, siRNA transfection, and DNA transfection by supercharged proteins. *Proceedings of the National Academy of Sciences* 106(15):6111-6116.

127. Cronican James J*, et al.* (2011) A class of human proteins that deliver functional proteins into mammalian cells *in vitro* and *in vivo*. *Chemistry & Biology* 18(7):833-838.

128. Morris MC, Depollier J, Mery J, Heitz F, & Divita G (2001) A peptide carrier for the delivery of biologically active proteins into mammalian cells. *Nature Biotechnology* 19(12):1173-1176.

129. Crombez L*, et al.* (2008) A new potent secondary amphipathic cell-penetrating peptide for siRNA delivery into mammalian cells. *Molecular Therapy* 17(1):95-103.

130. Thompson David B, Villaseñor R, Dorr Brent M, Zerial M, & Liu David R (2012) Cellular uptake mechanisms and endosomal trafficking of supercharged proteins. *Chemistry & Biology* 19(7):831-843.

131. Mäger I, Langel K, Lehto T, Eiríksdóttir E, & Langel Ü (2012) The role of endocytosis on the uptake kinetics of luciferin-conjugated cell-penetrating

peptides. *Biochimica et Biophysica Acta (BBA) - Biomembranes* 1818(3):502-511.

132. Milletti F (2012) Cell-penetrating peptides: classes, origin, and current landscape. *Drug Discovery Today* 17(15–16):850-860.

133. Waugh J, Lee J, Dake M, & Browne D (2011) Nonclinical and clinical experiences with CPP-based self-assembling peptide systems in topical drug development. *Cell-Penetrating Peptides,* Methods in Molecular Biology, ed Langel Ü (Humana Press), Vol 683, pp 553-572.

134. Miyaji Y*, et al.* (2011) Distribution of KAI-9803, a novel δ-protein kinase C inhibitor, after intravenous administration to rats. *Drug Metabolism and Disposition* 39(10):1946-1953.

135. Wiegler K, Bonny C, Coquoz D, & Hirt L (2008) The JNK inhibitor XG-102 protects from ischemic damage with delayed intravenous administration also in the presence of recombinant tissue plasminogen activator. *Cerebrovascular Diseases* 26(4):360-366.

136. Meyer-Losic F*, et al.* (2008) DTS-108, a novel peptidic prodrug of SN38: in vivo efficacy and toxicokinetic studies. *Clinical Cancer Research* 14(7):2145-2153.

137. Rothbard JB*, et al.* (2000) Conjugation of arginine oligomers to cyclosporin A facilitates topical delivery and inhibition of inflammation. *Nature Medicine* 6(11):1253-1257.

138. Flynn CR*, et al.* (2010) Internalization and intracellular trafficking of a PTD-conjugated anti-fibrotic peptide, AZX100, in human dermal keloid fibroblasts. *Journal of Pharmaceutical Sciences* 99(7):3100-3121.

139. Lopes LB*, et al.* (2009) Cell permeant peptide analogues of the small heat shock protein, HSP20, reduce TGF-beta1-induced CTGF expression in keloid fibroblasts. *Journal of Investigative Dermatology* 129(3):590-598.

140. Wasley A & Alter MJ (2000) Epidemiology of hepatitis C: geographic differences and temporal trends. *Seminars in Liver Disease* 20(01):0001-0016.

141. W.H.O. (2012) Guidance on prevention of viral Hepatitis B and C among people who inject drugs. *Geneva, World Health Organization*.

142. Hadziyannis SJ*, et al.* (2004) Peginterferon-alpha2a and ribavirin combination therapy in chronic hepatitis C: a randomized study of treatment duration and ribavirin dose. *Annals of Internal Medicine* 140(5):346-355.

143. Halfon P & Locarnini S (2011) Hepatitis C virus resistance to protease inhibitors. *Journal of Hepatology* 55(1):192-206.

144. Thompson AJ, Locarnini SA, & Beard MR (2011) Resistance to anti-HCV protease inhibitors. *Current Opinion in Virology* 1(6):599-606.

145. Roninson IB*, et al.* (1995) Genetic suppressor elements: new tools for molecular oncology--thirteenth Cornelius P. Rhoads Memorial Award Lecture. *Cancer Research* 55(18):4023-4028.

146. Holzmayer TA, Pestov DG, & Roninson IB (1992) Isolation of dominant negative mutants and inhibitory antisense RNA sequences by expression selection of random DNA fragments. *Nucleic Acids Research* 20(4):711-717.

147. Garkavtsev I, Kazarov A, Gudkov A, & Riabowol K (1996) Suppression of the novel growth inhibitor p33ING1 promotes neoplastic transformation. *Nature Genetics* 14(4):415-420.

148. Gudkov AV*, et al.* (1994) Cloning mammalian genes by expression selection of genetic suppressor elements: association of kinesin with drug resistance and cell immortalization. *Proceedings of the National Academy of Sciences* 91(9):3744-3748.

149. Levenson VV*, et al.* (1999) A combination of genetic suppressor elements produces resistance to drugs inhibiting DNA replication. *Somatic Cell Molecular Genetics* 25(1):9-26.

150. Novoa I, Zeng H, Harding HP, & Ron D (2001) Feedback inhibition of the unfolded protein response by GADD34-mediated dephosphorylation of eIF2alpha. *Journal of Biological Chemistry* 153(5):1011-1022.

151. Primiano T*, et al.* (2003) Identification of potential anticancer drug targets through the selection of growth-inhibitory genetic suppressor elements. *Cancer Cell* 4(1):41-53.

152. Dunn SJ*, et al.* (2004) Identification of cell surface targets for HIV-1 therapeutics using genetic screens. *Virology* 321(2):260-273.

153. Newcomer BW*, et al.* (2013) Effect of treatment with a cationic antiviral compound on acute infection with bovine viral diarrhea virus. *Canadian Journal of Veterinary Research* 77(3):170-176.

154. Yang T-T, Cheng L, & Kain SR (1996) Optimized codon usage and chromophore mutations provide enhanced sensitivity with the green fluorescent protein. *Nucleic Acids Research* 24(22):4592-4593.

155. Cowan S*, et al.* (2002) Cellular inhibitors with FV1-like activity restrict human and simian immunodeficiency virus tropism. *Proceedings of the National Academy of Sciences* 99(18):11914-11919.

156. Wölk B*, et al.* (2000) Subcellular localization, stability, and trans-cleavage competence of the hepatitis C virus NS3-NS4A complex expressed in tetracycline-regulated cell lines. *Journal of Virology* 74(5):2293-2304.

157. Gao L, Aizaki H, He J-W, & Lai MMC (2004) Interactions between Viral Nonstructural Proteins and Host Protein hVAP-33 Mediate the Formation of Hepatitis C Virus RNA Replication Complex on Lipid Raft. *Journal of Virology* 78(7):3480-3488.

158. Tu H*, et al.* (1999) Hepatitis C virus RNA polymerase and NS5A complex with a SNARE-like protein. *Virology* 263(1):30-41.

159. Miyanari Y*, et al.* (2007) The lipid droplet is an important organelle for hepatitis C virus production. *Nature Cell Biology* 9(9):1089-1097.

160. Carroll SS, *et al.* (2003) Inhibition of hepatitis C virus RNA replication by 2′-modified nucleoside analogs. *Journal of Biological Chemistry* 278(14):11979-11984.

161. Prasher DC, Eckenrode VK, Ward WW, Prendergast FG, & Cormier MJ (1992) Primary structure of the Aequorea victoria green-fluorescent protein. *Gene* 111(2):229-233.

162. Cormack BP, Valdivia RH, & Falkow S (1996) FACS-optimized mutants of the green fluorescent protein (GFP). *Gene* 173(1):33-38.

163. Marukian S, *et al.* (2008) Cell culture–produced hepatitis C virus does not infect peripheral blood mononuclear cells. *Hepatology* 48(6):1843-1850.

164. Burns JC, Friedmann T, Driever W, Burrascano M, & Yee J-K (1993) Vesicular stomatitis virus G glycoprotein pseudotyped retroviral vectors: concentration to very high titer and efficient gene transfer into mammalian and nonmammalian cells. *Proceedings of the National Academy of Sciences* 90(17):8033-8037.

165. Hahm B, Kim YK, Kim JH, Kim TY, & Jang SK (1998) Heterogeneous nuclear ribonucleoprotein L interacts with the 3′ border of the internal ribosomal entry site of hepatitis C virus. *Journal of Virology* 72(11):8782-8788.

166. Honda M, *et al.* (2000) Cell cycle regulation of hepatitis C virus internal ribosomal entry site-directed translation. *Gastroenterology* 118(1):152-162.

167. Maqbool MA, *et al.* (2013) Regulation of hepatitis C virus replication by nuclear translocation of nonstructural 5A protein and transcriptional activation of host genes. *Journal of Virology* 87(10):5523-5539.

168. Phan T, Kohlway A, Dimberu P, Pyle AM, & Lindenbach BD (2011) The Acidic Domain of Hepatitis C Virus NS4A Contributes to RNA Replication and Virus Particle Assembly. *Journal of Virology* 85(3):1193-1204.

169. Gastaminza P*, et al.* (2011) Antiviral stilbene 1,2-diamines prevent initiation of hepatitis C virus RNA replication at the outset of infection. *Journal of Virology* 85(11):5513-5523.

170. Zhang L & Wang A (2012) Virus-induced ER stress and the unfolded protein response. *Frontiers in Plant Science* 3(293):16.

171. Samuel CE (2001) Antiviral actions of interferons. *Clinical Microbiology Reviews* 14(4):778-809.

172. Rice CM, Levis R, Strauss JH, & Huang HV (1987) Production of infectious RNA transcripts from Sindbis virus cDNA clones: mapping of lethal mutations, rescue of a temperature-sensitive marker, and in vitro mutagenesis to generate defined mutants. *Journal of Virology* 61(12):3809-3819.

173. Garnier J, Gibrat JF, & Robson B (1996) GOR method for predicting protein secondary structure from amino acid sequence. *Methods in Enzymology* 266:540-553.

174. Simeon RL, Chamoun AM, McMillin T, & Chen Z (2013) Discovery and characterization of a new cell-penetrating protein. *ACS Chemical Biology*.

175. Ganz T & Lehrer RI (1995) Defensins. *Pharmacology & Therapeutics* 66(2):191-205.

176. Selsted ME, Szklarek D, Ganz T, & Lehrer RI (1985) Activity of rabbit leukocyte peptides against Candida albicans. *Infection and Immunity* 49(1):202-206.

177. Daher KA, Selsted ME, & Lehrer RI (1986) Direct inactivation of viruses by human granulocyte defensins. *Journal of Virology* 60(3):1068-1074.

178. Zhang L*, et al.* (2002) Contribution of human α-defensin 1, 2, and 3 to the anti-HIV-1 activity of CD8 antiviral factor. *Science* 298(5595):995-1000.

179. Selsted ME, Szklarek D, & Lehrer RI (1984) Purification and antibacterial activity of antimicrobial peptides of rabbit granulocytes. *Infection and Immunity* 45(1):150-154.

180. Buck CB*, et al.* (2006) Human α-defensins block papillomavirus infection. *Proceedings of the National Academy of Sciences* 103(5):1516-1521.

181. Chang TL, Vargas J, Jr., DelPortillo A, & Klotman ME (2005) Dual role of α-defensin-1 in anti–HIV-1 innate immunity. *The Journal of Clinical Investigation* 115(3):765-773.

182. REED LJ & MUENCH H (1938) A simple method of estimating fifty per cent endpoints. *American Journal of Epidemiology* 27(3):493-497.

183. Zennou V*, et al.* (2000) HIV-1 genome nuclear import is mediated by a central DNA flap. *Cell* 101(2):173-185.

184. Chamoun AM*, et al.* (2012) PD 404,182 is a virocidal small molecule that disrupts hepatitis C virus and human immunodeficiency virus. *Antimicrobial Agents and Chemotherapy* 56(2):672-681.

185. Yamauchi J*, et al.* (2010) The mood stabilizer valproic acid improves defective neurite formation caused by charcot-marie-tooth disease-associated mutant Rab7 through the JNK signaling pathway. *Journal of Neuroscience Research* 88(14):3189-3197.

186. Cronican JJ*, et al.* (2010) Potent delivery of functional proteins into Mammalian cells *in vitro* and *in vivo* using a supercharged protein. *ACS Chemical Biology* 5(8):747-752.

187. Kim D*, et al.* (2009) Generation of human induced pluripotent stem cells by direct delivery of reprogramming proteins. *Cell Stem Cell* 4(6):472-476.

188. Miller VM*, et al.* (2005) CHIP suppresses polyglutamine aggregation and toxicity *in vitro* and *in vivo*. *The Journal of Neuroscience* 25(40):9152-9161.

189. Shaner NC*, et al.* (2004) Improved monomeric red, orange and yellow fluorescent proteins derived from Discosoma sp. red fluorescent protein. *Nature Biotechnology* 22(12):1567-1572.

190. Patterson G, Day RN, & Piston D (2001) Fluorescent protein spectra. *Journal of Cell Science* 114(5):837-838.

191. Lammers G & Jamieson JC (1989) Studies on the effect of lysosomotropic agents on the release of Gal beta 1-4GlcNAc alpha-2,6-sialytransferase from rat liver slices during the acute-phase response. *The Biochemical Journal* 261(2):389-393.

192. Laporte J*, et al.* (2000) Comparative analysis of translation efficiencies of hepatitis C virus 5′ untranslated regions among intraindividual quasispecies

present in chronic infection: opposite behaviors depending on cell type. *Journal of Virology* 74(22):10827-10833.

193. Chen Z, Katzenellenbogen BS, Katzenellenbogen JA, & Zhao H (2004) Directed evolution of human estrogen receptor variants with significantly enhanced androgen specificity and affinity. *Journal of Biological Chemistry* 279(32):33855-33864.

194. Gao S, Simon MJ, Morrison B, 3rd, & Banta S (2009) Bifunctional chimeric fusion proteins engineered for DNA delivery: optimization of the protein to DNA ratio. *Biochimica et Biophysica Acta* 1790(3):198-207.

195. Dangoria NS, Breau WC, Anderson HA, Cishek DM, & Norkin LC (1996) Extracellular simian virus 40 induces an ERK/MAP kinase-independent signalling pathway that activates primary response genes and promotes virus entry. *Journal of General Virology* 77(9):2173-2182.

196. Macia E*, et al.* (2006) Dynasore, a cell-permeable inhibitor of dynamin. *Developmental Cell* 10(6):839-850.

197. Subtil A, Hémar A, & Dautry-Varsat A (1994) Rapid endocytosis of interleukin 2 receptors when clathrin-coated pit endocytosis is inhibited. *Journal of Cell Science* 107(12):3461-3468.

198. Shibata Y, Metzger WJ, & Myrvik QN (1997) Chitin particle-induced cell-mediated immunity is inhibited by soluble mannan: mannose receptor-mediated phagocytosis initiates IL-12 production. *The Journal of Immunology* 159(5):2462-2467.

199. Rothberg KG, Ying YS, Kamen BA, & Anderson R (1990) Cholesterol controls the clustering of the glycophospholipid-anchored membrane receptor for 5-methyltetrahydrofolate. *The Journal of Cell Biology* 111(6):2931-2938.

200. Macklis JD & Madison RD (1990) Progressive incorporation of propidium iodide in cultured mouse neurons correlates with declining electrophysiological status: a fluorescence scale of membrane integrity. *Journal of Neuroscience Methods* 31(1):43-46.

201. Safaiyan F*, et al.* (1999) Selective effects of sodium chlorate treatment on the sulfation of heparan sulfate. *Journal of Biological Chemistry* 274(51):36267-36273.

202. Hallbrink M*, et al.* (2001) Cargo delivery kinetics of cell-penetrating peptides. *Biochimica et Biophysica Acta* 1515(2):101-109.

203. Steinman RM, Mellman IS, Muller WA, & Cohn ZA (1983) Endocytosis and the recycling of plasma membrane. *Journal of Biological Chemistry* 96(1):1-27.

204. Ceresa BP, Lotscher M, & Schmid SL (2001) Receptor and membrane recycling can occur with unaltered efficiency despite dramatic RAB5(Q79L)-induced changes in endosome geometry. *Journal of Biological Chemistry* 276(13):9649-9654.

205. Heitz F, Morris MC, & Divita G (2009) Twenty years of cell-penetrating peptides: from molecular mechanisms to therapeutics. *British Journal of Pharmacology* 157(2):195-206.

206. Fonseca SB, Pereira MP, & Kelley SO (2009) Recent advances in the use of cell-penetrating peptides for medical and biological applications. *Advanced Drug Delivery Reviews* 61(11):953-964.

207. Pinto FM*, et al.* (2004) mRNA expression of tachykinins and tachykinin receptors in different human tissues. *European Journal of Pharmacology* 494(2-3):233-239.

208. Uddin S*, et al.* (2002) Protein kinase C-δ (PKC-δ) is activated by type I interferons and mediates phosphorylation of STAT1 on serine 727. *Journal of Biological Chemistry* 277(17):14408-14416.

209. Munoz M*, et al.* (2010) The NK-1 receptor is expressed in human melanoma and is involved in the antitumor action of the NK-1 receptor antagonist aprepitant on melanoma cell lines. *Laboratory Investigation* 90(8):1259-1269.

210. Munoz M, Rosso M, Casinello F, & Covenas R (2010) Paravertebral anesthesia: how substance P and the NK-1 receptor could be involved in regional block and breast cancer recurrence. *Breast Cancer Research and Treatment* 122(2):601-603.

211. Muñoz M, González-Ortega A, & Coveñas R (The NK-1 receptor is expressed in human leukemia and is involved in the antitumor action of aprepitant and other NK-1 receptor antagonists on acute lymphoblastic leukemia cell lines. *Investigational New Drugs*:1-12.

212. Medhurst AD, Hay DWP, Parsons AA, Martin LD, & Griswold DE (1997) In vitro and in vivo characterization of NK3 receptors in the rabbit eye by use of

selective non-peptide NK3 receptor antagonists. *British Journal of Pharmacology* 122(3):469-476.

213. Hargreaves R*, et al.* (2011) Development of aprepitant, the first neurokinin-1 receptor antagonist for the prevention of chemotherapy-induced nausea and vomiting. *Annals of the New York Academy of Sciences* 1222(1):40-48.

214. Fujita T*, et al.* (1988) Evidence for a nuclear factor(s), IRF-1, mediating induction and silencing properties to human IFN-beta gene regulatory elements. *The EMBO Journal* 7(11):3397-3405.

215. Lin C, Kwong AD, & Perni RB (2006) Discovery and development of VX-950, a novel, covalent, and reversible inhibitor of hepatitis C virus NS3.4A serine protease. *Infectious Disorders Drug Targets* 6(1):3-16.

216. Ganz T (1994) Biosynthesis of defensins and other antimicrobial peptides. *Antimicrobial Peptides, Ciba Foundation Symposium*, pp 62-71.

217. Taylor MJ, Perrais D, & Merrifield CJ (2011) A high precision survey of the molecular dynamics of mammalian clathrin-mediated endocytosis. *PLoS Biology* 9(3):e1000604.

218. Lua BL & Low BC (2005) Activation of EGF receptor endocytosis and ERK1/2 signaling by BPGAP1 requires direct interaction with EEN/endophilin II and a functional RhoGAP domain. *Journal of Cell Science* 118(12):2707-2721.

219. Qualmann B & Mellor H (2003) Regulation of endocytic traffic by Rho GTPases. *The Biochemical Journal* 371:233-241.

220. Tai AW*, et al.* (2009) A functional genomic screen identifies cellular cofactors of hepatitis C virus replication. *Cell Host & Microbe* 5(3):298-307.

221. Coller KE*, et al.* (2009) RNA interference and single particle tracking analysis of hepatitis C virus endocytosis. *PLoS Pathogens* 5(12):e1000702.